UPWIND 1A2 Metrology. Final Report

Eecen, P.J.; Wagenaar, J.W.; Stefanatos, N.; Friis Pedersen, Troels; Wagner, Rozenn; Hansen, Kurt Schaldemose

Publication date:
2011

Document Version
Publisher's PDF, also known as Version of record

ECN

Energy research Centre of the Netherlands

FINAL REPORT

UPWIND 1A2 METROLOGY

P.J. Eecen, J.W. Wagenaar (ECN)

N. Stefanatos (CRES)

T.F. Pedersen, R. Wagner (Riso-DTU)

K.S. Hansen (DTU-MEK)

UpWind

RISØ КАПЕ CRES ECN DTU

ECN-E--11-013

FEBRUARI 2011

Acknowledgement/Preface
The work described in this report is carried out within the framework of the European UPWIND research project under contract with the European Commission.
CE Contract Number: 019945 (SES6)
ECN Project number: 7.9466

Abstract
The UpWind project is a European research project that focuses on the necessary up-scaling of wind energy in 2020. Among the problems that hinder the development of wind energy are measurement problems. For example: to experimentally confirm a theoretical improvement in energy production of a few percent of a new design by field experiments is very hard to almost impossible. As long as convincing field tests have not confirmed the actual improvement, the industry will not invest much to change the turbine design. This is an example that clarifies why the development of wind energy is hindered by metrology problems (measurement problems). Other examples are in the fields of:

- Warranty performance measurements
- Improvement of aerodynamic codes
- Assessment of wind resources

In general terms the uncertainties of the testing techniques and methods are typically much higher than the requirements. Since this problem covers many areas of wind energy, the work package is defined as a crosscutting activity.

The objectives of the metrology work package are to develop metrology tools in wind energy to significantly enhance the quality of measurement and testing techniques. The first deliverable was to perform a state of the art assessment to identify all relevant measurands. The required accuracies and required sampling frequencies have been identified from the perspective of the users of the data (the other work packages in UpWind). This work led to the definition of the Metrology Database, which is a valuable tool for the further assessment and interest has been shown from other work packages, such as Training.

This report describes the activities that have been carried out in the Work Package 1A2 Metrology of the UpWind project. Activities from Risø are described in a separate report: T.F. Pedersen and R. Wagner, 'Advancements in Wind Energy Metrology UPWIND 1A2.3', Risø-R-1752.

Contents

1. Introduction

The UpWind project
UpWind is a European project funded under the EU's Sixth Framework Programme (FP6). The project looks towards the wind power of tomorrow, more precisely towards the design of very large wind turbines (8-10MW), both onshore and offshore. Furthermore, the research also focuses on the requirements to the wind energy technology of 20MW wind turbines.
The challenges inherent to the creation of wind farms of several hundred MW request the highest possible standards in design, complete understanding of external design conditions, the design of materials with extreme strength to mass ratios and advanced control and measuring systems geared towards the highest degree of reliability, and critically, reduced overall turbine mass.
The wind turbines of the future necessitate the re-evaluation of the turbine itself for its re-conception to cope with future challenges. The aim of the project is to develop accurate, verified tools and component concepts that the industry needs to design and manufacture this new type of turbine. UpWind focuses on design tools for the complete range of turbine components. It addresses the aerodynamic, aero-elastic, structural and material design of rotors. Critical analyses of drive train components will be carried out in the search for breakthrough solutions. The UpWind consortium, composed of over 40 partners, brings together the most advanced European specialists of the wind industry.

Expected results
In the UpWind project research will lead to accurate, verified tools and some essential component concepts the industry needs to design and manufacture the new breed of very large wind turbines. Among others, UpWind will address the aerodynamic, aero-elastic, structural and material design aspects of rotors. Future wind turbine rotors may have diameters of over 150 meters. These dimensions are such that the flow in the rotor plane is non-uniform as a result of which the inflow may vary considerably over the rotor blade. Full blade pitch control would no longer be sufficient. That is why UpWind will investigate local flow control along the blades, for instance by varying the local profile shape. New control strategies and new control elements must be developed and critical analyses of drive train components must be carried out in the search for breakthrough solutions.
Furthermore, wind turbines are highly non-linear, reactive machines operating under stochastic external conditions. Extreme conditions may have an impact a thousand times more demanding on, for instance, the mechanical loading than average conditions require. Understanding profoundly these external conditions is of the utmost importance in the design of a wind turbine structure with safety margins as small as possible in order to realise maximum cost reductions.
A similar argument applies to the response of the structure to external excitations. In order to make significant progress in this field, more accurate, linearly responding measuring sensors and associated software are needed. Preferably, the sensors should remain stable and accurate during a considerable part of the operational lifetime of a wind turbine. UpWind will explore measuring methods and will look more in detail into new remote sensing techniques for measuring wind velocities. The validation and verification of the analyses, tools and techniques depend on reliable and appropriate measurements. The task of the work package ‘Metrology’ is to identify the critical issues in measurement techniques and to find solutions for the most critical ones.

More information on the UpWind project is found on the website:
www.upwind.eu

1.1 Work Package 1A2 Metrology

As the project includes many scientific disciplines which need to be integrated in order to arrive at specific design methods, new materials, components and concepts, the project's organisation structure is based on work packages which variously deal with scientific research, the integration of scientific results, and their integration into technical solutions. Since the measurement problems are related to several areas in the wind energy, the work package Metrology is defined as an integrating work package.

The metrology problems to develop wind turbine technology are the focus of this work package since the development of wind energy is hindered by measurement problems. In particular the fluctuating wind speed introduces large uncertainties and these fluctuations in the wind are experienced throughout the entire wind turbine. An example of a problem through measurement uncertainties is that it is almost impossible to confirm anticipated small performance improvements resulting from design modifications by means of field tests. As long as convincing field tests have not confirmed the actual improvement, the industry will be hesitant in investing in turbine design improvements. Furthermore, the developments within the UpWind project will require validation that is based on reliable and appropriate measurements.

The objective of the metrology work package is to develop metrology tools in wind energy to significantly enhance the quality of measurement and testing techniques. The first deliverable has been published being the first step to reach this objective and the list of parameters that should be measured in wind energy. The list has been developed in close collaboration with the other UpWind project work packages. The second deliverable is to find theoretical solutions for the identified metrology problems. Based on the deliverable 1 [1], the list of measurement problems, it has been analysed what the precise consequences of the identified problems are and in which directions possible solutions can be found. This has been reported [2] and a database structure has been designed to make the detailed information available to the other work packages.

1.2 References

[1] P.J. Eecen, N. Stafanatos, S.M. Petersen, K.S. Hansen, UpWind METROLOGY Deliverable D1A2.1: List of Measurement Parameters, ECN-E--07-015

[2] P.J. Eecen, N. Stefanatos, T.F. Pedersen, K.S. Hansen, UpWind METROLOGY. Deliverable D 1A2.2; Metrology Database - Definition ECN-E--08-079

2. Deliverable D 1A2.1: List of Measurement Parameters

The development of metrology tools to significantly enhance the quality of measurement and testing techniques in wind energy is carried out in three steps. These steps are described in the work programme and are defined as deliverables. The three steps (deliverables) are

1. Problem identification: determination of the parameters that must be measured for the various problems encountered in wind energy and the required accuracies.
2. Available techniques and theoretical solutions: for the identified parameters the state-of-the-art measurement techniques are described, the problems that may be encountered are described and possible theoretical solutions are presented.
3. The practical value of the proposed solutions is demonstrated.

After finishing the second step where the theoretical solutions are presented, a work programme for the demonstration phase is defined.

This report presents lists of parameters that should be measured for the various subjects in wind energy. Since the work packages in the UpWind project are divided along these subjects, the lists are specified for the different work packages. The lists have the intention not only to include the present-day techniques, but rather describe required or desired measurement techniques for the future 20MW wind turbines. The list has been made after interaction with the work packages in the UpWind project. All members of these work packages did have the opportunity to comment on the list or add further required measurements.

When setting up the lists of parameters, it was found that the most valuable list limits itself to the following columns

Parameter / Signal	Unit	Desired accuracy	Traceable (Y/N)	Sampling frequency range [Hz]	Required / Optional	Measurement position

Where the columns are:

- **Parameter / Signal:** The name of the parameter or signal that must be measured.
- **Unit:** The unit in which the parameter should be measured.
- **Desired accuracy:** The desired accuracy with which the parameter should be determined for the specific task. This means that a single parameter could have quite different requirements for the different applications (work packages).
- **Traceability:** Whether or not the parameter should have a traceable value. In general all values that are measured should be traceable, otherwise you will have a 'floating' value. Although almost all values should be traceable, it is still included in the list to remind the experimenters and users of experimental data of the importance of traceability. Further information on traceability is presented in section 2.1.2.
- **Sampling frequency range:** The required frequency range for the specific purpose. For many parameters a minimum sampling frequency is provided. For some of the more general parameters, the reader is reminded that the sampling frequency should be eight times larger than the highest frequency to be studied.
- **Required or Optional:** indicate whether the parameter is required for the purpose or can be optional. Optional is also indicated when we expect that it will be required for future techniques but at the moment it is (only) optional. It must be noted that in many cases the optional measurements can improve the final accuracy and reliability of the measurements.
- **Measurement position:** the location where the parameter should be measured.

There are some remarks:

1. Measurands could be used for various applications. For the different applications, usually there are different requirements with respect to accuracy, sampling frequency or reliability.
2. For each measurand is indicated whether or not it is required. One should keep in mind that what is optional today might be required in the future because of for example advancements in turbine control or measurement techniques.
3. The measurement position does not include the mounting, since this is specific for each instrument and measurement technique. The mounting will be included in the list of measurement devices (deliverable D 1A2.2). In the list presented in this report is indicted the location in the turbine, or around the turbine where the measurement should be performed.
4. For offshore wind farms, it should be noted that the relative importance of certain parameters may differ from the onshore cases. For example, under low-turbulence ambient conditions, wake effects within wind farms are more pronounced. In addition, not only the single parameters are of relevance, but also the correlation with other parameters e.g. the correlation of wind and wave parameters. Another example is the description of the vertical wind speed profile. Thermal stratification of the atmosphere as well as the surface roughness has a major impact on the profile. While the surface roughness strongly depends on the actual sea state the thermal stratification is influenced by a number of conditions such as the ambient air and water temperature and the location of the site under consideration. This might require other methods to determine the vertical wind speed profile.
5. In the case of voltage measurements and current measurements, it is tempting to put the required class 0.5 (or other class) as desired accuracy. This is not done here: the total accuracy is indicated here, including the mounting, sampling etc., which is similar to the other measurands.
6. Controller signals may be measured in different ways. In some cases, a voltage signal representing the controller signal is measured. This should be traceable. In other cases, where the digital signal is 'measured' or obtained directly, this is considered traceable.
7. The accuracies of the derived parameters are not stated in the lists. The accuracies of the derived parameters are fully determined from the input parameters.
8. The time scale is an important parameter when analyzing and validating flow structures inside wind farms because of large transportation time and bad correlation.

This report describes the measured parameters and the required accuracies and required frequency range for measurements on wind turbines. The areas that are investigated are covered by the various other work packages in the UpWind project. It is advantageous to combine the lists of parameters for some of the other work packages. The following subdivision is used throughout this report.

Work Packages	**Parameter list**
WP2 Aerodynamics & Aero elastics WP3 Rotor structure and materials WP4 Parameters Foundations	Table A.1 Table A.1 Table A.1
WP5 Control systems WP7 Condition Monitoring	Table B.1 Table B.1
WP1B2 Transmission and conversion WP9 Electrical Grid	Table C.1 Table C.1
WP8 Flow WP6 Remote Sensing	Table D.1 Table D.1

From the many IEC documents, three have been selected to be included in the lists of parameters. These are:

IEC Documents		**Parameter list**
Noise Measurements	IEC 61400-11	Table F.1
Power Performance Measurements	IEC 61400-12-1	Table E.1
Power Quality Measurements	IEC 61400-21	Table C.1

For reference, the following IEC documents are indicated. The selection is quite arbitrary.

Design requirements	IEC 61400-1	
Measurement of mechanical loads	IEC 61400-13	
Wind turbine certification	IEC 61400-22	
Full scale blade testing	IEC 61400-23	
Lightning protection	IEC 61400-24	
Communications for monitoring and control of wind power plants	IEC 61400-25	

The tables in the Appendices of the lists of measurands also indicate a column with 'parameter number'. This parameter number is added for further analyses on the data. The parameter numbers indicate the following:

Parameter number	Indication
1	Structural parameters
2	Operational and control parameters
3	Meteorological parameters
4	Hydrological parameters
5	Geotechnical parameters
6	Acoustic parameters

2.1 Other areas of investigation

Other areas of investigation that are not included in the analyses of the Metrology work package are:

1. **Wind tunnel measurements**. Although for some measurands wind tunnel measurements could be a tool for the further improvement, the accuracies and measurement techniques connected to wind tunnel measurements is not included in the scope of this report.
2. **Material coupon testing**. The work package WP3 Rotor structures and Materials was one of the first work packages to send us the information required to build the lists of measurands. Despite the useful list, the UpWind work package leader meeting decided that coupon testing is not considered in the scope of WP1A2 Metrology.
3. **Blade testing** (although there is a common standard covering this subject) and requirements to the testing might need a revision, as the size of blades increases. Right now the increasing problems are subject for a discussion among the testing laboratories (outside the scope of UpWind WP1A2 Metrology).

2.1.1 Air Foil data

From the interaction with other work packages, the issue of air-foils did come up. The determination of the exact shape of the air foils is an issue not completely covered. The questions that did arise are:

- How to determine the outer shape of the blade
- How to determine the weight distribution in the blade

- How to determine the structural characteristics of the blade

Required accuracies should come from the aerodynamics work package (WP2).

2.1.2 Traceability in measurements

The definition of traceability as it appears in the ISO/IEC Guide 43-1:1997 is [VIM:1993, 6.10]**:**

"Traceability is the property of the results of the measurement or the value of a standard whereby it can be related to stated references, usually national or international standards through an unbroken chain of comparisons , all having stated uncertainties"

This report includes a brief working analysis of this definition in this section. More details can be found in [1].

"Traceability is the property of the results of a measurement ...
Whereby it can be related to stated references ..."

ANY measurement result MUST BE TRACEABLE, in order to be comparable with values measured at different locations or different times.

"it can be related to stated references, usually national or international standards …"

Traceability is assured by comparing the output of a "measurement system" to a globally accepted value and establishing a correction function (= calibration coefficients of the measurement system) connecting the measurement system output to the "real globally accepted value" of the measurand.

" ….related to stated references, ….., through an unbroken chain of comparisons …"

It is not necessary to compare our measurement system (say a load cell) directly to the International Standard (for Mass) stored in Geneva. We can compare it to our reference load cell (Step 1) which was compared to the reference load cell of a calibration laboratory (Step 2) which was compared to the National Standard (Step 3) for Mass, which was compared to the International Standard (Step 4) in Geneva. In theory, unlimited number of in-between comparisons are accepted, provided that there is a continuous (unbroken) chain leading up to global values. However, the following comment should be taken into account:

"… all having stated uncertainties …"

For each comparison step made in the chain, an uncertainty factor should be included to the "calibration uncertainty" for our measurement system. This uncertainty relates to the limited accuracy of the "reference value" and to other uncertainty factors related to the comparison procedure (effect of ambient conditions, effects of mounting etc). In other words, the more steps in

the comparison of our system to the globally recognised values, the greater the calibration uncertainty. The calibration certificate issued by the calibration laboratory must include an evaluation of the total uncertainty in the calibration step performed. It is assumed that the calibration uncertainties of all previous steps up to the Globally Accepted Value (International Standard) are included in the uncertainty evaluation of the calibration.

Important Note: The calibration uncertainty is only ONE of the uncertainty parameters that must be included in the measurement uncertainty analysis.
Other factors like
- limited resolution of the instrument,
- long term deviation,
- ambient conditions (e.g. temperature, humidity) effects,
- mounting,
- and signal conditioning and transmission

just to name a few, should always be evaluated in the uncertainty analysis.

"A traceable calibration assures a globally accepted value for the results of the measurement but it cannot reduce uncertainty related to other factors"

2.2 Integration with other work packages in UpWind

In this Chapter the work packages are indicated for which lists of measured parameters are generated. Each section includes a short description of the work package and includes the relevance of Metrology for that work package. The lists of measured parameters are combined for several work packages.

WP2 Aerodynamics & Aero-elastics, WP3 Rotor structures and WP4 Turbine Foundations

The list of parameters for these work packages has been combined. The list is indicated in Appendix A. The four applications of the measured parameters in this list are

1. WP2 and WP3 Turbine Monitoring: measurements of a single turbine mainly intended for the verification of simulation codes
2. Farm Monitoring: Measurements to characterise the conditions within and around the wind farm
3. WP4 Design code verification: design code verification for offshore foundations
4. WP4 Advanced Control strategies: development of advances control strategies of single offshore wind turbines to reduce the loads on the structure (including foundations).

WP2 Aerodynamics & Aero-elastics

The objective of the work package "Aerodynamics & Aero-elastics" is to develop a basis for aerodynamic and aero-elastic design of large multi-MW turbines in order to ensure that the wind turbine industry will not be limited by insufficient models and tools in their future design of new turbines, including possible new and innovative concepts.

The specific objectives are:

- Development of structural dynamic models for the complete wind turbine or subcomponents that can handle highly non-linear effects e.g. from flexible blades with complex laminated composite and/ or composite sandwich skins and webs, spanning from micro-mechanics to structural scale.
- Development and application of advanced models on rotor and blade aerodynamics, covering full 3D CFD rotor models, free wake models and improved BEM type models.

- Aerodynamic and aero-elastic modelling of aerodynamic control features and devices. This represents the theoretical background for the smart rotor blades.
- Development of methods and models for analysis of aero-elastic stability and total damping including hydro-elastic interaction.
- Development of models for computation of aerodynamic noise in order to design new airfoils and rotors with less noise emission.

Relevance of Metrology: The verification of the simulation codes requires measurements that are reliable and accurate. The measurements should fit the requirements from the simulation codes verification process.

WP3 Rotor structures and materials

The objectives of the work package "Rotor structures and materials": For larger wind turbines, the potential power yields scales with the square of the rotor diameter, but the blade mass scales to the third power of rotor diameter (square-cube law). With the gravity load induced by the dead weight of the blades, this increase of blade mass can even prevent successful and economical employment of larger wind turbines. In order to meet this challenge and allow for the next generation of larger wind turbines, higher demands are placed on materials and structures. This requires more thorough knowledge of materials and safety factors, as well as further investigation into new materials. Furthermore, a change in the whole concept of structural safety of the blade is required.

The specific objectives are:

- Improvement of both empirical and fundamental understanding of materials and extension of material database.
- Study on effective blade details.
- Establishment of tolerant design concepts and probabilistic strength analysis.
- Establishment of a material testing procedure and design recommendations.

Relevance of Metrology: The verification of the simulation codes requires measurements that are reliable and accurate. The measurements should fit the requirements from the simulation codes verification process. Coupon testing of materials is another issue, where measurement problems can be identified. Unless input was received from the work package regarding the requirements and problems encountered in measurement techniques, the subject of coupon testing is not included in this report (see also section 2.1).

WP4 Offshore Foundations and Support Structures

The objective of WP 4 "Offshore Foundations and Support Structures" is to develop innovative, cost-efficient wind turbine support structures to enable the large-scale implementation of offshore wind farms across Europe, from sheltered Baltic sites to deep-water Atlantic and Mediterranean locations, as well as other emerging markets worldwide. The work package will achieve this by seeking solutions which integrate the designs of the foundation, support structure and turbine machinery in order to optimise the structure as a whole. Particular emphasis will be placed on large wind turbines, deep water solutions and designs which are insensitive to site conditions, allowing cost-reduction through series production.

Relevance of Metrology to the work package Foundations is the determination and measurement of parameters that are relevant for offshore wind energy application in general and such that are directly related to future work of WP4. In this context the parameters are intended for a variety of purposes. These are:

- Design basis, site specific design of offshore wind farms.
- Advanced control & load mitigation concepts.

In addition, condition monitoring is important for the WP4 'Foundations'. This is taken into account when describing the list for WP7 "Condition Monitoring". Another important aspect re-

lates to the verification and further development of existing state-of-the-art simulation tools. Especially the measurement of the structural parameters becomes necessary as well as the environmental parameters and operational parameters. Due to the offshore specific environment, the hydrological and geological parameters are essential.
Here we elaborate a little on the **geotechnical parameters**. The range of demanded geotechnical parameters strongly depends on the actual foundation type and furthermore strongly depends on the modelling approach. Typically, the geotechnical investigations of a specific site comprise determination of the soil strata and their corresponding physical and engineering properties by in-situ tests and sample tests in the laboratory. Not only the initial values for these parameters are required, but also their variation over the lifetime due to the presence of the wind turbine. However, the sampling rate will not be high and these measurements will in most cases be performed by companies specialised in these geotechnical measurements.

WP5 Control systems and WP7 Condition Monitoring

The list of parameters for these work packages has been combined. The list is indicated in Appendix B. The applications of the measured parameters in this list are

1. WP5 Operational Control Systems; measurements needed for day-to-day control of the turbine. Main requirement is reliability.
2. WP5 Development of Control strategies; measurements needed for optimisation of control of the turbine and measurements to validate developments. Accuracy could be of more importance than reliability.
3. WP7 Condition Monitoring; measurements for condition monitoring. The condition monitoring is treated to focus primarily on the drive train. Main requirement is reliability.

WP5 Control systems

Further improvements in the cost-effectiveness of wind turbines drive designers towards larger, lighter, more flexible structures, in which more 'intelligent' control systems plays an important part in actively reducing the applied structural loads. This strategy of "brain over brawn" will therefore avoid the need for wind turbines to simply withstand the full force of the applied loads through the use of stronger, heavier and therefore more expensive structures. To reach this point it is necessary to demonstrate these load reductions in full-scale field tests on a well-instrumented turbine. **The objective of WP5 "Control Systems"** is to develop new control techniques can then be used with more confidence in the design of new, larger and innovative turbines.

As the penetration of wind energy increases, real issues are already arising relating to the control of the electrical network and its interaction with wind farms. These issues must be resolved before the penetration of wind power can increase further.

The specific objectives of this work package are:

- Further development of control algorithms for wind turbine load reduction, of the sensors and actuators which are required for the algorithms to be effective, of efficient methods of adjusting and testing controllers, and the application of these techniques to new larger and innovative turbines.
- Investigation and evaluation of different load estimation algorithms, using various sets of available sensor signals. Incorporation of promising structures to load reducing controller algorithms. Identification of potential problems to overcome when taking into account fault prediction information in controller dynamics.
- Field tests to demonstrate that the load reductions and estimated loads can be achieved reliably, so that future designs can take advantage of the implied reduction in capital costs.

Development of wind turbine and wind farm control techniques aimed at increasing the acceptable penetration of wind energy, by allowing wind turbines to ride through network distur-

bances, and to contribute to voltage and frequency stability and overall reliability of the network.

Relevance of Metrology to the work package "Control Systems" extends to two applications. The first application requires measurements for day-to-day control of the turbine. Apart from the accuracy of the measurements, the reliability shall be equally important. These measurements should extend at least 20 years. The second application requires measurement techniques to facilitate the development of new control strategies. These measurements are needed for optimisation of control of the turbine and measurements to validate new developments.

WP7 Condition Monitoring

The objective of work package "Condition Monitoring" is to support the integration of new approaches for condition monitoring, fault prediction and operation & maintenance (O&M) strategies into the next generation of wind turbines for offshore wind farms. Main aspects for these items are the cost effectiveness of the required condition monitoring hardware equipment, the introduction of optimised signal processing routines and the adaptation of fault prediction algorithms or O&M strategies. The results will be used in the educational part of the UpWind project and will have impact into the work packages dealing with material research and rotor blade sensor integration.

Relevance of Metrology to the work package "Condition Monitoring" are measurement techniques to measure during long periods the condition of the turbine, for example the drive train, and the analyses techniques required to obtain the required information from the large amount of vibration data.
From the work package it is stipulated that for condition monitoring purposes, most of the measured quantities are not evaluated according to their absolute values, but according to the deviation from a defined level ("base line") as a trend analysis. This base line level can be derived, for example, from a measurement taken under a fault free condition of the component to be monitored. It can also be a component manufacturer's recommendation. For the trend analysis, the absolute accuracy of the measured values is not that important. What is important for condition monitoring is the long term stability of the measured values to allow a reliable trend analysis.

WP1B2 Transmission and conversion and WP9 Electrical Grid

The list of parameters for these work packages has been combined. The list is indicated in Appendix C. The applications of the measured parameters in this list are

1. WP9 Electrical Grid, measurements needed for the work package electrical grid. Only a limited number of parameters could be identified. The assumption is that the work package limits itself to the components after the generator.
2. WP1B2 Transmission; measurements needed for the work package transmission and conversion. The parameters identified include the forces on the main shaft etc. Therefore also the bending moments on the blade root are the input for this work package.

The issue of Power Quality measurements (IEC 61400-21) is included in this table.

WP1B2 Transmission and conversion

This work package covers the entire drive train including mechanical and electrical components. The overall purpose is to develop the technology necessary to overcome the present limitations in turbine size, power, and effectiveness and to increase predictability and reliability. The work package is divided in three: Mechanical Transmission, Generators and Power Electronics. The interaction of Metrology primarily is with the Mechanical Transmission.

Objectives – Mechanical Transmission.

In terms of reliability the drive train today is the most critical component of modern wind turbines. Nowadays the typical design of the drive train of modern wind turbines consists of an integrated serial approach where the single components, such as rotor shaft, main bearing, gear-

box and generator are as much closed together as possible with the aim of compactness and mass reduction. Field experiences throughout the entire wind industry show that this construction approach results in many types of failures (especially gearbox failures) of drive train components, although the components are well designed according to contemporary design methods and all known loads. It is assumed that the basic problem of all these unexpected failures is based on a principal misunderstanding of the dynamic behaviour of the complete system "wind turbine" due to the lack of an integral approach ready to use which at the same time integrates the structural nonlinear elastic behaviour with the coupled dynamic behaviour of multi body systems together with the properties of electrical components.
Beneath of the principal understanding of the actual loads within the gearboxes the turbine manufacturers increasingly request for a test to prove the reliability of the gearboxes. As the lifetime should be up to 20 years, the test has to be performed in a significantly reduced period of time. But within such test procedures the product needs to be stressed in the same way as if it has endured the designed lifetime. It is not sufficient to simply raise the load, but an intelligent combination of load cycles and speed is necessary. The theory for the layout of such accelerated lifetime tests up to now is still unclear and not state of the art.
Within this work package three main issues for the construction of future large scale wind turbines are addressed: 1st the in-depth and realistic simulation of the complete system behaviour for the design of reliable and cost effective components and 2nd the systematically analysis and test of gearboxes to ensure and verify a desired lifetime and at the same time reduce noise excitation. 3rd to verify common load assumptions for drive train design through long-term measurement technique and development of low-cost down counting technique of remaining drive train life-time due to actual measured stresses.
Relevance of Metrology to this work package is development of a measurement list required for the validation of models and the characterisation of the mechanical transmission.

WP9 Electrical Grid
The objective of work package "Electrical Grid" is to investigate the requirements to wind turbine design due to the need for reliability of wind farms in power systems, and to study possible solutions that can improve the reliability. The task is particularly important for large offshore wind farms because failure of a large wind farm will have significant influence on the power balance in the power system and because offshore wind farms are normally more difficult to access than land-sited wind farms.
The reliability of the power production from a wind farm depends on the wind turbine, the collecting grid of the wind farm including transformers, the power grid, and also the wind farm monitoring system can have an influence. However, critical situations are where the complete wind farm trips thus the influence of the grid is the most important, because grid abnormalities normally affect all the wind turbines in a large wind farm simultaneously. The consequences of grid abnormalities such as voltage dips, outages and unbalance, depend on the "ride-through" capability of the wind turbines. Finally, extreme wind conditions are important if all wind turbines are affected, i.e. if cut-out wind speed is reached or when the wind speed drops after a front passage.
The work package will investigate operational as well as statistical aspects of wind farm reliability. Investigating grid code requirements, extreme wind conditions and specific wind farm control options to cope with these requirements will cover the operational aspects. The statistical aspects will be covered by the development of a database and by statistical modelling of the reliability of wind energy.
The list of measurands for the work package "Electrical Grid" limits itself to the measurement of the electrical properties of the power evacuation system, some temperatures to monitor the system and the wind speed at the nacelle. Meteorological aspects are treated in connection to other work packages.

WP6 Remote Sensing and WP8 Flow
The list of parameters for these work packages has been combined. The list is indicated in Appendix D. The applications of the measured parameters in this list are

1. WP6 Remote Sensing. This is a specific work package where measurement techniques are being developed. The parameters to be determined from remote sensing devices are the wind speed and direction in the rotor plane including turbulence parameters with sufficiently high frequency.
2. WP8 Flow; Characterisation of the flow field within and around wind farm. For this work package, the wind conditions within and around the wind farm are important. Waves etc. are not included. Wake effects and validation of wakes is included, so that some turbine parameters are necessary to include.

WP6 Remote Sensing

The modern wind turbines are getting larger, requiring larger measuring heights. The instrumented mast installations of comparable height to these turbines are already more expensive than intelligent remote-sensing alternatives. Two such alternatives are Sodar (an acoustic version of a RADAR) and Lidar (an optical version of a RADAR). The Sodar obtains reflections from atmospheric fluctuations and measures the mean horizontal speed of the turbulence. The Lidar obtains reflections from atmospheric particles and measures their mean horizontal speed. The potential for remote sensing methods has been demonstrated, however, further research is required in a number of key areas. Recently new Lidar technologies have arisen which are targeted toward wind measurements over a distance range appropriate to turbines, and which do not require the expense and logistic overheads of liquid nitrogen cooling or very stable optical platforms.

The objectives of WP6 "Remote Sensing" is to concentrate the research on Lidars, the monostatic Sodars and the bistatic Sodars. There exist already examples of work on these instruments showing their capabilities (power curves using Sodars and Lidars, site assessment and comparisons to cup anemometer measurements). It is the intention of this work package to mature the work, which has already taken place, on the Lidar and the monostatic Sodar techniques, through a coordinated effort. By the end of this work the remote sensing methods will be introduced into the existing standards (the relevant IEC and MEASNET documents) as valid alternatives to the existing methods for wind speed and direction measurements which use mast-mounted instruments. For the bistatic Sodar the intention is to investigate further this technique, since the theory shows that it possesses large potential.

Relevance of Metrology to the work package "Remote Sensing" is the validation of the new remote sensing techniques against existing techniques. The differences mainly exist in the heights that could be measured and in the principle difference between point measurement of the wind speed and a volume measurement of the wind speed. Apart from measurement techniques, this will require analyses techniques and further refinement of standards and guidelines to include these techniques in the day-to-day operation of wind energy.

WP8 Flow

The objective of WP8 "Flow" is to provide input on free stream and wake (within wind farm) wind (shear) and turbulence. The research focuses on the interaction between wind turbines and the boundary-layer – including both the impact of the boundary layer on downwind wake propagation (affecting downwind turbines) and the impact of wakes on the boundary-layer affecting downwind free stream conditions. Each wind turbine generates a wake and a neighbouring wind turbine in that wake will be exposed to a lower wind speed and a higher turbulence than the unobstructed wind turbine and thus yield less energy but experience higher loads. In ideal circumstances, wind and turbulence on a fine mesh (horizontal and vertical) for the whole wind farm would be predicted. However, there is a gap between engineering solutions and CFD models and a bridge is needed for this prediction in order to provide more detailed information for modelling power losses, for better wind farm and turbine design, for more sophisticated control strategies and for load calculation.

Work package "Flow" focuses on individual wake model performance in the offshore environment and complex terrain and in further developing a whole wind farm model that can be used to evaluate impacts downwind for siting of multiple wind farm clusters. In large wind farms,

other than accurate resource prediction, the largest impact on power output is losses through wind turbine wakes. Emphasis is placed on optimal performance of the wind farm as a unit through reduced wakes. Hence an additional task is to evaluate whether wake losses and turbulence can be minimized by close crosswind spacing, by better characterisation of the wake-induced loading, by controls on the turbines or by using turbine yawing to create enhanced farm level circulation. The specific objectives are:

- Further development of large wind farm models for offshore also incorporating downstream flow.
- Better prediction of flow and wakes in wind farms in complex terrain, taking into account flow turning and wind rose narrowing.
- Collection and dissemination of data sets (wind speed and power output, mainly for wake studies).
- Investigation of reduction of wake losses and turbulence by close crosswind spacing, by controls on the turbines or by using turbine yawing to create enhanced farm level circulation.
- Demonstration of the value of load-optimal layout design and wind farm operation in overall cost-effectiveness.

Relevance of Metrology to the work package Flow is the study of existing measurement techniques and analyses techniques. The integration will give better insight in the main uncertainties, their origin and if and how they can be reduced or removed. Furthermore, emphasis could be placed on the spatial and temporal correlation of the wind field across large offshore wind farms.

2.3 Discussion and Conclusions

The UpWind consortium research covers a wide area of expertise in wind energy. The required measurement and analysis techniques covering this wide range are identified after successful and extensive interaction between the various work packages of the UpWind project. The lists of measurands for a number of applications are added to the report. With this report the deliverable D 1A2.1 is presented. Further work within the work package 1A2 Metrology will concentrate on the further analyses and demonstration of the measurement techniques and analysis techniques.

2.4 References

[1] EAL-G12: Traceability of Measuring and Test Equipment to National Standards. European cooperation for Accreditation of Laboratories, Ed. 1, November 1995 See in http://www.european-accreditation.org/

3. The Metrology Database

The Metrology Database is defined to structuring all topics relating to metrology. The implemented dedicated database consists of a number of inter-related tables. This Chapter describes the tables and their interrelation together with a small tutorial on how to open the database.

3.1 Introduction

A dedicated database has been designed to substitute the large number of MS-Excel sheets used during the initial project definition period. The database has been designed in OpenSource software package, named MySQL®, which is compatible with MS-Windows and Linux computers.
The metrology database consists of a number of individual tables, which are linked together through a number of variables. The applications, defined in the other UpWind Work Packages during the integration process, have been defined as key parameters and the tables contains a registration of methods, problems, references, measurands, techniques, sensors and commercial sensors.
It has been of great importance to use the cross references defined in database between applications, methods, parameters and sensors during the process of identifying problems between the state-of-art-analysis-technique and the state-of-art-technique.

3.2 Database structure

The metrology database consists of 11 tables, where the structure and contents of each table is defined in the sections below. The main tables are connected as shown on Figure 1, the remaining tables contain additional information.

The database structure and the contents of the tables represent three different aspects:
1) Application types.
2) State-of-art-analysis-techniques, derived problems and documentation.
3) Identification of measurands and the state-of-art-technology.

The database furthermore includes tables with sensor types, available sensors and links to sensor information.

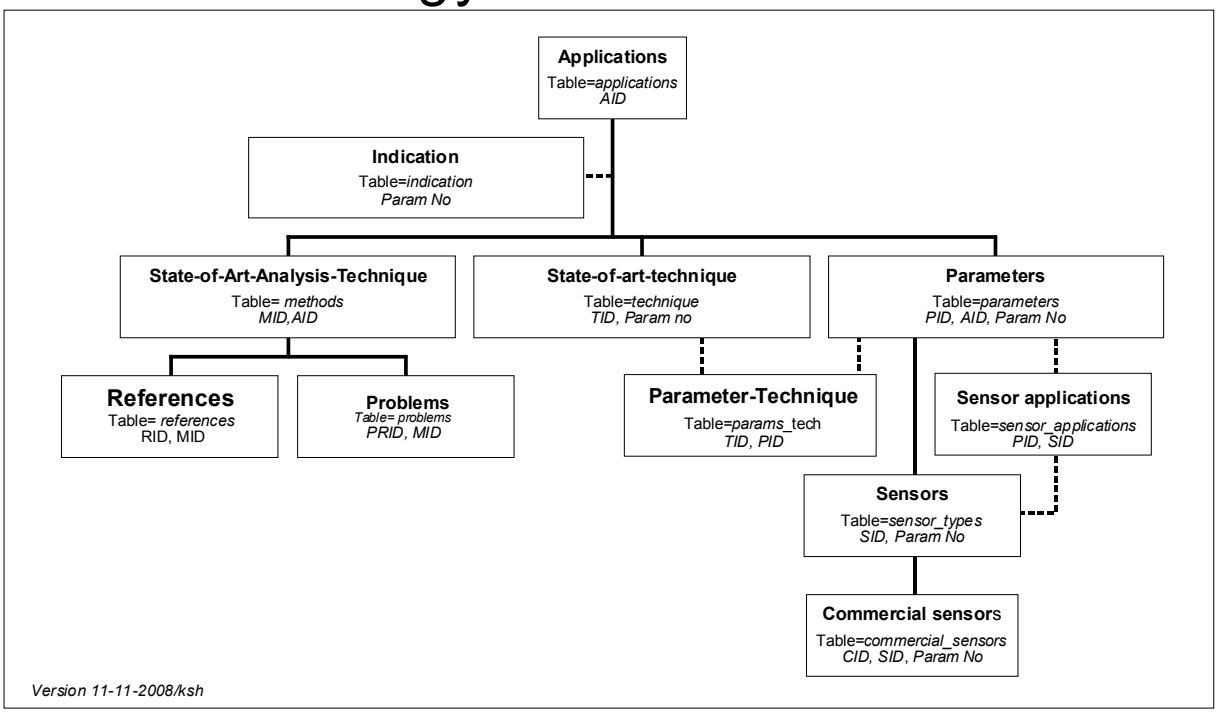

Figure 3.1 *Structure of the metrology database.*

Table 3.1 *Summary of ID parameters used in the metrology database*.

Parameters	***Definitions***
AID	Definition of application ID
CID	Commercial sensor ID
CRID	Commercial sensor reference ID
MID	State-of-art-analysis-technique ID
Param No	Indication of parameter location ID
PID	Parameter ID, referring to a physical parameter
PRID	Problem ID, referring to a method
RID	Reference ID, referring to method description
SID	Sensor type ID, referring to a principle
TID	State-of-art-technique ID

Detailed definitions of each table structure are listed in [1].

Table 3.2 *Parameter cross references for all tables.*

Tables	AID	CID	CRID	MID	Param No	PID	PRID	RID	SID	TID
Applications	X									
Indication					X					
Methods	X			X						
Technique					X					X
Parameters	X				X	X				
References				X				X		
Problems				X			X			
Sensor applications						X			X	
Sensor types					X				X	
Commercial sensors		X			X				X	
Data sheet		X	X							

The application definition table contains information about different applications as listed in Appendix A.

3.3 Access to the database

The database has been developed on a database-server located at DTU, Lyngby. During the process of the UpWind project the database is a prototype and is continuously being updated. User access information is presented in the Table below.

Table 3.3 *Driver information to access the Metrology database through ODBC.*

DRIVER (MS-Windows XP):	MySQL ODBC 3.51 Driver
Database-server IP:	130.226.17.201
Port (default):	3306
Database name:	Metrologi
User name (UID):	
Password (PWD):	

User names (UID's) and Passwords (PWD's) will be distributed when the database is ready for release. The ODBC 3.51 driver is used to access MySQL® version 4.0 and different commercial and freeware tools can be used to access the database:

Table 3.4 *Tools for accessing the Metrology database.*

Tool	***Note***
MySQl® Control center	Based on SQL scripts
MySQL® Query Builder	Based on SQL scripts
MS-Excel®	Requires an ODBC installation of MySQL® ODBC 3.51 Driver
MS-Access®	Requires an ODBC installation of MySQL® ODBC 3.51 Driver
MS-Word®	Requires an ODBC installation of MySQL® ODBC 3.51 Driver

Using MS-Access with linked MySQL® tables enables the user to work in a MS-Access environment but requires access to the Internet. MS-Access® includes all necessary tools for querying and reporting the contents of the database. A MS-Excel link enables import of table(s) or queries to a MS-spreadsheet.

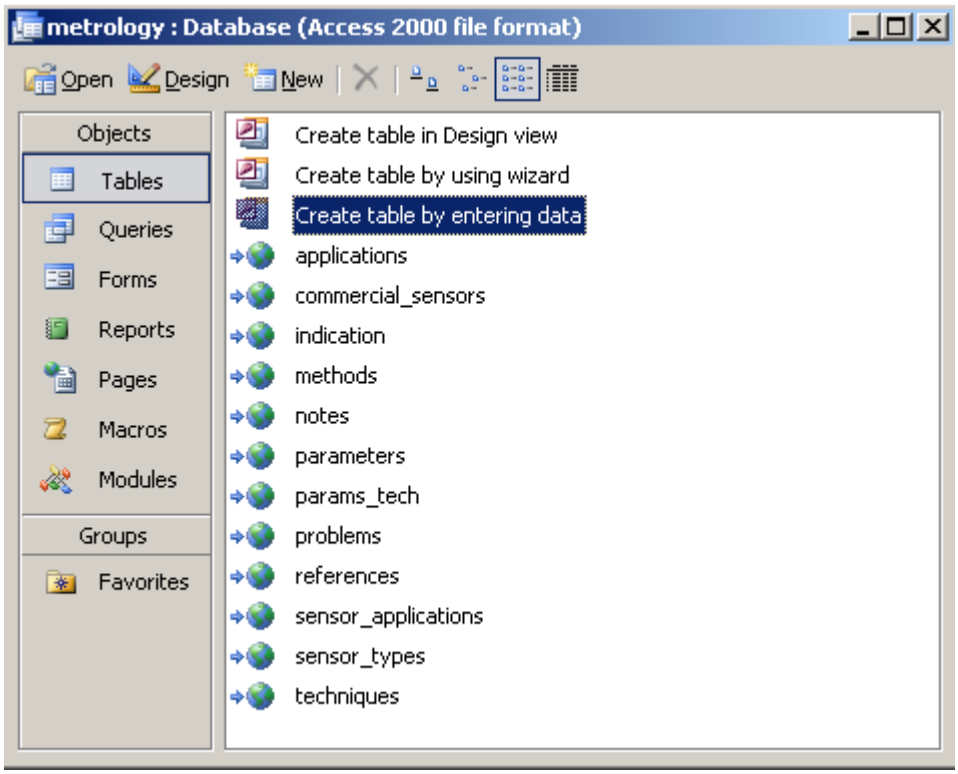

Figure 3.2 *List of linked tables in MS-Access from the Metrology database.*

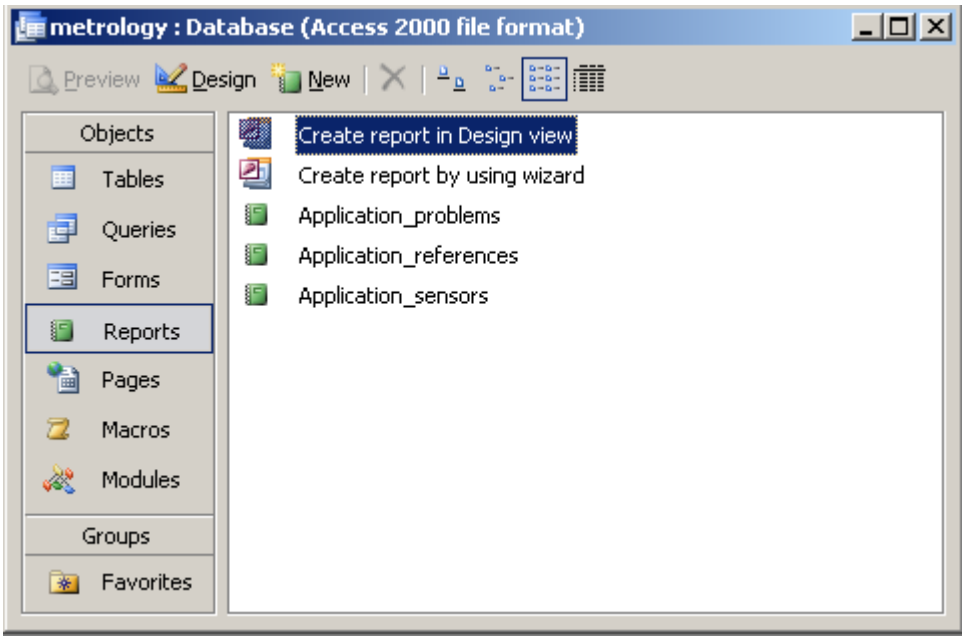

Figure 3.3 *List of predefined, dedicated reports based on linked tables.*

3.4 Discussion and Conclusions

The UpWind consortium research covers a wide area of expertise in wind energy. The required measurement and analysis techniques covering this wide range are identified after successful and extensive interaction between the various work packages of the UpWind project.

The second deliverable is to find theoretical solutions for the identified metrology problems. Based on the deliverable 1, the list of measurement problems, it has been analysed what the precise consequences are of the identified problems and in which directions possible solutions can be found.

In order to process the large amounts of data, and especially the many relations, a database structure has been designed. A dedicated database is designed to systematically organise the information that has been generated. First of all, the identified measurement problems are included, the state-of-the-art measurement techniques, including lists of sensors applied to measure the various measurands. Furthermore, a list of commercially available sensors is included.

The database has been developed in MySQL, which can be installed on both Linux and MS-Windows personal computers. The metrology database consists of a number of individual tables, which are linked together through a number of variables. The applications from the different UpWind Work Packages have been used as key parameters and the other tables contain the derived and necessary methods, measurands, techniques, etc.

Further work within the work package 1A2 Metrology will concentrate on the further analyses and demonstration of the measurement techniques and analysis techniques.

3.5 References

[1] P.J. Eecen, N. Stefanatos, T.F. Pedersen, K.S. Hansen, UpWind METROLOGY. Deliverable D 1A2.2; Metrology Database – Definition, ECN-E--08-079

4. Turbulence normalization combined with the equivalent wind speed method

Rozenn Wagner and Julia Gottschall

4.1 Introduction

The power performance of a wind turbine has to be measured according to the IEC 61400-12-1 standard [1]. The power curve is obtained with 10 minute mean power output from the turbine plotted against simultaneous 10 minute average wind speeds. The standard only requires the wind speed the wind speed at hub height and the air density (derived from temperature and pressure measurement). However it has been shown that other characteristics of the wind field influence the power performance measurement too. These parameters are the wind shear (see chapter 5 and 6) and the turbulence intensity [1, 2]. Turbulence intensity (TI) is defined as the ratio between 10-minute standard deviation and mean wind speed.

4.2 Effect of the turbulence intensity

When the wind speed fluctuates around the rated wind speed, the power extracted is limited to the rated power. Therefore only "negative fluctuations'" (i.e. the instantaneous wind speeds below rated speed) of the wind are transformed into power fluctuations. Consequently, 10 minute mean power obtained with a given turbulence intensity is generally smaller than the power that would be obtained with the same mean wind speed and a laminar flow (TI=0%), and the mean power decreases as the turbulence intensity increases, see Figure 4.1. In the same way, as the wind speed fluctuates around the cut-in wind speed, only the positive fluctuations are transformed in power fluctuations. Therefore, near the cut-in wind speed, the mean power is expected to increase with the turbulence intensity. Between the cut-in and rated speeds, the turbine is expected to respond to any wind speed fluctuations (positive or negative). Within the wind speed range where the C_P is nearly constant, the turbine power increases with the turbulence intensity as the power is then proportional to the cube of the wind speed. Moreover, according to BEM simulations (with HAWC2Aero), the scatter increases around the mean power curve with the turbulence intensity.

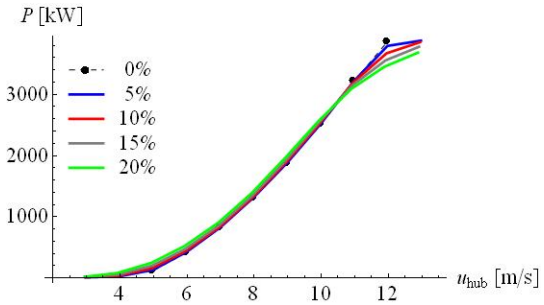

Figure 4.1 *Mean power curves for various turbulence intensities*

The effect of the turbulence intensity on the power curve can be seen as the combination of one effect on the mean power curve that varies with the turbulence intensity (especially around rated speed) and one effect on the scatter that increases with the turbulence intensity. The scatter in the power curve results from both effects as it usually results from a distribution of various turbulence intensities.

4.3 Equivalent wind speed and turbulence

The effects of turbulence intensity on the power curve cannot be taken into account with a simple definition of equivalent wind speed similar to the one used to account for the shear [2]. Albers suggested a method aiming at representing the non linear relation between the 10 minute mean power and the 10 minute mean wind speed [1]. This method is based on the fact that the 10 minute average of the power is not linearly related to the mean wind speed but to the wind speed distribution during the considered 10 minute and the shape of the power curve.

4.4 Description of Albers' method

The model is based on the assumption that the wind turbine follows the same power curve at each instant. This power curve is the curve that should be theoretically obtained with 0% turbulence intensity. According to this assumption, the power output of the turbine for any turbulence intensity can be simulated by:

$$P_{sim}(v,TI)=\int_{v=0}^{\infty} P_{0\%}(v)\, f(v)\, dv \qquad (4.1)$$

where $P_{0\%}(v)$ is the power given by the 0%-TI power curve for the wind speed v, and f(v) is the wind speed distribution within the 10 minutes. This distribution is assumed to be Gaussian, denoted by $f(v)=N(v,\sigma^2)$, it only depends on the 10 minute wind speed average, v, and variance, σ^2. The variance here is given by $\sigma^2 = v^2 \times TI^2$. Albers' method therefore consists of 2 steps:
The estimation of the 0%-TI power curve;
The simulation of the power curve for a chosen turbulence intensity: TI_{target}.

Step1: definition of the 0%TI power curve
The 0%-TI power curve is derived from a few parameters characteristic of the turbine: the rated power, the cut-in wind speed and the maximum C_P [1]. The values taken for these parameters are tuned with an iterative process in order to minimize the error between the simulated mean power curve and the measured mean power curve. The simulated mean power curve is the power curve obtained by applying (4.1) to each wind speed bin (i.e. the wind speed bins used to average the power curve as described in the IEC 61400-12-1 standard) statistics: $P_{sim}(v_i, TI_i)$ where v_i is the bin-averaged speed and TI_i is the bin-averaged turbulence intensity in the i^{th} bin.

Step2: Simulation of the power output with TI_{target}
Once the 0%-TI power curve has been determined, each 10 minute measured power output is corrected for the TI_{target} by applying the formula:

$$P^{(10)}_{TI_{target}}(v^{(10)}_{meas}) = P^{(10)}_{sim}(v^{(10)}_{meas}, TI_{target}) + P^{(10)}_{meas} - P_{sim}(v^{(10)}_{meas}, TI^{(10)}_{meas}) \qquad (4.2)$$

where $P^{(10)}_{meas}$ and $v^{(10)}_{meas}$ are the simultaneous measured 10 minute mean power and wind speed and $TI^{(10)}_{meas}$ is the 10 minute measured TI. $P^{(10)}_{sim}(v^{(10)}_{meas}, TI^{(10)}_{means})$ is the power output expected if the assumption that the turbine follows the 0% TI power curve at each instant was true. But there is actually a difference between the actual power output and the simulated power output as the power curve is influenced by other parameters than the turbulence intensity such as the speed shear for example. Albers' method can only reduce the scatter due to the distribution of the turbulence intensity during the power curve measurement. Figure 4.2 shows the measured power curve scatter plot, the simulated power curve for $TI_{target}=10\%$ and the predicted power curve scatter plot for $TI_{target}=10\%$

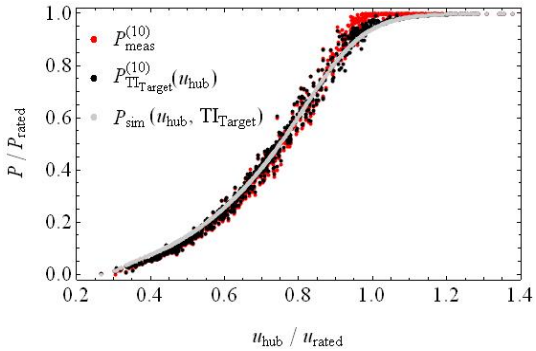

Figure 4.2 *Measured power curve scatter plot ($P^{(10)}_{meas}$), simulated power output for $TI_{target} = 10\%$ ($P^{(10)}_{sim}(v^{(10)}_{meas}, TI_{target})$), resulting simulated power curve scatter plot ($P^{(10)}_{TI_{target}}$).*

4.5 Combination with the equivalent wind speed

Albers' method was designed to normalize the standard power curve to a chosen TI: TI_{target}. On the other hand, the equivalent wind speed method "normalizes" the power curve for the effect of shear, the combination of these two methods would result in a power curve less sensitive to the wind characteristics, and therefore less dependent on the site and season.

The turbulence normalisation changes the power value whereas the equivalent wind speed method changes the wind speed. It is therefore quite simple to combine both method in order to obtain a power curve less sensitive to shear and turbulence intensity.

Albers' method was initially designed to normalize the standard power curve, i.e. based on wind speed measurements at hub height, for the turbulence intensity. In order to compare the results to those obtained by combining Albers' method with the equivalent wind speed, the turbulence normalisation was applied to both power curves: with hub height wind speed and with equivalent wind speed. Therefore for a given TI_{target} value, four results can be compared:

	Measured power	Normalized power
u_{hub}	Standard power curve	Alber's method
U_{eq}	Equivalent wind speed power curve	Combined method

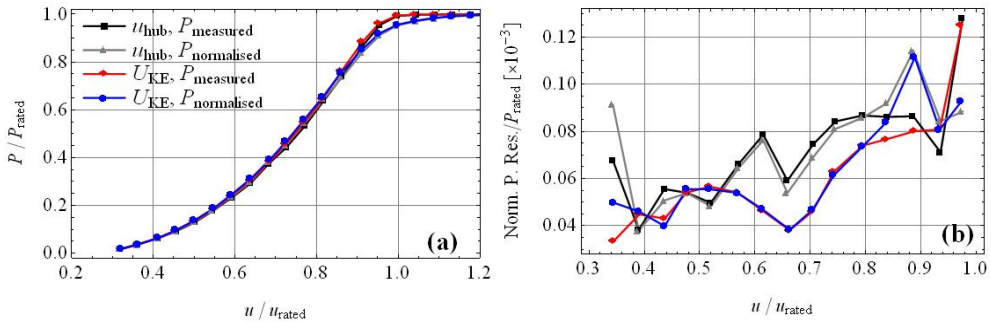

Figure 4.3 *Mean power curve and scatter in the power curve obtained with wind speed measurements at hub height and equivalent wind speed, both with and without turbulence normalization using Albers' method*

The power curve obtained by combining both the equivalent wind speed and Alber's turbulence normalization presents both a modification of the shape of the mean power curve (due to the different TI) and a reduction of the scatter around the mean power curve (scatter due to the shear).

4.6 Conclusions

The equivalent wind speed method reduces scatter due to shear also when the power has been normalized for the turbulence intensity according to Albers' method for turbulence normalization, except near rated speed where the mean power curve slope is significantly changed.
The mean power curve obtained with the combination of both methods is less sensitive to shear and is representative for a given TI. Such a power curve can give a better representation of the power curve that would be obtained at another site, with different wind shears and turbulence intensities from the power curve measurement site. In this sense, it is transferable from one site to another. Therefore it would give a better Annual Energy Production (AEP) estimation.

4.7 References

[1] Kaiser K, Hohlen H, Langreder W, *Turbulence correction for power curves*, EWEC 2008

[2] Albers A, *Turbulence normalisation of wind turbine power curve data*, EWEC 2010

[3] Wagner R, *Accounting for the speed shear in wind turbine power performance measurement*, PhD thesis (chapters 4 and 9), 2010.

5. Improvements in power performance measurement techniques

Jan Willem Wagenaar and Peter Eecen

This part of the report focuses on the analyses of the largest sources of uncertainties in power performance testing. The work is directly relevant for work being performed in the context of the IEC61400-12-1 and MEASNET [1]. It is known that the power performance of a wind turbine depends on atmospheric conditions as for instance the air density. The IEC regulations for power performance [2] already include an air density correction. Besides that it is also known that other atmospheric conditions play a role as well, such as turbulence and wind shear, which was already noticed in [3]. Other authors notice this dependence as well, such as for instance [4] [5] [6] [7]. Corrections for turbulence and wind shear have been suggested and have been shown to be effective.

We examine the power performance of a 2.5MW ECN research turbine on the ECN test field on those atmospheric conditions. A site description is give together with a description of necessary data selection. The dependence of the power performance on the air density, stability, turbulence and vertical wind shear is examined in subsequent sections.

5.1 EWTW and Data taking

ECN has made available the 'ECN Wind Turbine test station Wieringermeer' (EWTW) since the end of 2002. A site description is given in section 5.1.1. Data selection and correction procedures are described in section 5.1.2.

5.1.1 Site description

The EWTW is located in the North East of the province North Holland, 3 km North of the town Medemblik and 35 km East of ECN Petten. It consists of research turbines, prototype turbines and scaled wind turbines, all accompanied with meteorological masts. For this work the research turbines (green squares) and the nearby meteorological mast (meteo mast 3) are of interest and are indicated in Figure 5.1.

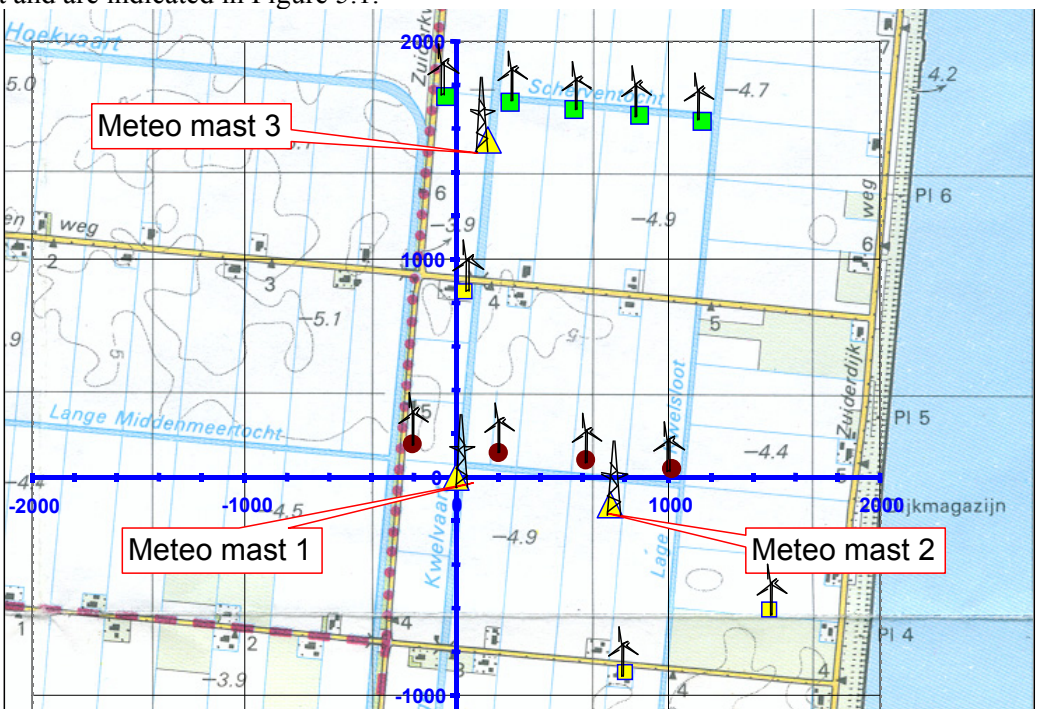

Figure 5.1 *Map of EWTW*

The surroundings of the test site are characterized by flat terrain, consisting of mainly agricultural area, with single farmhouses and rows of trees. The lake “IJsselmeer” is located at a distance of 1 to 2 km East. For more details see [8].

The 5 research turbines, named T5 – T9 (West to East), are 2.5MW ECN research turbines with a rotor diameter (D) of 80m, a hub height (H) of 80m and a rated power of 2.5MW. The nearby meteorological mast measures, among others, the wind speed and direction at 52m, 80m and 108m, pressure, temperature and temperature difference. A detailed description of the mast can be found in [8]. From now on, if not mentioned differently, the wind speed and direction always refers to the wind speed and direction at 80m.

All data taken from the turbines and the meteorological mast are stored in the “Long Term Validation Measurements” (LTVM) database [9] of the Wind Data Management System (WDMS) [10]. This database structure ensures high quality data. Data has been taken from September 2004 until April 2010, which makes it possible to analyse a large amount of data.

5.1.2 IEC Standards and data selection

To perform power performance measurements the IEC 61400-12-1 regulations [2] have been followed, where possible. The distance of turbines T5 and T6 to the meteorological mast is such (3.5D and 2.5D, respectively) that these turbines only are close enough to the meteorological mast for power performance measurements. In this work T6 is considered. An undisturbed wind sector is identified by choosing wind directions between 347° - 354°, 126° - 133° and 212° - 244°.

Besides the wind direction selection, other obviously erroneous data points are neglected as well.

For the entire period of about 6 years of data taking, the power curve of turbine T6 is constructed and depicted in the upper plot of Figure 5.2. Here, the scatter data as well as the binned values are shown. The lower plot shows the AEP against the reference wind speed. We note that the scatter plot in Figure 5.2 has 3 tails (15-20 m/s), which influences the standard deviation of the “method of bins”. In the remainder different (sub) data sets will be considered and the distribution of the data points for wind speeds above 15m/s over the three ‘tails’ may be different from one situation to another. This influences the power and the standard deviation of the power. Therefore, when comparing the power or the standard deviations of the power, wind speeds above 15m/s are not considered in this chapter.

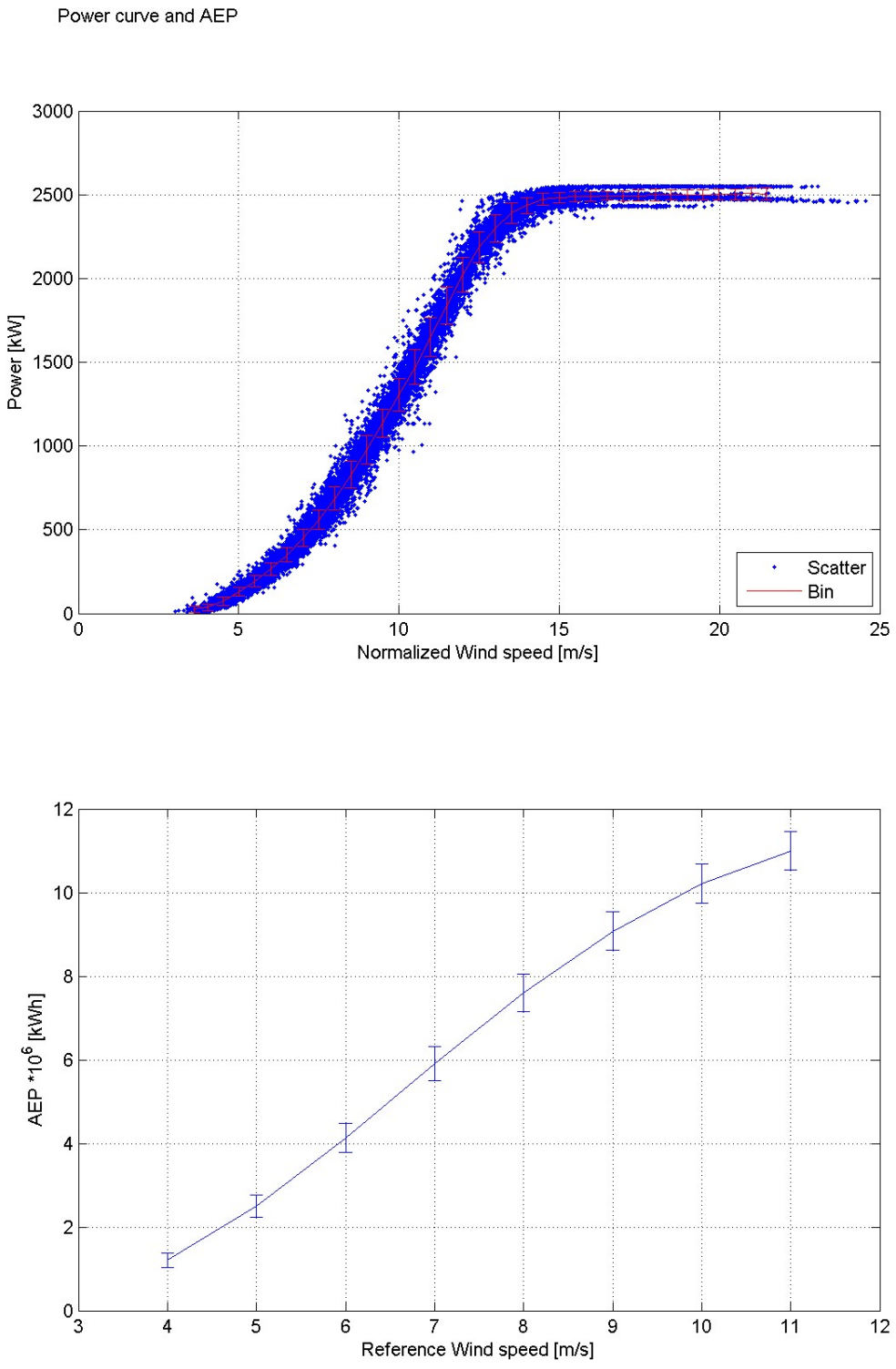

Figure 5.2 *Scatter plot (blue) and IEC "method of bins" (red) of power against normalized wind speed (upper plot). The lower plot contains the AEP as function of the reference wind speed.*

5.2 Atmospheric conditions

In this section the dependence of the power curve on atmospheric conditions as air density, temperature, stability, turbulence and wind shear is examined. Possible cross correlations are also studied.

5.2.1 Air density

The power that a turbine can extract from a volume of wind is [11]

$$P = \frac{1}{2} \cdot c_p \cdot A \cdot \rho \cdot U^3 \quad , \qquad (5.1)$$

where U is the horizontal wind speed, A is the rotor swept area, ρ is the air density and c_p is the power coefficient. P is the power. Clearly, the power depends on the air density and therefore also the power curve. In this section we want to see to what extend the power curve depends on the air density.

Before studying this effect of air density Figure 5.3 shows the distribution of the encountered air density values[1]. It is noticed that most values lay between 1.20 kg/m^3 and 1.27 kg/m^3. The mean value is 1.237 kg/m^3.

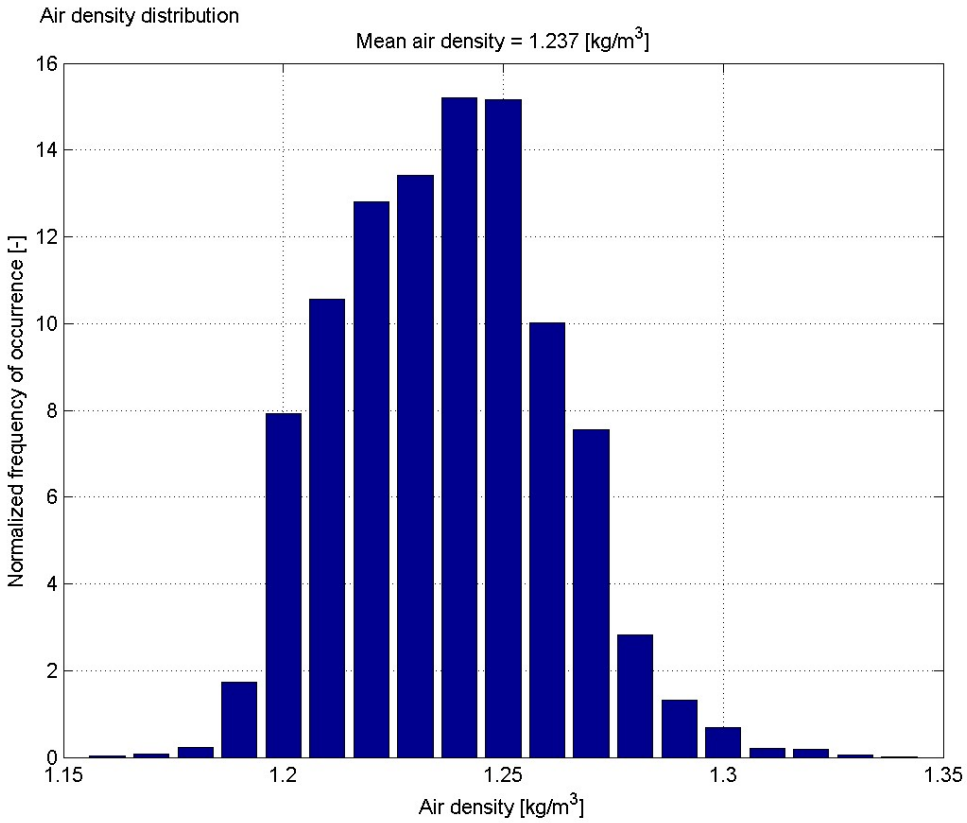

Figure 5.3 *Distribution of the air density.*

[1] The air density distribution is extracted from the same data set as used for the power performance. This will also be valid for the distributions of other atmospheric quantities.

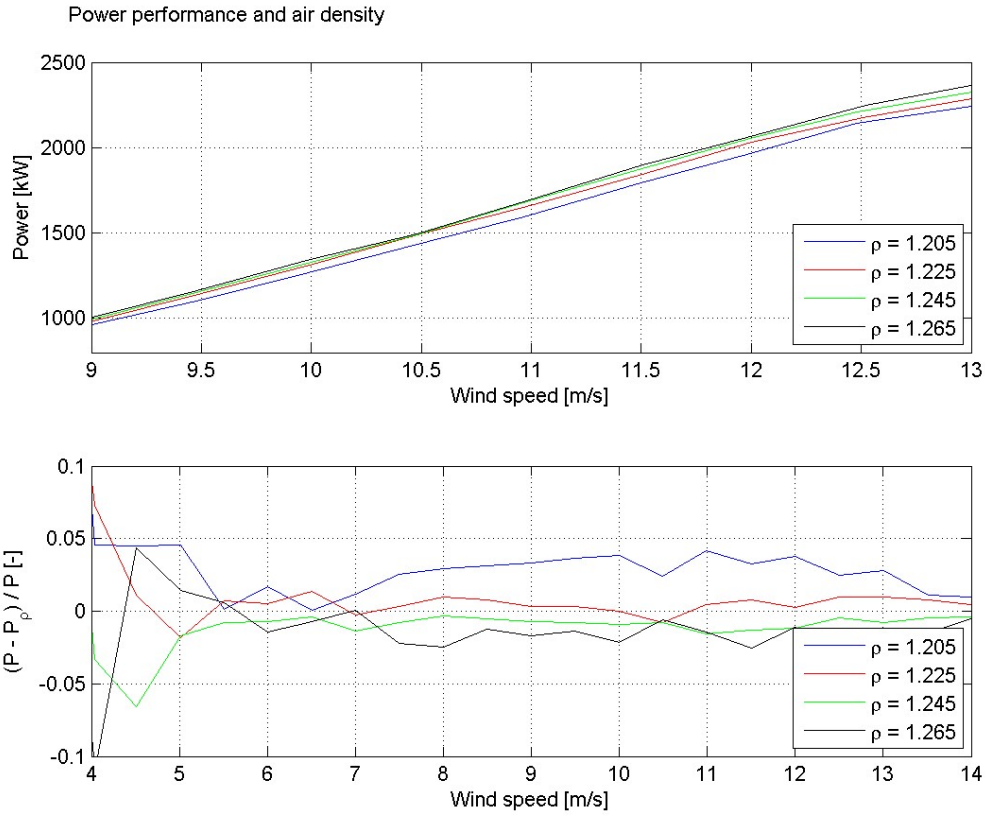

Figure 5.4 *Power as function of the (not normalized) wind speed for various values of the air density (upper plot). Difference between the power for all values of the air density and the power for various values of the air density as function of the (not normalized) wind speed (lower plot).*

Power curves for various values of the air density are shown in the upper plot of Figure 5.4. They can clearly be distinguished. The lower plot shows the difference between the power for all values of the air density and the power for various values of the air density. The maximum difference occurs for the power curve for ρ=1.205 kg/m^3. This difference is at most 4% for (not normalized) wind speeds above 5m/s.

Also for different values of temperature power curves can be distinguished. However, because the air density is calculated from temperature (and pressure) measurements, it is obvious that the two are related. This is also reflected in the power curves.

5.2.2 Stability

The stability of the atmosphere is determined by means of the environmental lapse rate:

$$-dT/dh < 6K/km \quad = \text{ stable atmospheric conditions}$$
$$6K/km < -dT/dh < 10K/km \quad = \text{ conditionally unstable atmospheric conditions}$$
$$-dT/dh > 10K/km \quad = \text{ unstable atmospheric conditions,}$$

where T is the temperature and h is the height. Here, the lapse rate is determined using the temperature difference instrument, which measures the temperature difference between a height of 37m and 10m. The distribution of the stability is exposed in Figure 5.5. It is clearly seen that unstable conditions happen the most during daytime and during summer. For stable conditions the opposite is valid.

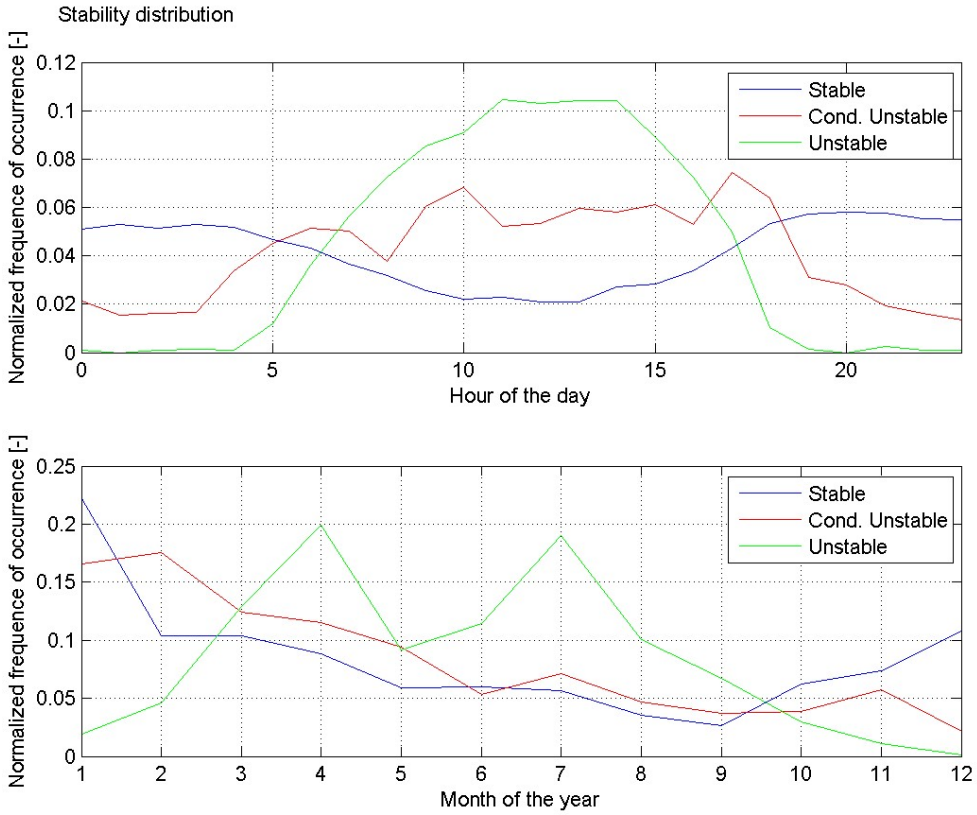

Figure 5.5 *Normalized frequency of occurrence of different stability conditions as function of the hour of the day (upper plot) and as function of the month of the year (lower plot).*

Within the considered period stable conditions occur the most: the number of data points with stable conditions is about 7 times higher than the number of data points with conditionally stable or unstable conditions.

The power curves for stable, unstable and all atmospheric conditions are given in Figure 5.6, as are the relative differences and the relative differences in the standard deviation. For wind speeds above, say, 6m/s the difference between the power for all atmospheric conditions and stable conditions and the between the power curve all atmospheric conditions and unstable conditions is lower than about 4%.

More interesting are the differences in the standard deviation of the power. Again we consider the wind speed range 4m/s – 13m/s. We see that the standard deviation for unstable conditions is up to 50% larger than the standard deviation for all conditions. Furthermore the standard deviation for stable conditions is smaller (~10%) than the standard deviation for all conditions.

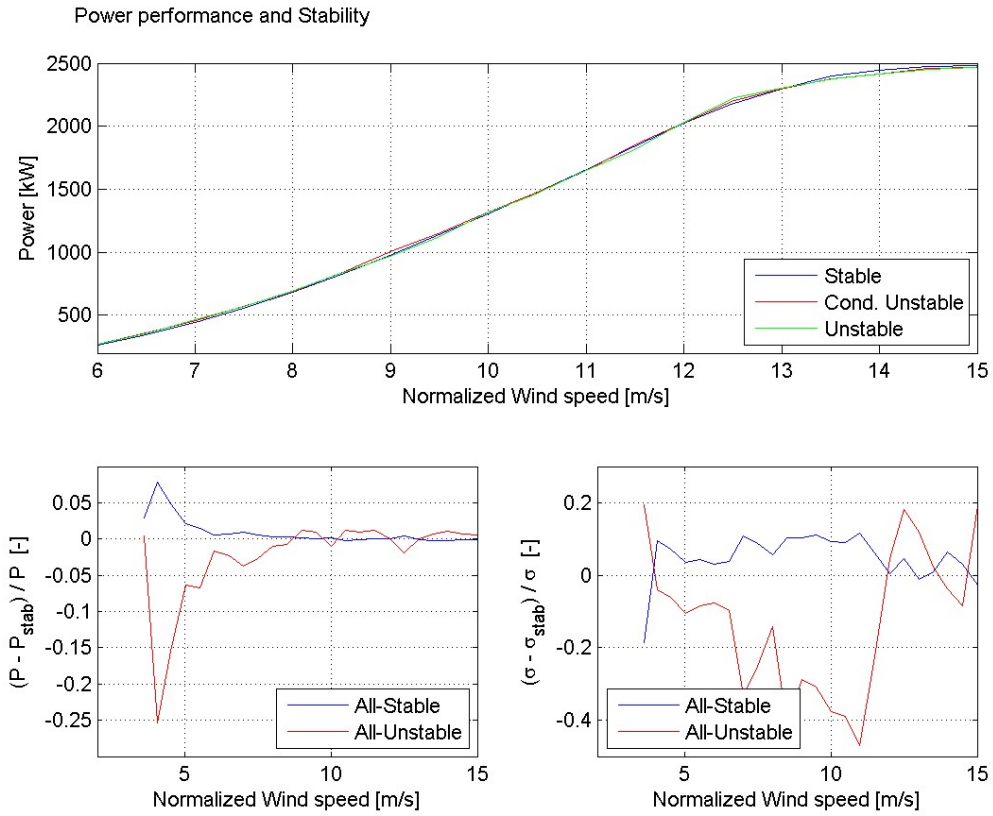

Figure 5.6 *Power curve (upper plot) for different stability conditions. Relative difference in power (lower left plot) between all and stable conditions (blue) and between all and unstable conditions (red). Relative difference in standard deviation (lower right plot) between all and stable conditions (blue) and between all and unstable conditions (red).*

5.2.3 Turbulence

The turbulence intensity is defined as [3]

$$TI = \frac{\sigma_U}{U} \quad , \qquad (5.2)$$

where σ_U is the standard deviation of the wind speed. We note here that occasionally the turbulence intensity is exposed as a percentage. In that case (5.2) is multiplied with 100.

In Figure 5.7 the distribution of the turbulence intensity (in percentage) is given. It is seen that most values are between 2% and 12% and the mean is 8.1%. It is also seen that the TI is somewhat higher during daytime.

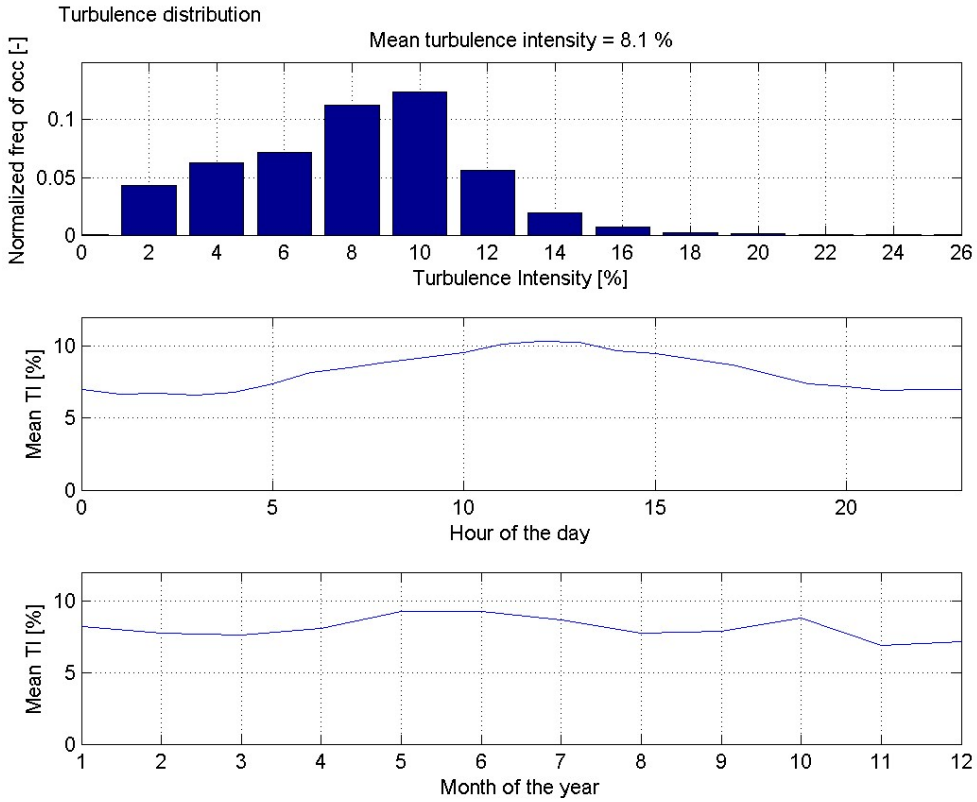

Figure 5.7 *Normalized frequency of occurrence of the turbulence intensity (upper plot). Normalized frequency of occurrence of the turbulence intensity as function of the hour of the day (middle plot). Normalized frequency of occurrence of the turbulence intensity as function of the month of the year (lower plot).*

The power curve for different turbulence intensity classes is given in Figure 5.8, as are the relative differences and the relative differences in the standard deviation. As noticed before [12] we see that for low wind speeds (4m/s-10m/s) high TI classes yield the most power and for high wind (12m/s-14m/s) speeds low TI classes yield the most power. Also, differences in the standard deviations of the power are clearly seen. In the wind speed range 6m/s – 13m/s we see that the standard deviation of certain turbulence intensity classes (4%-6% and 12%-14%) differ up to about 50% with the standard deviation for all turbulence intensities. Furthermore, it is noticed that the standard deviation of the power for high turbulence intensities is larger than the standard deviation of the power for all turbulence intensities up to wind speeds of 10m/s. For low turbulence intensities the opposite is valid.

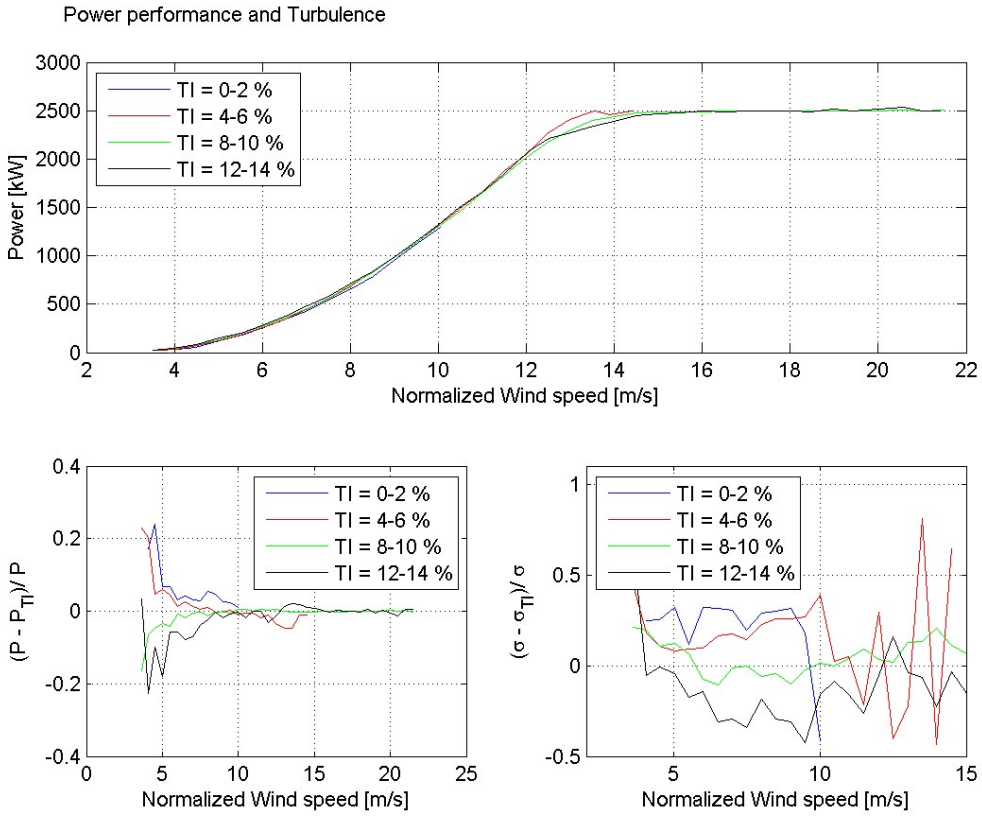

Figure 5.8 *Power curve (upper plot) for different turbulence intensity classes. Relative differences in power (lower left plot) between all and various TI classes. Relative difference in standard deviation (lower right plot) between all and various TI classes.*

5.2.4 Vertical wind shear

The horizontal wind speed varies with height. Since the horizontal wind speed is measured on the meteorological mast at 3 different heights, namely at 52m, at 80m (hub height) and 108m, this vertical wind shear can be measured.

In Figure 5.9 the (horizontal) normalized wind speeds are given for the various heights. Here, the wind speeds are normalized to 9.5m/s at 80m. Specification of this vertical wind shear is given with respect to the hour of the day and the month of the year. It is clearly seen that the wind shear is highest for around midnight and winter period.

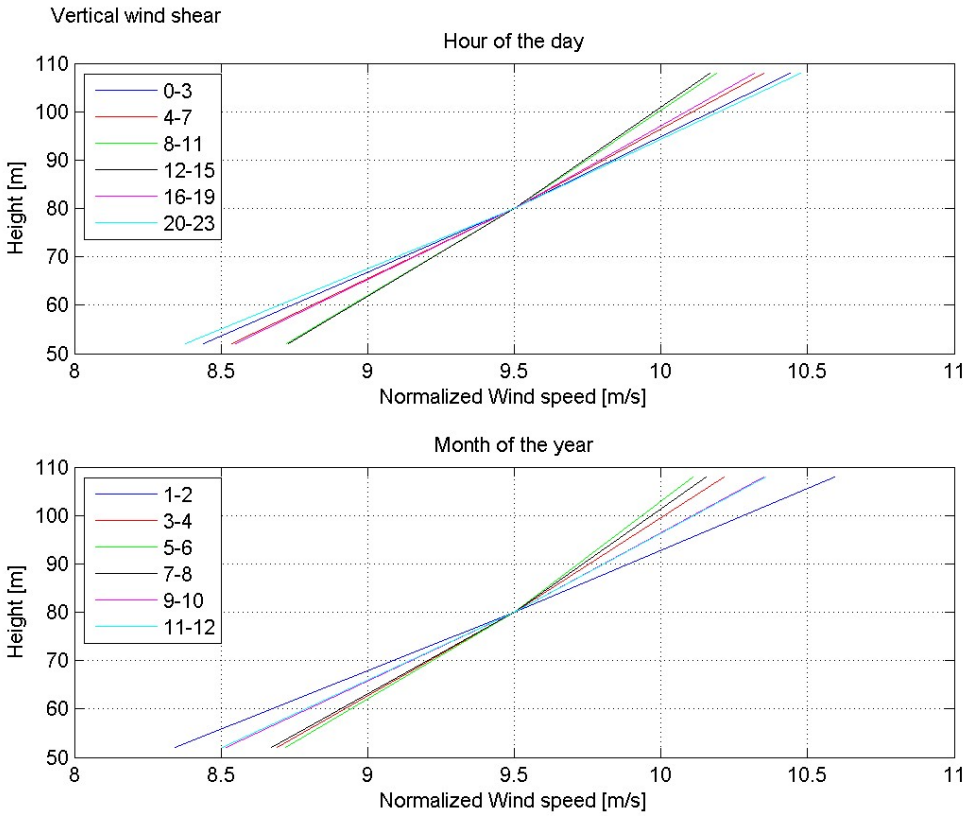

Figure 5.9 *Normalized (horizontal) wind speed as function of height. Specification is made with respect to the hour of the day (upper plot) and the month of the year (lower plot). The wind speeds are normalized to 9.5m/s at 80m.*

Power law profile

The vertical wind shear can be quantified by assuming a power law profile [11]:

$$U(z) = U(z_r) \cdot \left(\frac{z}{z_r} \right)^{\alpha}, \qquad (5.3)$$

where U(z) is the horizontal wind speed at height z. The subscript r indicates the reference height and α is a dimensionless constant.

Because the horizontal wind speed is measured at three different heights, two α exponents are determined: α_1 for the heights 108m and 80m and α_2 for the heights 80m and 52m. Both α exponents are distributed over bins of 0.1 wide. Those cases are considered where both α exponents are in the same bin. In 1/3 of all possibilities the wind shear shows a profile as assumed in (5.3).

The distribution of the α parameter is shown in Figure 5.10. It is noticed that most values are within α=0.1 and α=0.4. The mean value is α=0.3.

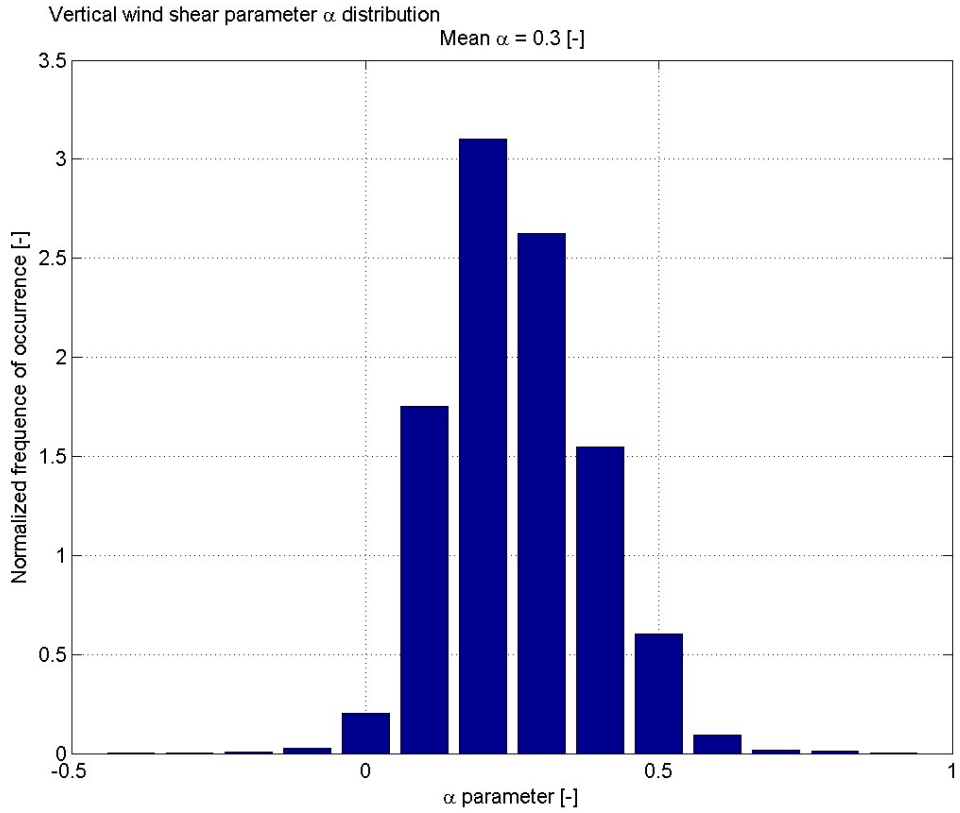

Figure 5.10*Distribution of the α parameter.*

In Figure 5.11 the power curves for different values of α are shown. Also shown are the relative differences with the power curve for all α as well as the relative difference of the standard deviation for various values of α with those for all α.

The differences between the various power curves are relatively small; the differences of the power curves for different values of α with the power curve for all values of α are a few percent. However, differences in the standard deviation of the power are clearly seen. In the wind speed range, say, 5m/s – 13m/s the standard deviation of the power for different values of α differs up to about 30% with the standard deviation of the power for all values of α. It is also seen in this same wind speed range that the standard deviation for a low values of α (α=0.1) is larger than the standard deviation for all values of α and the standard deviation for a higher value of α (α=0.3, 0.5) is smaller.

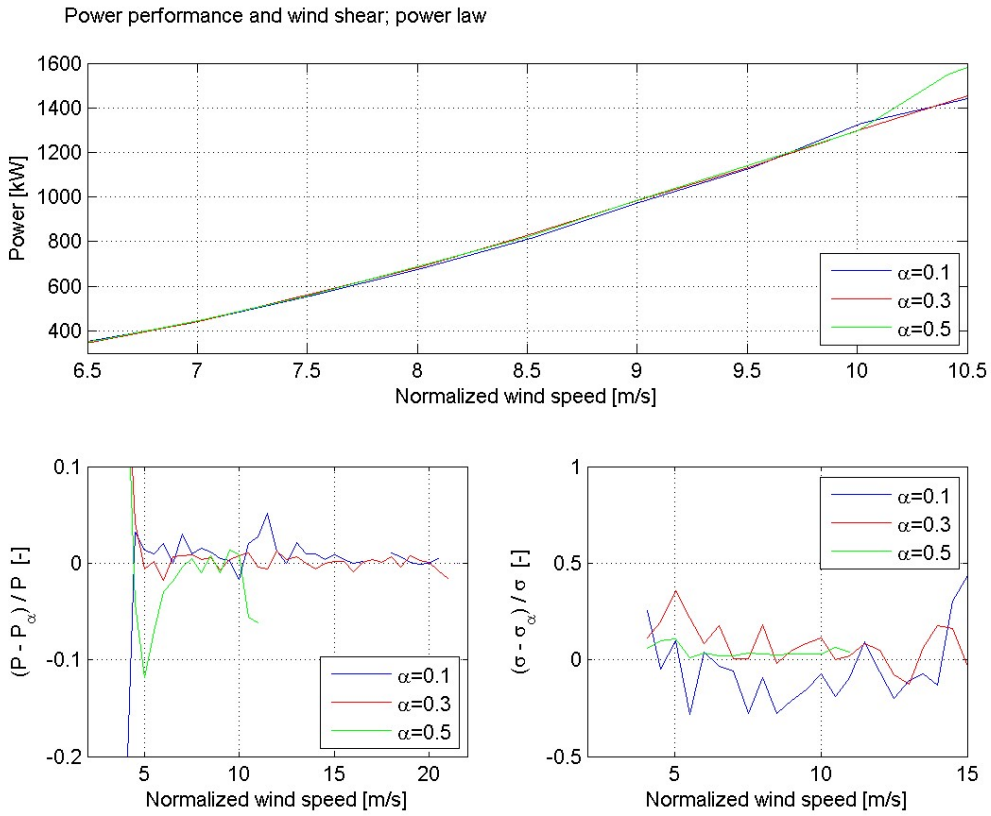

Figure 5.11 *Power for different values of α (upper plot), relative difference in power (lower left plot) between all and various values of α and relative difference in σ of power (lower right plot) between all and various values of α as function of the normalized wind speed.*

Linear profile

Here, the vertical wind shear is quantified by assuming a linear profile:

$$U(z) = U(z_r) + \beta \cdot \frac{z - z_r}{R}, \qquad (5.4)$$

Where β is the coefficient determining the steepness of the linear profile. All other symbols are as before. The inclusion of the rotor radius R is to make the parameter β have the same dimension as the wind speed (m/s).

Again, two β coefficients can be determined based on measurements at three different heights. Both β coefficients are distributed over bins of 0.1 wide. Those cases are considered where both coefficients are in the same bin. In 40% of all possibilities the wind shear shows a profile as assumed in (5.4).

The distribution of the β coefficient is shown in Figure 5.12. It is noticed that most values are within β=0.5m/s and β=2m/s. The mean value is β=1.25m/s.

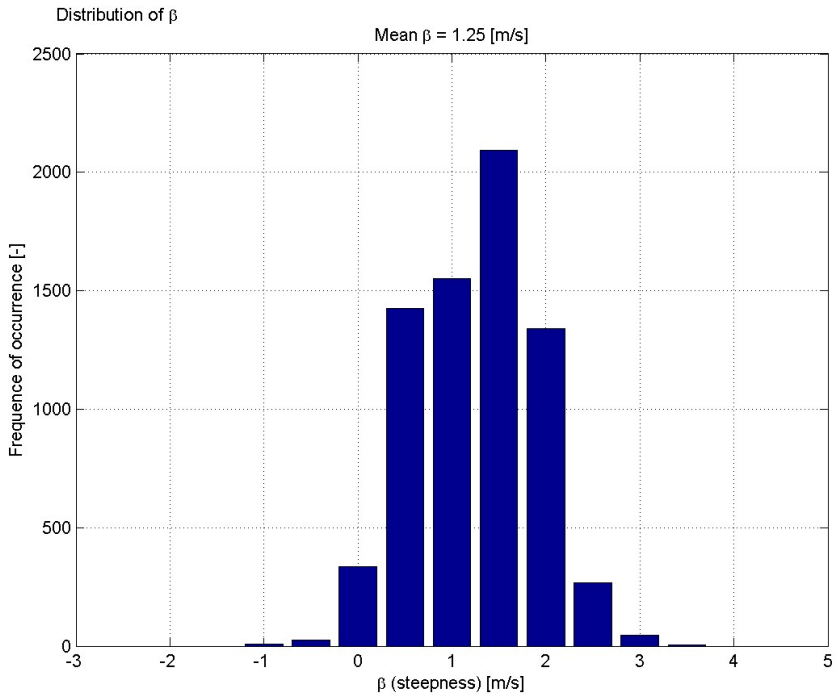

Figure 5.12*Distribution of the β parameter.*

In Figure 5.13 the power curves and the standard deviation of the power for different values of β are shown. Also shown are the relative differences with the power curve for all β as well as the relative difference of the standard deviation for various values of β with those for all β.

It is seen that the power for β values of 1m/s-2m/s is at most about 10% larger at a wind speed of 5m/s with respect to the power for all values of β. Furthermore, it is seen that the standard deviation of the power for lower values of β (0.5m/s-1m/s) is up to 50% higher than the standard deviation for all values of β. For higher values of β the standard deviation is lower than the standard deviation for all values of β.

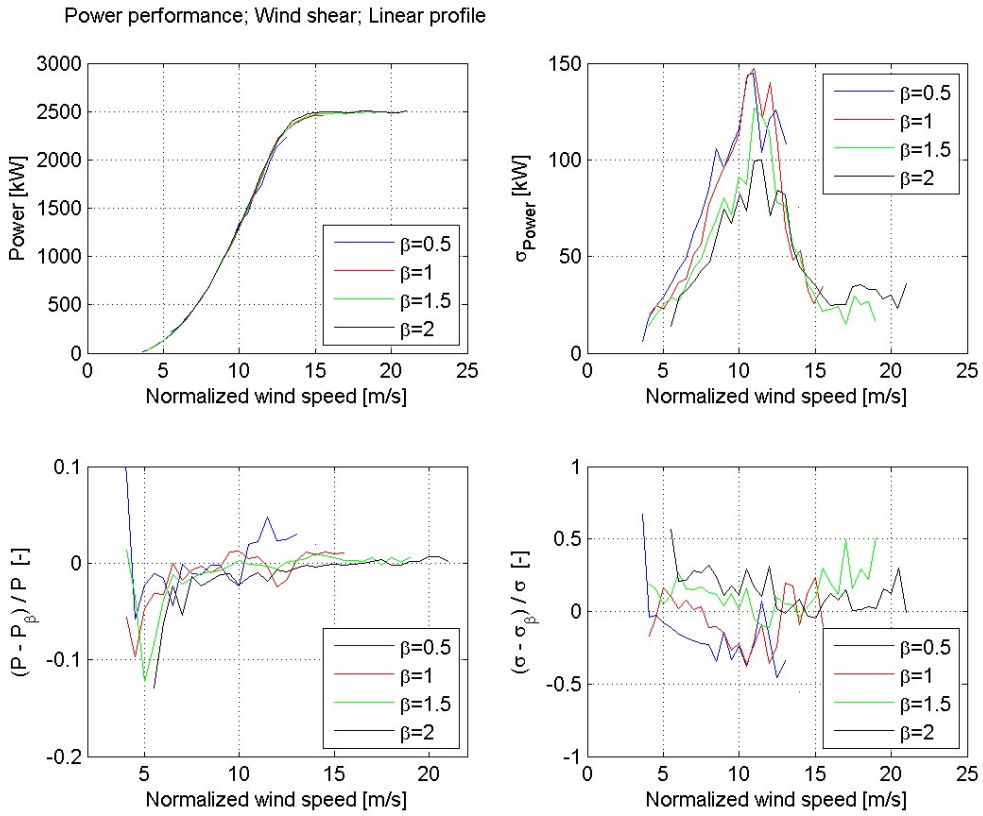

Figure 5.13 *Power (upper left plot) and σ of power (upper right plot) for different values of β, relative difference in power (lower left plot) between all and various values of β and relative difference in σ of power (lower right plot) between all and various values of β as function of the normalized wind speed.*

5.2.5 Cross correlations

Although stability, turbulence and vertical wind shear are treated separately in the foregoing, it may be expected that these phenomena are correlated. Therefore, Figure 5.14 shows the distribution of the α parameter for different stability conditions and for different TI classes. Also shown are the vertical wind speed profiles for different stability conditions and for different TI classes. The β parameter is not considered in this analysis of correlation.

From the distribution of α for different stability conditions it is clearly seen that the value of α that occurs the most for unstable conditions is α=0.1. For stable conditions this is α=0.3. It is also seen that the distribution of α for unstable conditions is sharper then for stable conditions. From the distribution of α for different turbulence intensities a sharp distribution of α is seen for high TI, centred around α=0.1. The value of the α parameter that occurs the most for low TI is α=0.4. These phenomena are explained by the fact that for unstable conditions and high turbulence different layers of air mix, which increases the correlation of the horizontal wind speeds at different heights. This decreases the value of α and broadens the distribution. For a value of α=0 all horizontal wind speeds at different heights are the same.

This mixing of air layers is also reflected in the vertical wind shear profiles (lower plots of Figure 5.14), where a low wind shears are seen for unstable conditions and high turbulence.

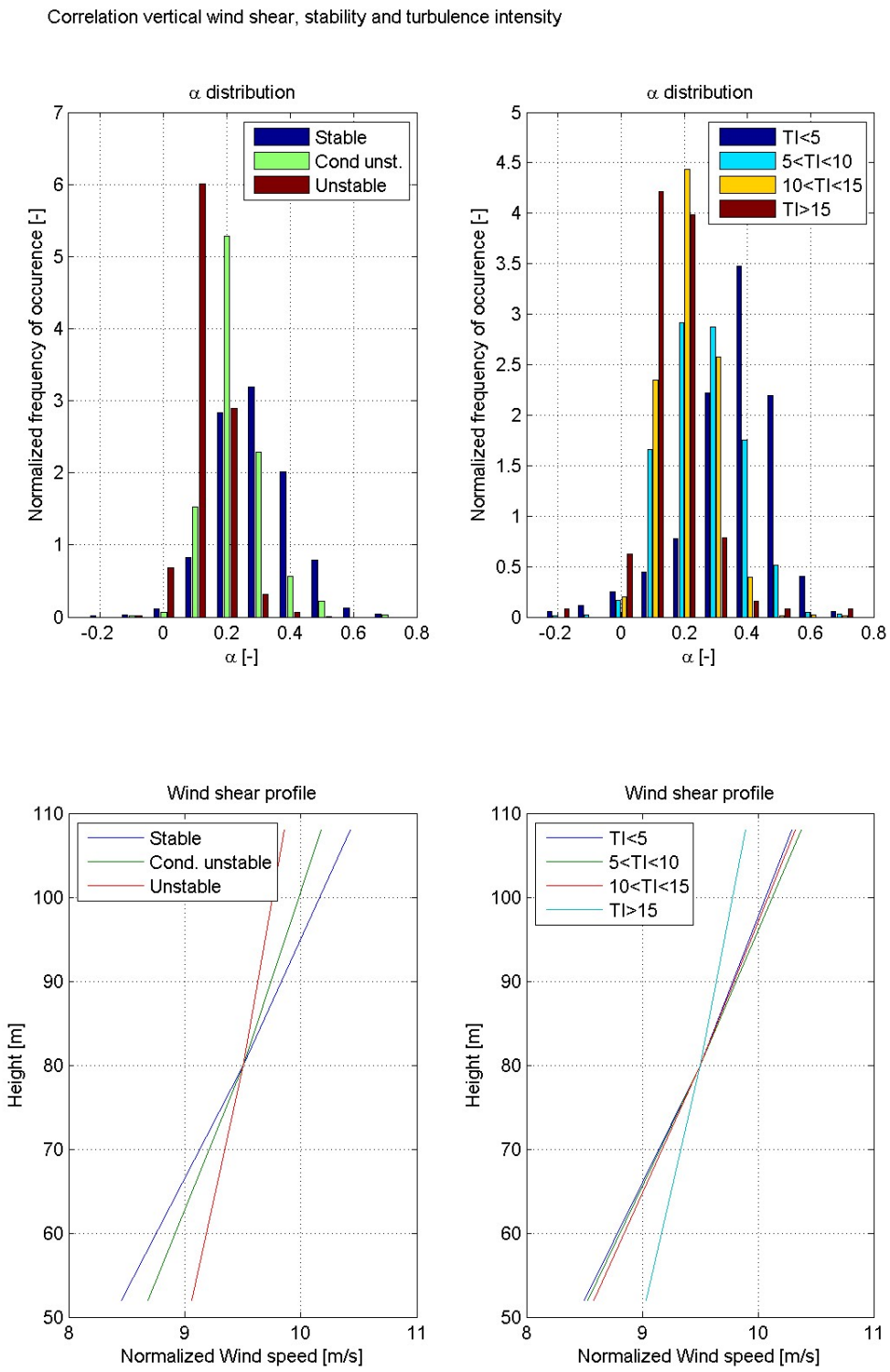

Figure 5.14 *Distribution of α for different stability conditions (upper left plot) and different TI (upper right plot). Wind shear profiles for different stability conditions (lower left plot) and different TI (lower right plot).*

5.3 Power Curve Corrections

In the previous section we have shown that the power curve depends on different atmospheric conditions as stability, turbulence and wind shear. In this section we study correction of these effects on the power curve. We have not found a correction with respect to stability, however, as we have shown, stability is correlated to turbulence and wind shear. Therefore we study correction with respect to turbulence and wind shear, only.

5.3.1 Air density

Because the turbine is a pitch-regulated machine an air density correction is performed on the wind speed

$$U_{norm} = U \cdot \left(\frac{\rho}{\rho_0} \right)^{1/3} . \qquad (5.5)$$

Here, U is the measured wind speed. ρ is the air density, derived from pressure and temperature measurements ([2]) and ρ_0 is the reference air density.

The effect of the normalization is depicted in Figure 5.15. The upper plots show power curves for different values of the air density, where the left plots is before and the right plot is after correction. From the upper left plot clear differences in the power curves are seen for different values of the air density. It is also clear from the upper right plot that the corrected power curves for different values of the air density are closer together. The wind speed range 9m/s – 14m/s is shown, because in this range the effect is best seen. It is concluded that the dependence of the power curve on the air density is reduced by using (5.5).

This point is further illustrated in the lower plots of Figure 5.15. The left plot shows the relative difference in normalized and unnormalized power. The difference is at most 2% -3%. More importantly the lower right plot shows the relative difference in the standard deviation of the power. It is clearly seen that the standard deviation is reduced by means of the correction (5.5) in the wind speed range 4m/s – 13m/s. In this range the cubic dependence of the power on the wind speed is most pronounced and (5.5) is here most effective. A reduction of the standard deviation of about 9% is seen.

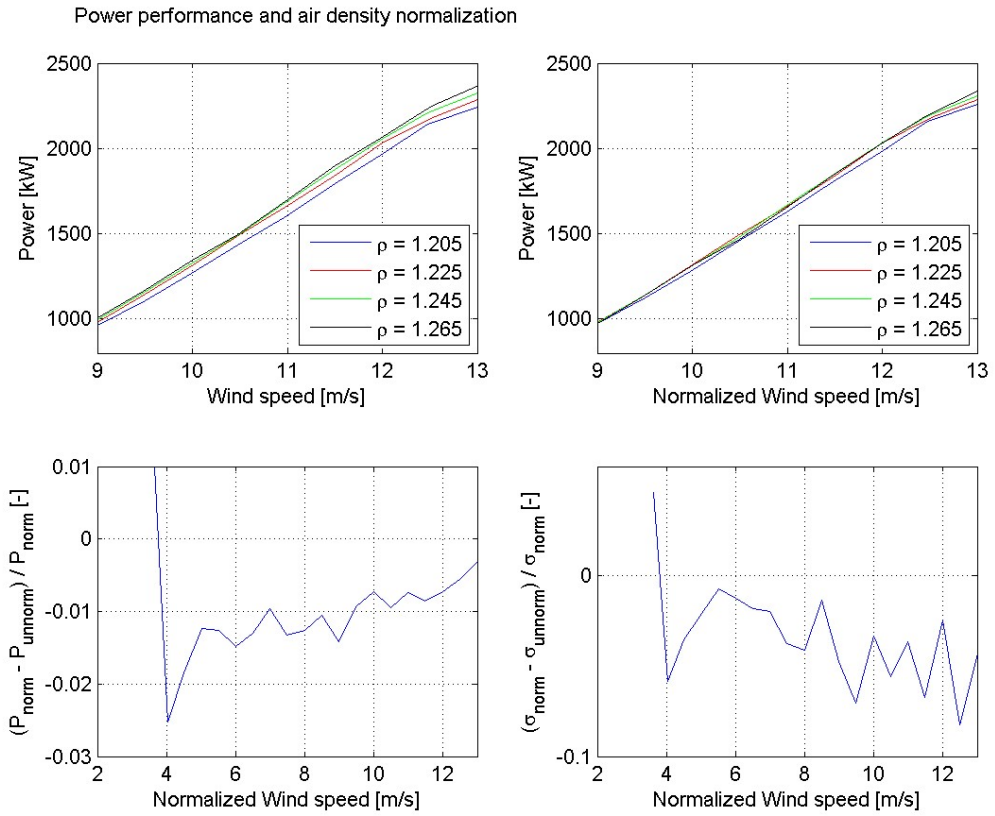

Figure 5.15 *Power curves for different values of the air density before (upper left plot) and after (upper right plot) air density correction. Relative difference in normalized and unnormalized power as function of the normalized wind speed (lower left plot). Relative difference in normalized and unnormalized standard deviation of the power as function of the normalized wind speed (lower right plot).*

As mentioned before temperature and air density are correlated. Therefore air density correction is implicitly also temperature correction. It is indeed observed that the air density correction is also effective for reducing the dependence of the power curve on the temperature. Nevertheless, a small influence of the temperature on the power curve remains, as is the case for the air density.

5.3.2 Turbulence

1D Turbulence

In (2) it is shown that the power depends cubically on the wind speed. Implicitly, the third power of the averaged wind speed was considered. However, the average of the power depends on the average of the cubed wind speed. It can be shown [6] that in this way a correction factor is added or, equivalently, a corrected wind speed is defined

$$U_{corr} = U_{norm} \cdot \left(1 + 3 \cdot \left(\frac{\sigma_U}{U} \right)^2 \right)^{1/3} . \qquad (5.6)$$

Here, σ_U/U is the TI (5.2).

The turbulence corrected power is shown in Figure 5.16 for different values of TI. Also shown is the uncorrected power for different values of TI (as in Figure 5.8) for comparison. The various curves are in the corrected case somewhat closer together with respect to the uncorrected case. This is made more quantitative in the relative difference in the standard deviation of the power before and after the correction. Here, the standard deviation of the corrected power is for almost all wind speeds in the range up to 12m/s lower than the standard deviation of the uncor-

rected power. A reduction up to 9% is seen. The correction (5.6) is based on the cubical dependence of the power on the wind speed. This behaviour is most pronounced in the mentioned wind speed range. Therefore, it is concluded that the turbulence correction (5.6) is effective.

A difference in power is seen up to 7%; above 6m/s this is at most 2%. For almost all wind speeds the corrected power is lower than the uncorrected power. This is caused by the fact that the corrected wind speed is always larger that the uncorrected wind speed.

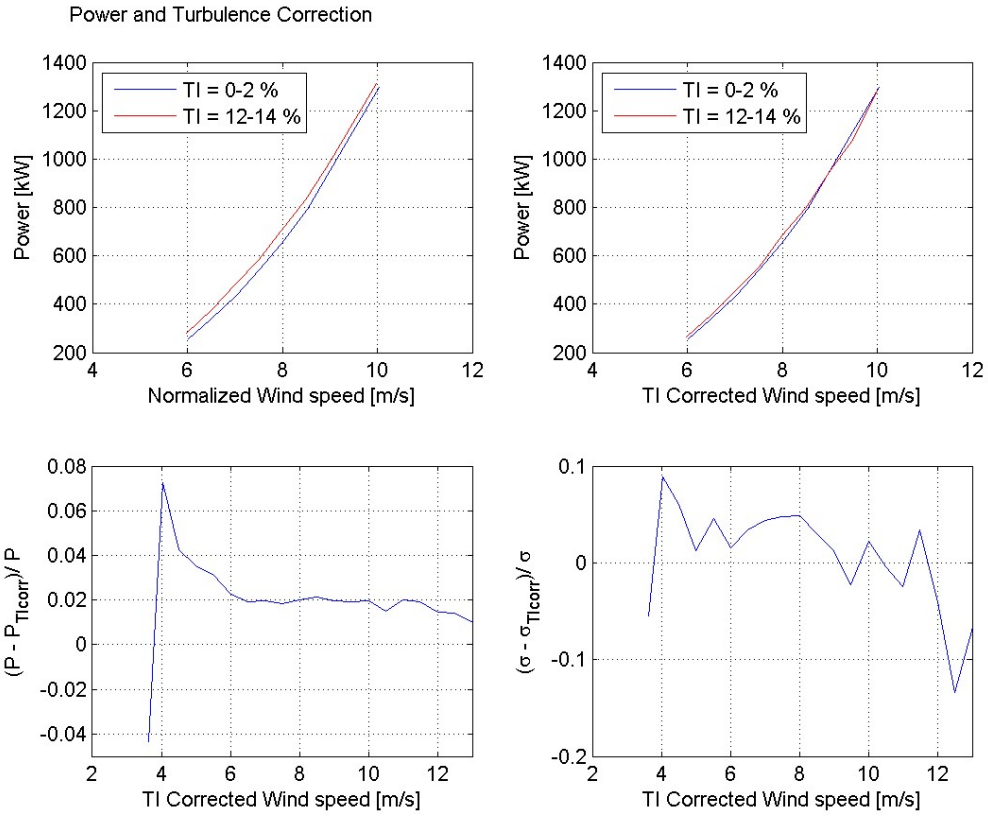

Figure 5.16*Power for different values of TI as function of the normalized wind speed (upper left plot) and the TI corrected wind speed (upper right plot). Relative difference in power (lower left plot) before and after TI correction. Relative difference in σ of power (lower right plot) before and after TI correction.*

3D Turbulence

Taking 3D turbulence into account, it can be shown [4] that a 3D turbulence corrected wind speed is defined as follows

$$U_{corr} = U_{norm} \cdot \left(1 + 5 \cdot \left(\frac{\sigma_U}{U}\right)^2\right)^{1/3} . \qquad (1.7)$$

Here, isotropic turbulence is assumed and yaw misaligned and vertical inflow is neglected.

The relative change in the standard deviation of the power as a result of the correction in (5.7) is shown in Figure 5.17. Below 10m/s a decrease in the standard deviation of the power is seen; an even stronger decrease than was seen in the 1D case. At 4m/s the decrease is 10%. Above 10m/s we see an increase in standard deviation. This increase is even stronger than in the 1D case. It is mentioned that the correction (5.7) is based on the cubic dependence of the power curve on the wind speed. This is in any case not valid above 12m/s.

The relative change in power is at most about 9% and for all cases the corrected power is smaller than the uncorrected power, as was the case in the 1D case. However, in this case the difference is larger, i.e. we see a larger deviation from the uncorrected situation. For wind speeds above 6m/s the change in power is at most 3-4%.

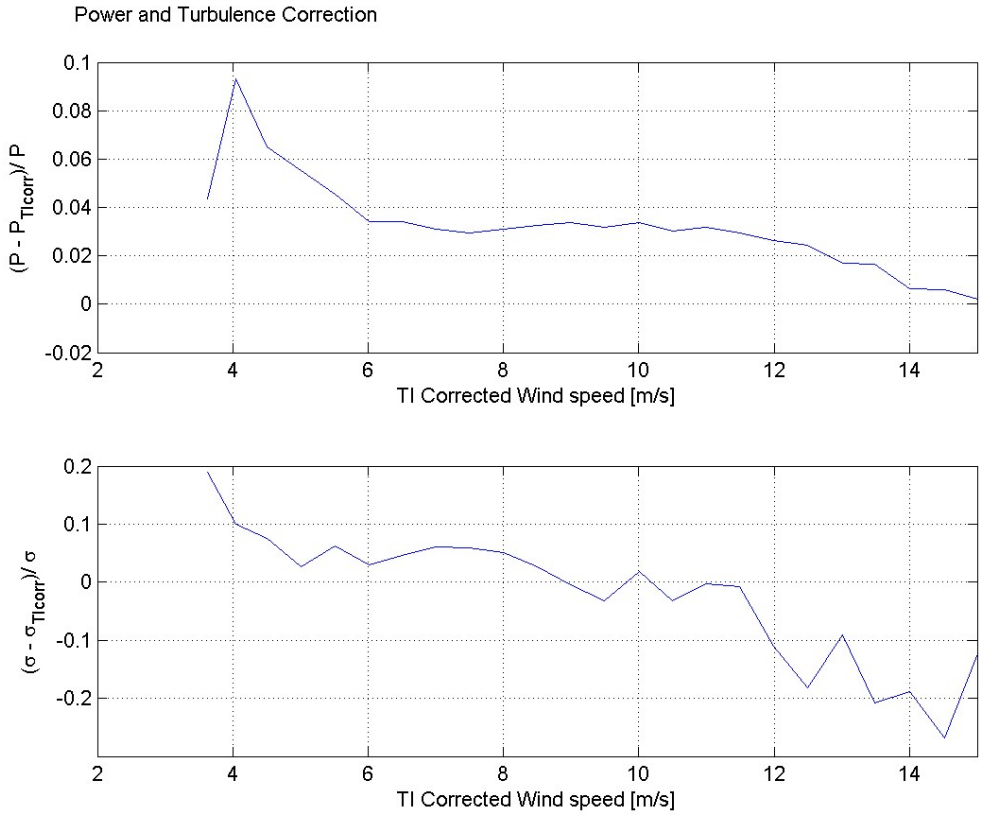

Figure 5.17*Relative difference in standard deviation of power before and after TI correction (6).*

5.3.3 Vertical wind shear: Wind speed corrections

To correct for the wind shear various approaches are considered. The first approach is to directly use the measurements at multiple heights in a redefinition of the wind speed. Other approaches are to determine vertical wind shear profile based on these measurements and to correct the wind speeds according to these profiles. A power law and a linear profile is considered.

Multiple measurements

The measurements at the various heights are used in a redefinition of the wind speed: the so-called rotor averaged wind speed

$$U_{rotor-averaged} = \frac{1}{A}\left(A_{52}\cdot U_{52} + A_{80}\cdot U_{80} + A_{108}\cdot U_{108}\right), \qquad (5.8)$$

Here, U_i (i=52, 80 and 108) is the wind speed at height i. A is the entire rotor swept area and $A_{52,}$ A_{80} and A_{108} are different sections of this area defined by height x

$$A = \pi R^2$$

$$A_{80} = 2\cdot R^2 \cdot \arcsin\left(\frac{x}{2R}\right) + x\cdot\sqrt{R^2 - \frac{x^2}{4}}, \qquad (5.9)$$

$$A_{52} = A_{108} = \frac{A - A_{80}}{2}$$

where R=D/2=40m. The meaning of these entities becomes clear when looking at Figure 5.18.

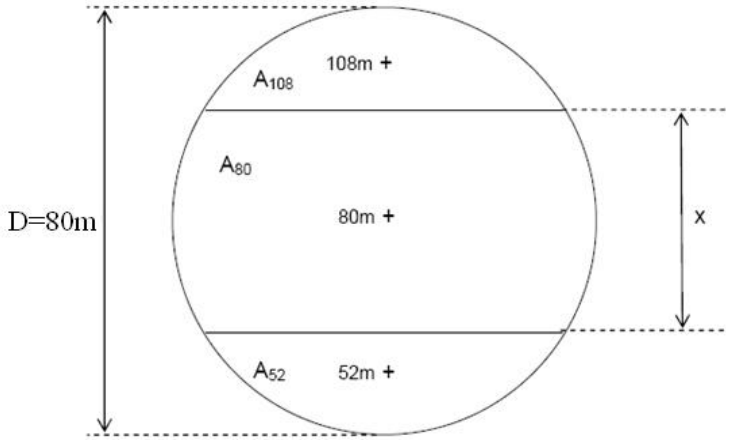

Figure 5.18*Rotor swept area divided in three sections.*

We notice that for x=80m the rotor averaged wind speed is equal to the wind speed at hub height. So, no correction takes place.

The rotor averaged wind speed corrected power is shown in Figure 5.19 for different values of x. Also shown are the relative difference between the corrected (x dependent) and the uncorrected power (x=80m) as well as the relative difference in the standard deviation of the corrected and uncorrected power.

The different corrected power curves differ only up to 4% for wind speeds above 4m/s from the uncorrected power curve. In practically all cases (all x-values and wind speeds) the corrected power is larger than the uncorrected power. Based on Figure 5.19, only for x=60m the standard deviation of the power shows for most wind speeds a decrease about 3%. In practice, for values of x above 50m the standard deviation of the power is decreased of about a few percent. Therefore, this correction is only effective for these values of x, although the effect is relative small.

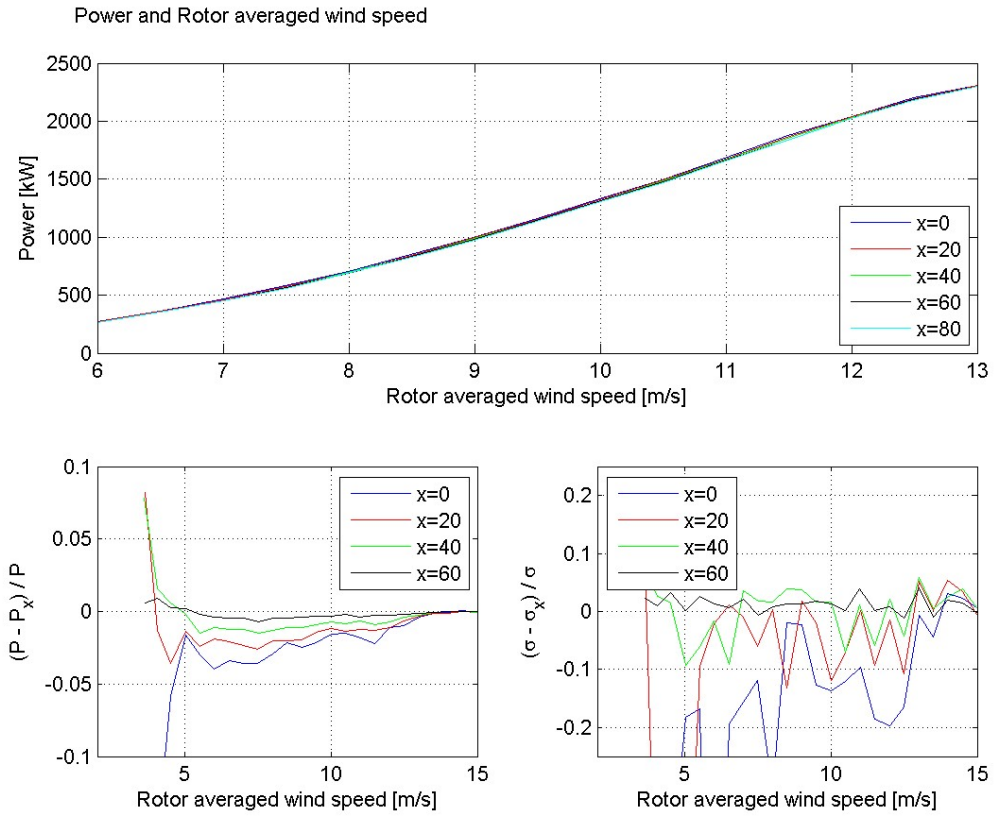

Figure 5.19 *Power curve for various values of x (upper plot). Relative difference in power with respect to the power at x=80m as function of the rotor averaged wind speed for various values of x (lower left plot). Relative difference in standard deviation of power with respect to the standard deviation at x=80m as function of the rotor averaged wind speed for various values of x (lower right plot).*

Power law profile

Further attempts to correct for vertical wind shear are sought in the assumption of a power law profile of the wind shear. Here, we first average the (horizontal) wind speed vertically

$$U_{\alpha,vertical} = \frac{1}{2R}\int_{H-R}^{H+R} U(z)dz = U(H)\cdot\frac{1}{\alpha+1}\cdot\left(\left(\frac{3}{2}\right)^{\alpha+1} - \left(\frac{1}{2}\right)^{\alpha+1}\right), \qquad (5.10)$$

where U(z) is defined in (5.3) and $z_r = H$. Furthermore, it has been used that H=2R. From (5.10) it is obvious that the hub height wind speed U(H) is α corrected based on the profile it is experiencing. These corrections are in the range 0.989 - 1.0353 for the α values in the range -0.5 to 1.

A second possibility is to average the wind speed over the rotor plane [5]. Again, a power law wind profile is assumed (5.3)

$$U_{\alpha,rotor} = \frac{1}{A}\int_{H-R}^{H+R} U(z)dA = U(H)\cdot\frac{2}{\pi}\cdot\int_{-1}^{1}\sqrt{1-y^2}\cdot\left(\frac{y}{2}+1\right)^{\alpha} dy, \qquad (5.11)$$

where y is a dummy integration variable. Also in this case the hub height wind speed is α corrected based on the profile it is experiencing. Now, the corrections are in the range 0.9918 - 1.0259 for the same α range as before.

The results of this vertically averaging and rotor averaging of the wind speed are shown in Figure 5.20. Here, the relative difference between the corrected and the uncorrected power is

shown as well as the relative difference in the standard deviation of the corrected and uncorrected power. Both corrections have more are less the same effect. The corrected power differs 12% from the uncorrected power at 4m/s. At higher wind speeds (>6m/s) the difference is at most 4% percent. In all cases the corrected power is larger than the uncorrected power.

For most wind speeds a decrease of the standard deviation of at most 10% is seen as a result of the α correction. However, for some wind speeds in this regime an increase is seen.

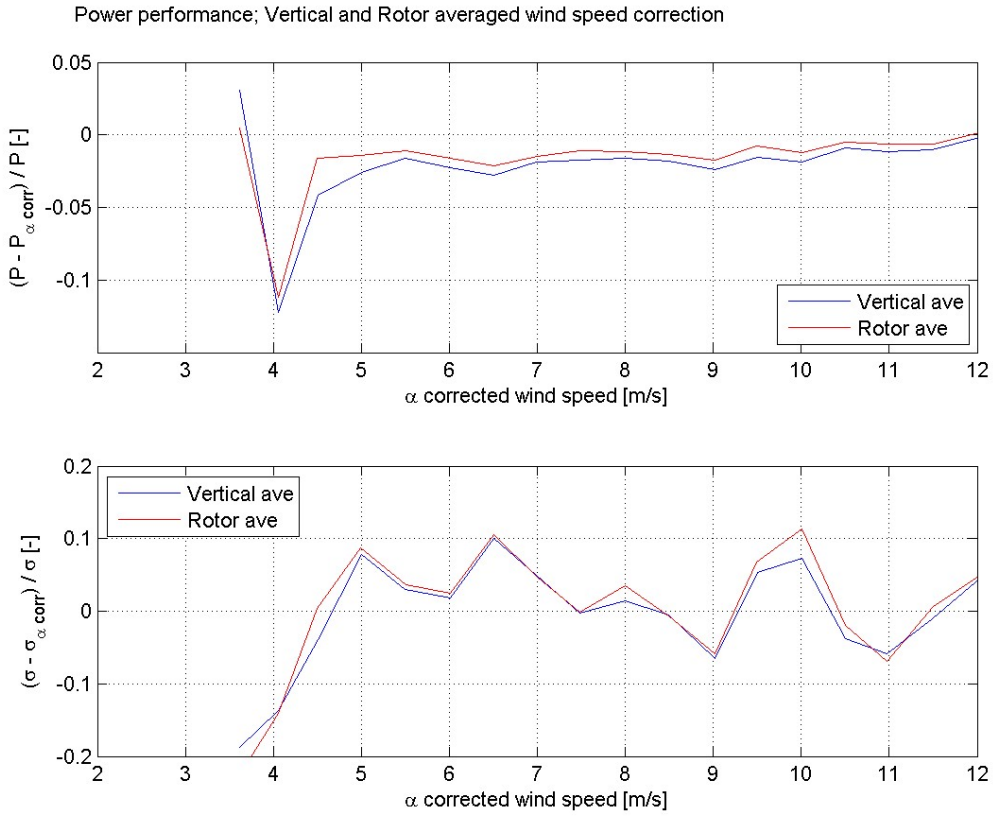

Figure 5.20*Relative difference in power (upper plot) before and after vertical averaged wind speed correction (blue) and rotor averaged wind speed correction (red). Relative difference in standard deviation of power (lower plot) before and vertical averaged wind speed correction (blue) and rotor averaged wind speed correction (red).*

Linear profile

Averaging the wind speed vertically or over the rotor plane assuming a linear wind shear profile (5.4) does not yield a correction factor to the hub height wind speed

$$U_{\beta,vertical} = \frac{1}{2R}\int_{H-R}^{H+R} U(z)dz = U(H), \qquad (5.22)$$

$$U_{\beta,rotor} = \frac{1}{A}\int_{H-R}^{H+R} U(z)dA = U(H). \qquad (5.33)$$

Therefore, with this set-up no corrected power curves can be obtained. However, we will come back to the point of linear profiles in the next subsection.

5.3.4 Vertical wind shear: Power corrections

In the previous subsection the focus for correcting for wind shear has been on the wind speed itself. However, here we want the focus to be on the power that can be extracted from that wind, which is

$$P = \frac{1}{2} \cdot \rho \cdot c_p \cdot \int U^3(z) dA \,, \qquad (5.44)$$

where the infinitesimal surface element dA is also a function of the height z. With this approach we are going to consider multiple measurements and wind shear profiles, again.

Multiple measurements

Based on (5.14) it is shown that multiple measurements are used to correct the cube of the wind speed. A redefinition is obtained as follows

$$P = \frac{1}{2} \cdot \rho \cdot c_p \cdot \int U^3(z) dA = \frac{1}{2} \cdot \rho \cdot c_p \sum_i A_i \cdot U_i{}^3$$

$$P \equiv \frac{1}{2} \cdot \rho \cdot c_p \cdot A \cdot U_{rotor-averaged,cube}{}^3 \quad . \qquad (5.55)$$

$$U_{rotor-averaged,cube} = \left(\frac{A_{52} \cdot U_{52}{}^3}{A} + \frac{A_{80} \cdot U_{80}{}^3}{A} + \frac{A_{108} \cdot U_{108}{}^3}{A} \right)^{1/3}$$

The results of this redefinition are shown in Figure 5.21. It is seen that for the x values shown the power is decreased up to about 7% at 4m/s; for wind speeds above 6m/s this is less than 1%. For almost all wind speeds up to 15 m/s the corrected standard deviation is decreased for x values above 40m. This decrease is at most 5%, which is of the same order, but a bit more as in the linear case (section 5.3.3). So, the correction based on (5.15) (cubically) is a bit more effective than the correction based on (5.8) (linearly).

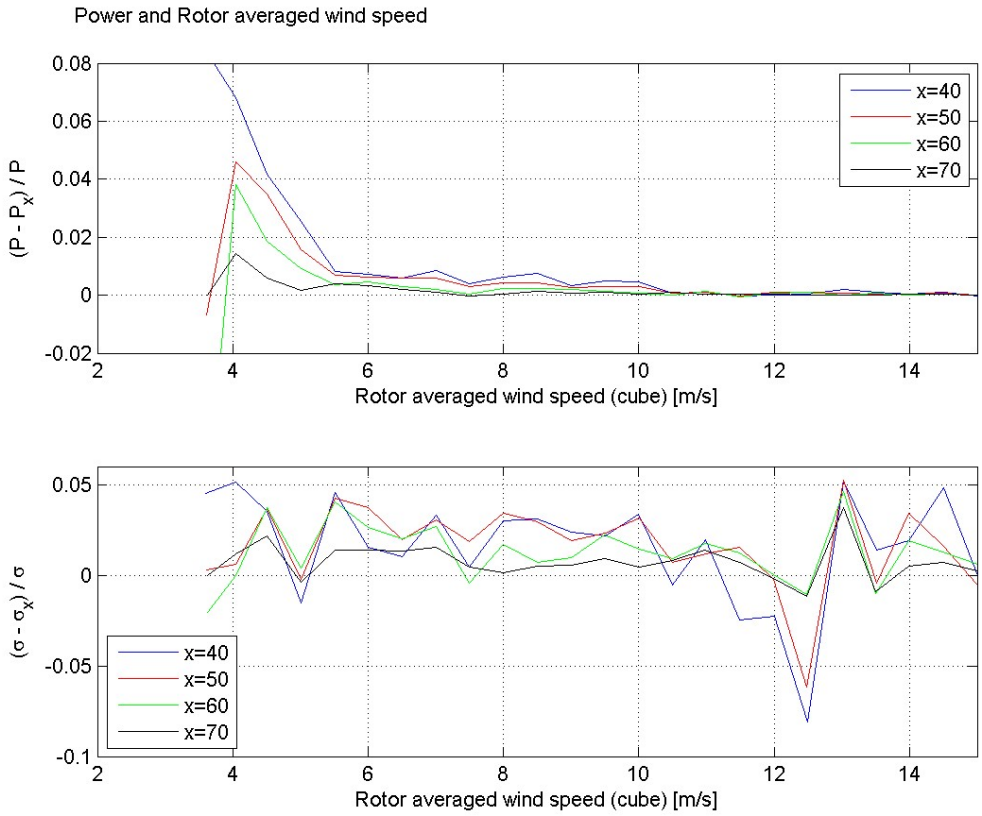

Figure 5.21 *Relative difference in power with respect to the power at x=80m as function of the rotor averaged wind speed for various values of x (upper plot). Relative difference in standard deviation of power with respect to the standard deviation at x=80m as function of the rotor averaged wind speed for various values of x (lower plot).*

Power law profile

The approach started in (5.14) can be applied assuming a power law profile, for which an α corrected wind speed is defined

$$U_{\alpha,cube} = \left(\frac{1}{A} \int_{H-R}^{H+R} U^3(z) dA(z) \right)^{1/3} = U(H) \cdot \left(\frac{2}{\pi} \int_{-1}^{1} \sqrt{1-y^2} \cdot \left(\frac{y}{2} + 1 \right)^{3\alpha} dy \right)^{1/3} . \qquad (5.66)$$

Again, we see that the hub height wind speed is α corrected. In Figure 5.22 these corrections are shown as function of the wind shear parameter α. Also shown are the corrections obtained in section 5.3.3, equations (5.11), for comparison. The blue line indicates the correction due to the linearly averaging the wind speed over the rotor plane (5.11) and the red line is the correction due to cubically averaging the wind speed over the rotor plane (5.16). As can be seen from Figure 5.10 most values of α are within 0 and 0.5. In this range the corrections differ only a few percent.

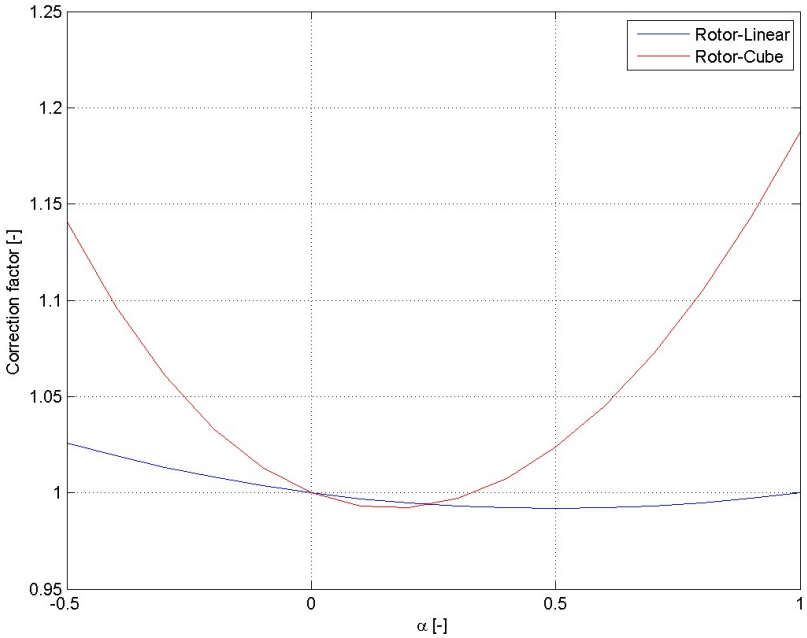

Figure 5.22 *Correction factors to the hub height wind speed as a result of the wind shear correction based on a power law profile. Distinction is made between the linear wind speed (blue) and the cube of the wind speed (red).*

The result of the wind shear correction (5.16) to the power (upper plot) and the standard deviation of the power (lower plot) are shown in Figure 5.23. Also shown is the correction due to (5.11). As indicated the blue lines are the corrections as a result of averaging the wind linearly and the red lines are the corrections as a result of averaging of the cube of the wind speed.

Regarding the standard deviation of the power we see that the difference between linear averaging or cubically averaging the wind speed is small, i.e. the effect of cubically correcting the wind speed is the same as linearly correcting the wind speed. Therefore, with respect to the standard deviation of the power, the same conclusions can be drawn for the effect of the wind shear correction based on a power law profile as in section 5.3.3.

A clear difference with respect to the change in power is seen between linearly averaging the wind speed and cubically averaging the wind speed. In the latter case we see that the corrected power generally is about 1% smaller than the uncorrected power for wind speeds above 4m/s. The linear averaged wind speed correction causes the power to be larger with respect to the uncorrected case.

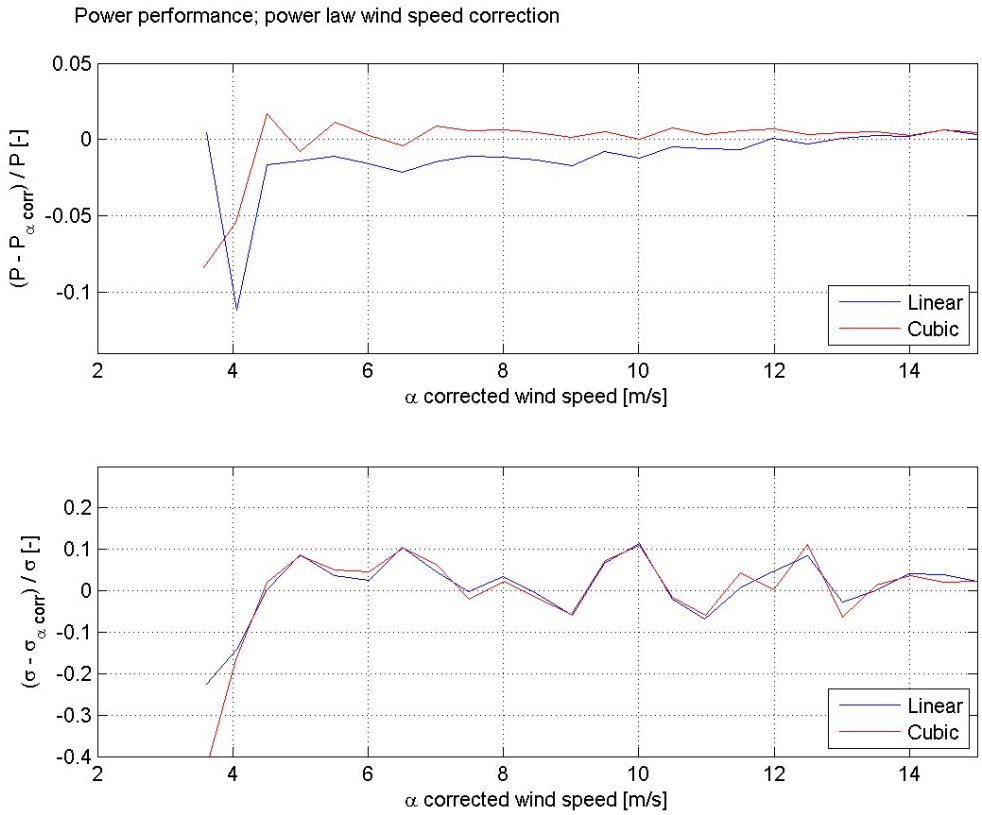

Figure 5.23 *Relative change in power (upper plots) and relative change in standard deviation of the power (lower plots) as result of wind shear correction based on a power law profile. Distinction is made between vertically (left plots) and rotor (right plots) averaging the wind speed and between averaging the linear wind speed (blue) and the cube of the wind speed (red).*

Linear profile

Assuming a linear profile for the vertical wind shear (5.4) and following the set-up as in (5.14) it is shown that the wind speed is corrected as follows

$$U_{\beta,cube} = \left(\frac{1}{A} \int_{H-R}^{H+R} U^3(z) dA \right)^{1/3} = U(H) \cdot \left(\frac{2}{\pi} \int_{-1}^{1} \sqrt{1-y^2} \cdot \left(U(H) + \beta \cdot y \right)^3 dy \right)^{1/3} \quad (7.17)$$

$$U_{\beta,cube} = U(H) \cdot \left(1 + \frac{3\beta^2}{4U^2(H)} \right)^{1/3}$$

The effect of this correction is shown in Figure 5.24. We see that the standard deviation of the power is decreased up to about 5% for wind speeds below 8m/s. For higher wind speeds the standard deviation is generally increased.

For the power we see that the correction causes the power to be lower as compared to the uncorrected case. For wind speeds above 4m/s this only is at most 2%.

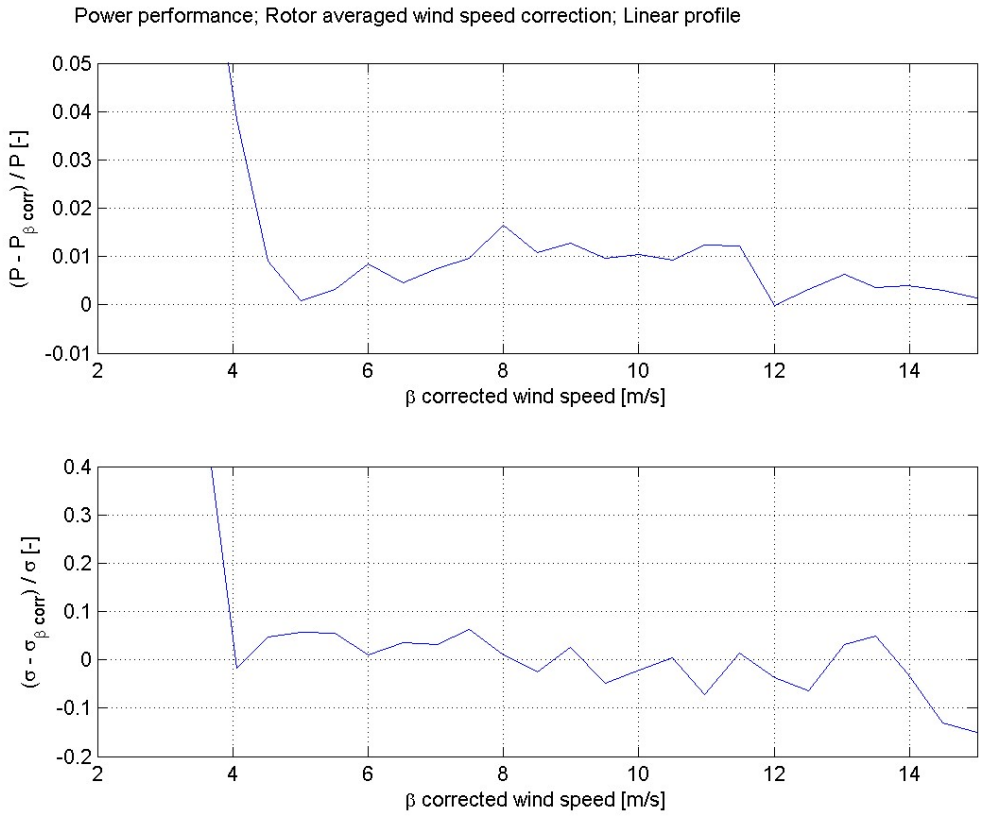

Figure 5.24 *Relative change in power (upper plot) and relative change in standard deviation of the power (lower plot) as result of wind shear correction based on a linear profile.*

5.4 Conclusions

All atmospheric conditions that have been considered, i.e. air density, temperature, turbulence and vertical wind shear, have been shown to have effect on either the power curves themselves or on the standard deviation of the power.

Corrections with respect to air density, as prescribed by [1], turbulence and vertical wind shear are examined. Corrections with respect to temperature and stability are not considered. This because temperature is correlated to air density and stability is correlated to turbulence and wind shear, as we have seen.

Correction with respect to air density and turbulence (1D and 3D) have been shown to be effective for (most) wind speeds in the range where the cubic dependence of the power on the wind speed is most pronounced, say 4m/s - 12m/s. In case of the air density the standard deviation is reduced up to about 8% and in case of the turbulence a reduction up to about 9% (1D) and 10% (3D) is seen. For the 3D turbulence correction the standard deviation of the power is increased above 10m/s. The air density correction and the 1D and 3D turbulence corrections cause the power to be lower than the uncorrected power. For the air density correction and the 1D turbulence correction these differences are at most 2% above 6m/s. For the 3D turbulence correction these are at most 3-4% above 6m/s.

In case of the rotor averaged wind speed correction, only for x values above 50m an improvement in the standard deviation is seen of about 3% in the linear case. In the cubic case the standard deviation is decreased up to 5% for x>40m. The effect of the corrections are considered to be small. In practically all cases (all x-values and wind speeds) the corrected power is larger than the uncorrected power. The difference is at most 4% above 4m/s in the linear case and less

than 1% above 6m/s in the cubic case. The corrections in the cubic case are slightly better as compared to the linear case.

Both (linear) vertical wind shear corrections based on the α parameter basically show the same result. In the most interesting wind speed regime the standard deviations are in most cases reduced up to about 10%, but for some wind speeds an increase of the standard deviation is seen. The increase in power is at most 4% for wind speeds above 6m/s. Also considered is the vertical wind shear correction based on cubically averaging the wind speed over the rotor plane assuming a power law profile. The effect of this correction on the standard deviation is basically the same as for linear averaging over the rotor plane. The change in power is however much less, this is at most (+/-) 1% for wind speeds above 5m/s.

The last vertical wind shear correction is to average the wind speed (cubically) over the rotor plane assuming a linear profile. The effect of this correction on the standard deviation of the power is that it is decreased up to about 5% for wind speeds below 8m/s. For higher wind speeds the standard deviation is generally increased. For the power we see that the correction causes the power to be lower as compared to the uncorrected case. For wind speeds above 4m/s this is at most 2%.

5.5 References

[1] MEASNET - International Network for Harmonised and Recognised Measurements in Wind Energy.

[2] "IEC 61400-12-1:2005(e): Wind turbines - Part 12-1: Power performance measurements of electricity producing wind turbines," 2005.

[3] Elliott and Cadogan, "Effects of wind shear and turbulence on wind turbine power curves," *Proceedings European Community Wind Energy Conference*, 1990.

[4] Pedersen, Gjerding, Ingham, Enevoldsen, Hansen, and Jorgensen, "Wind turbine power performance verification in complex terrain and wind farms," *Riso Report*, April 2002. Riso-R-1330(EN).

[5] Sumner and Masson, "Influence of atmospheric stability on wind turbine power performance curves," *Journal of Solar Energy Engineering*, vol. 128, 2006.

[6] Antoniou, Wagner, Pedersen, Paulsen, Madsen, Jorgensen, Thomsen, Enevoldsen, and Thesbjerg, "Influence of wind characteristics on turbine performance," *Proceedings EWEC*, 2007.

[7] Rareshide, Tindal, Johnson, Graves, Simpson, Bleeg, Harris, and Schoborg, "Effects of complex wind regimes on turbine performance," *Proceedings AWEA Windpower*, 2009.

[8] P. J. Eecen and J. P. Verhoef, "EWTW Meteorological database. Description June 2003 - May 2007," *ECN Report*, June 2007. ECN-E–07-041.

[9] Eecen, Machielse, Braam, and Verhoef, "LTVM statistics database," *ECN Report*, 2005.

[10] D. H. van Dok, *Wind Data Management System, Reference Manual*. ECN TS&C, release 3, version 99, k.3718-gr 05/05 ed., 2005.

[11] Manwell, McGowan, and Rogers, *Wind Energy Explained; Theory, Design and Application*. Wiley, 2002.

[12] Kaiser, Hohlen, and Langreder, "Turbulence correction for power curves," *Proceedings EWEC*, 2003.

6. Power performance measurement

Rozenn Wagner

6.1 Influence of shear - Introduction

Power performance measurement is central to the wind industry since it forms the basis for the power production warranty of the wind turbine. The power curve measurement has to be realized according to the IEC 61400-12-1 standard [1]. The power curve is obtained with 10 minutes mean power output from the turbine plotted against simultaneous 10 minutes average wind speeds. The standard requires the wind speed to be measured by a cup anemometer mounted on top of a mast having the same height as the turbine hub and located at a distance equivalent to 2.5 rotor diameters from the turbine.

Such a plot usually shows a significant spread of values and not a uniquely defined function. The origin of the scatter can mainly be grouped to four categories: the wind turbine operation and maintenance, lack of correlation due to mast distance, sensor uncertainties and the wind characteristics. Within the last group, the current standard only requires the wind speed at hub height and the air density measurement. However, other wind characteristics can influence the power production like the variation of the wind speed with altitude (i.e. wind speed shear). The influence of wind speed shear on the power performance was shown in several studies: some based on aerodynamic simulations [2] others based on measurements [3],[4].
A major issue is to experimentally evaluate the wind speed shear. The wind speed profile is usually assumed to follow one of the standard models such as the logarithmic or power law profiles. However, these models are true for some particular meteorological conditions, and therefore they cannot represent all the profiles that can be experienced by a wind turbine. Measurements are then a better option but are also challenging. Indeed characterizing the speed profile in front of the rotor of a multi-megawatt wind turbine requires measurements of wind speed at several heights, including some above hub height, i.e. typically above 100m. Remote sensing instrument such as Lidar or Sodar then appear as a very attractive solution.
This chapter starts with a description of the influence of the speed shear on the power performance of a multi-megawatt turbine. The challenge of describing the speed profile is then discussed followed by a description of an experiment using a Lidar to characterize the speed profile. This is followed by the introduction of the definition of an equivalent wind speed taking the wind shear into account resulting in an improvement of the power performance measurement. Finally, some recommendations about remote sensing instruments are given to successfully apply this method.

6.2 Shear and turbine aerodynamics

When the flow is axial and homogeneous, i.e. the wind speed is the same at any point, the wind speed seen from a given point on one of the wind turbine blades is the same for any azimuth position. The angle of attack and the relative wind speed are therefore independent on the blade azimuth position (the nacelle tilt is ignored for simplification here), and so is the resulting tangential force. On the contrary, if the flow in front of the turbine presents a shear (vertical variation of the horizontal wind speed), the wind speed seen by a given point on a rotating blade varies with the azimuth position of the blade, so does the tangential force on all blades which affects the resulting torque, see Figure 6.1.

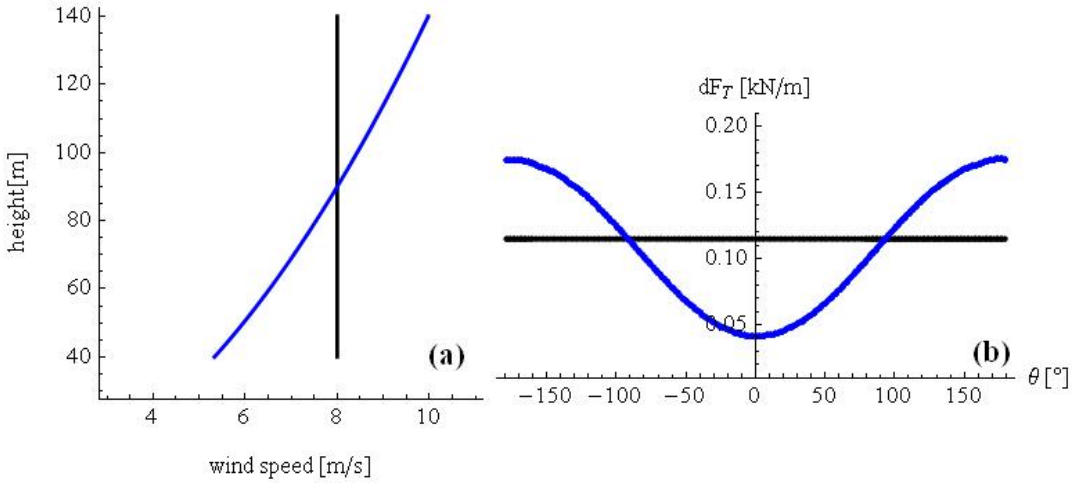

Figure 6.1 *(a): Constant wind speed profile at 8m/s (black), power law profile with a wind speed at hub height (90m) of 8 m/s and a shear exponent of 0.5; Local tangential force for one blade at a radius of 60m obtained with HAWCAero simulations for the 2 wind speed profiles shown in (a).*

The power law profile in Figure 6.1 (a) is not linear and the tangential force in Figure 6.1 (b) is not sinusoidal. Therefore different power output can be obtained for the same wind speed at hub height depending on the complete wind speed profile affecting the rotor, i.e. the speed profile between the lower and higher tip heights, see Figure 6.2.

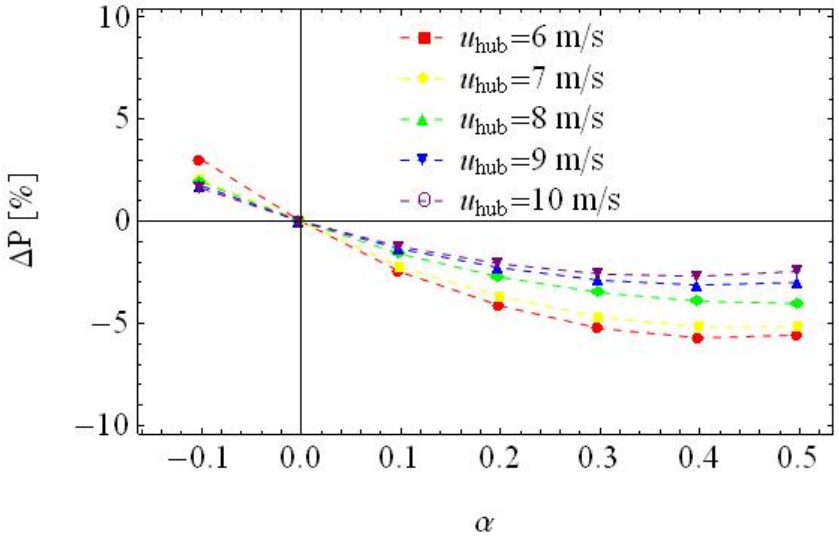

Figure 6.2 *Relative difference in power output (simulated with HAWC2Aero) between a constant free wind speed profile and a power law profile with the same wind speed at hub height, shown as a function of the shear exponent. The simulated power output of the wind turbine is smaller for a power law profile than for a constant profile and the magnitude of the difference depends on the wind speed at hub height.*

6.3 Equivalent wind speed

One of the main differences between a sheared inflow and a uniform inflow, regarding power production, is the kinetic energy flux conveyed by each profile. According to this idea, an "equivalent wind speed" was defined based on the kinetic energy flux of the flow going through the rotor swept area, assuming horizontal homogeneity of the flow. This wind speed is equivalent to the wind speed of a profile constant with height giving the same kinetic energy flux the actual profile (not constant). Contrary to the traditional power curve, which depends on only one

wind speed (at hub height), the use of this equivalent wind speed results in a power curve accounting for the influence of shear.

This method was first tested with aerodynamic (BEM) simulations of a MW wind turbine subjected to various shears [2]. The use of the equivalent wind speed was found to reduce the scatter due to vertical shear in the power curve.

6.4 Experimental validation of the method

The major challenge in the experimental application of the equivalent wind speed method is to characterize the speed profile in front of the wind turbine. As Lidars measure the wind speed at several heights, it enables us to measure the horizontal wind speed profile in front of the wind turbine rotor. Better than a hub height mast, with a Lidar, measurements can be taken up to the highest tip height, i.e. nor assumptions neither extrapolation are needed above hub height. A good approximation of the kinetic energy flux can thus be obtained.

A Lidar was installed in front of a MW wind turbine in order to measure the upcoming wind speed profile. The power curves scatter plot obtained with the equivalent wind speed derived directly from the Lidar measurements presented less scatter than the traditional power curve obtained with measurements at hub height only, see Figure 6.3. This method therefore results in a power curve which is less dependent on the shear than the current standard power curve. It is to be noted though that it is not completely independent of the shear as the power performance of the turbine does not depend only on the kinetic energy flux but also on the response of the turbine to various shear conditions.

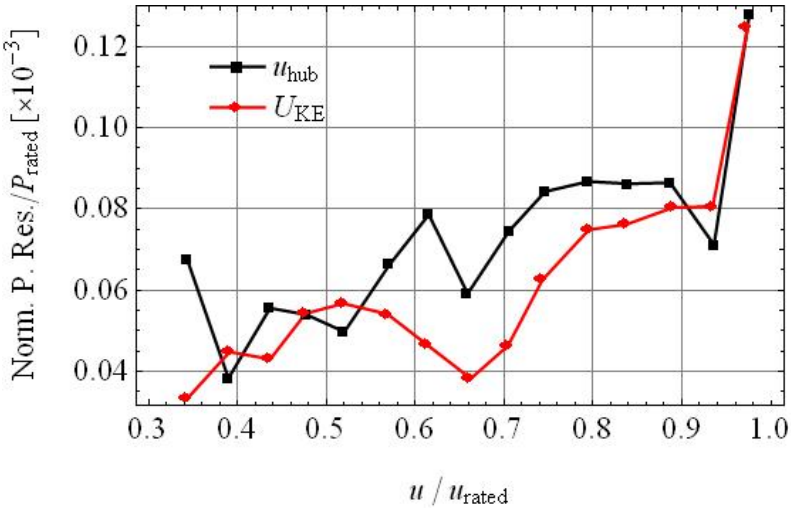

Figure 6.3 *Scatter (quantified as the normalized residuals) in the power curves obtained with the wind speed at hub height only and the equivalent wind speed (derived from Lidar wind speed profile measurement). The use of the equivalent wind speed reduce decreases the scatter due to shear in the power curve.*

6.5 Conclusions

As it is less dependent of the shear, this power curve is more repeatable, i.e. nearly identical power curve can be obtained for various shear conditions, e.g. various seasons and/or various locations. Such a power curve not only facilitates the comparison of the performance of various turbines, but also improves the AEP prediction. Indeed the AEP prediction at a site potentially selected to build a wind farm is usually based on a power curve measured prior to the installation of the turbines at another site.

Furthermore, the reduction of scatter in the power curve results in the decrease of the category uncertainty in power curve measurement (according to IEC 61400-12-1 definitions). However the combined uncertainty in power curve measurement was not reduced because the reduction in category A uncertainty was counterbalanced by an increase in the category B wind speed measurement uncertainty. This is due to the fact that the wind speed was measured by a Lidar, of which, as an instrument recently introduced to wind energy, the measurement uncertainty was defined relative to the uncertainty of cup anemometers, and also that the category B uncertainty due to wind shear in IEC 61400-12-1 is not taken into account.

6.6 References

[1] IEC 61400-12-1 Power performance measurements of electricity producing wind turbines, Ed.2 , 2005

[2] Wagner R., Antoniou I., Pedersen S.M., Courtney M.S. and H.E. Jørgensen, 2009: *The influence of the wind speed profile on wind turbine performance measurements*, Wind Energy, **12**:348-362.

[3] Elliott DL and Cadogan JB, *Effect of wind shear and turbulence on wind turbines power curve*, EWEC 1990

[4] Sumner J and Masson M, *Influence of atmospheric stability on wind turbine power performance curves*, Journal of solar energy engineering, 128:531—538,2006

7. Influence of offshore wakes on power performance at large distances

Jan Willem Wagenaar

7.1 Introduction

The issue of turbulence intensity or rather added turbulence intensity due to offshore wind turbines is addressed. The turbulence intensity is measured in the wake of the turbine. By making proper wind direction selections, various turbines can be addressed and therefore the turbulence intensity can be measured at various distances from a wind turbine. These turbulence intensities are not only considered in single wakes, but also in multiple wakes. Studying increased turbulence intensity levels is done by considering data where turbines are on or off.

The relevance to power performance is that the standard IEC 61400-12-1 [1] states that objects are considered to be disturbing up to 20 diameters (20D). By measuring and analysing the turbulence intensity it can be studied to which distances added turbulence is still present. The presence of added turbulence of one turbine to another influences the power performance of the latter turbine.

The wind farm under consideration is the OWEZ wind farm. It consists of 36 Vestas V90 turbines, having a rotor diameter (D) of 90m and a rated power of 3MW, and a meteo mast measuring the wind speed and direction at least at hub height. More details can be found in [2]. A lay-out of the farm is given in Figure 7.1. The coloured lines indicate single and multiple wake directions as seen from the meteo mast.

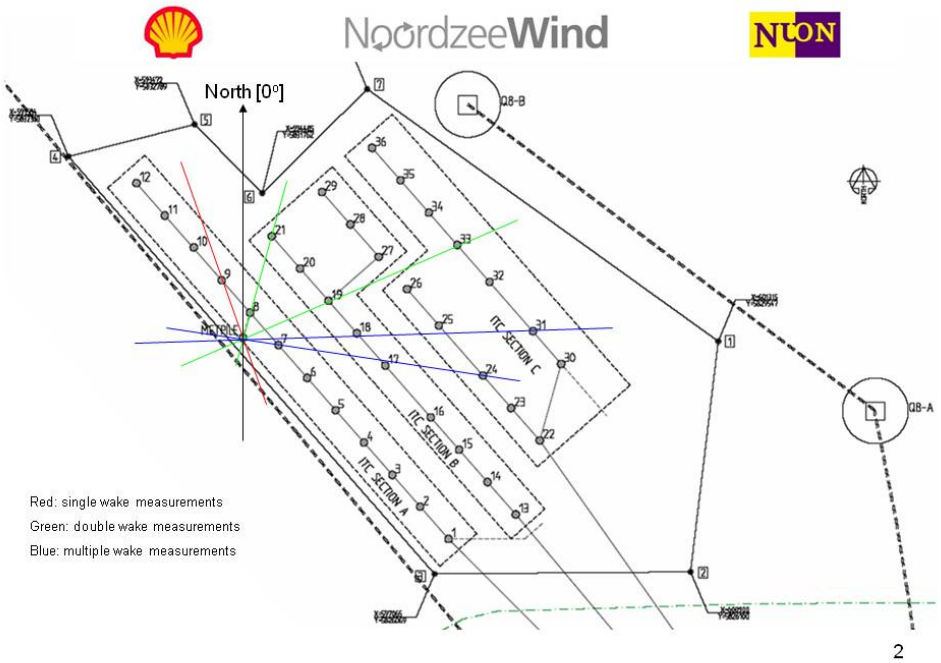

Figure 7.1 *OWEZ lay-out with wake indication.*

7.2 Data selection

The meteo mast was installed in the summer of 2005 [3] and the turbines were erected in the last part of 2006. For the latter activities the possible influence on the wind measurements are examined in [4]. Those measurement points that were found to be effected are removed from the dataset.

In the same period, i.e. the last half year of 2006 test runs of the turbines took place. Because those dates could not be retrieved, all data points that were taken in that period and for which the wind was from the disturbing sector are left out.

All other obviously wrong data points are removed from the set as well.

For all three heights at the meteo mast a wind speed and a wind direction has been defined for which the mast influences are minimised (see [5]). Those are called the "true" wind speed and "true" wind direction, respectively. In the remainder of this document the wind speed refers to the "true" wind speed at 70m (hub height) and the wind direction refers to the "true" wind direction at 70m as measured by the meteo mast. The turbulence intensity is defined as

$$TI = \frac{\sigma_{U_{70}}}{U_{70}}, \qquad (7.8)$$

Where U_{70} is the 10 minute mean value of the (true) wind speed and σ_{U70} is the standard deviation. For most analyses wind speeds are selected above 4m/s; these selections are however explicitly mentioned.

In the remainder of this chapter data will be selected based on turbines being "on" or "off"; a turbine is "on" when it is producing power below rated (0<P<3000 kW) and "off" when it is not producing power. For all other turbines, i.e. for those turbines that are not explicitly mentioned in the text regarding data selection, it is not know whether these turbines are producing power or not. For some data points these unmentioned turbines are on, for others they are off.

Those data selections that are used, but are not listed above, are explicitly mentioned in text.

7.3 Null measurements

Before investigating the turbulence in the wake of the turbines, it is interesting to see what the turbulence level is, when there are no power producing turbines. This can be considered as a null measurement.

Figure 7.2 shows the turbulence intensity as function of the wind direction. The data considered are data points taken before the turbines became active, i.e. before the 1st of January 2007. The upper plot shows scatter data and the lower plot shows the binned values. Here, a bin size of 2.5 degrees is chosen and wind speeds above 4m/s are considered. The uncertainty bars are the standard uncertainty of each bin mean.

The turbulence intensity is lowest around 150 degrees with a value of about 5%. The highest values are found around 350 degrees, which are about 7.5%. Similar figures are presented in [5] where the half-yearly data are presented.

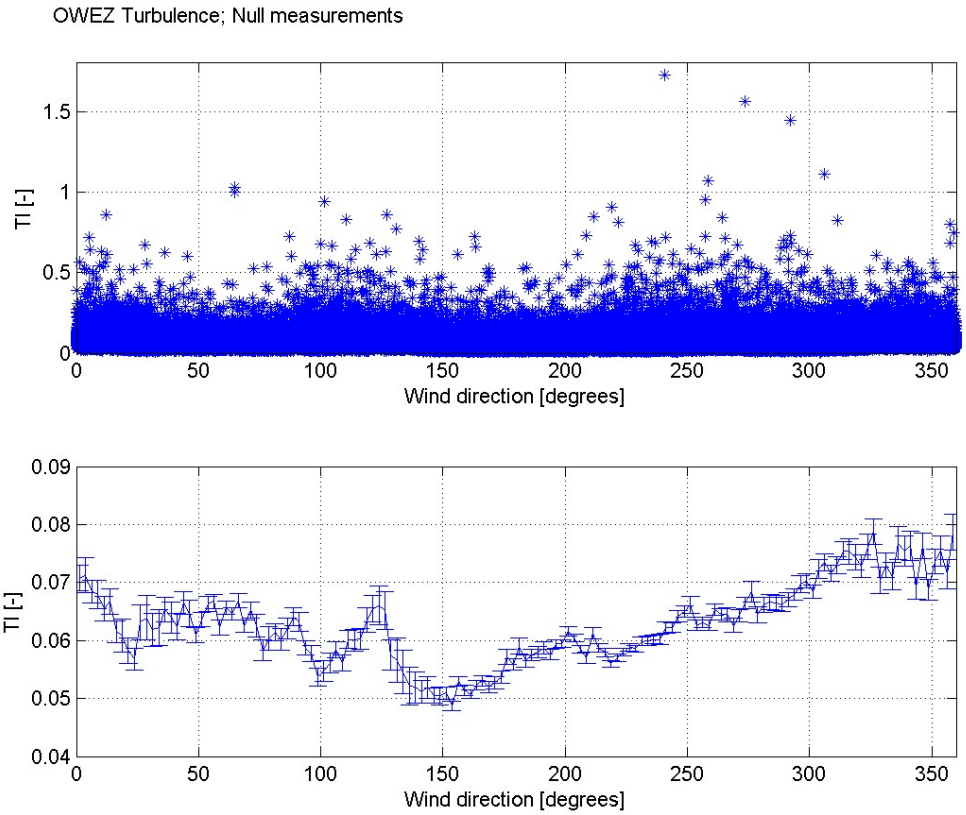

Figure 7.2 *Turbulence intensity as function of wind direction when there are no power producing turbines.*

7.4 Single Wakes

7.4.1 Turbulence intensity: Wind speed dependency

To see to what extend the turbulence intensity depends on the wind speed, turbine T9 is considered. This turbine is located at a distance of 916m (=10.2D) from the meteo mast and at an angle of 340 degrees. A wind direction window of 5 degrees is chosen. With respect to the meteo mast T9 produces a single wake, when it is active.

Figure 7.3 shows the turbulence intensity as function of the wind speed, where wind speed refers to the wind speed in the wake. The upper plot shows the scatter data and the lower plot the binned values, where a bin size of 1m/s is chosen. Distinction is made whether turbines are on or off. For the scatter data no wind speed selection is made, however a few extreme data points are not shown, i.e. are not within the shown window of TI and wind speed. For the binned values in the lower plot, only wind speeds between 4m/s and 16m/s are considered. The uncertainty bars are the standard uncertainty of the bin mean.

When the turbines are on, it is seen in the lower plot of Figure 7.3 that the turbulence intensity decreases with increasing wind speed. From about 9.5m/s to 15.5m/s the turbulence intensity drops from about 11.5% to 8.5%.

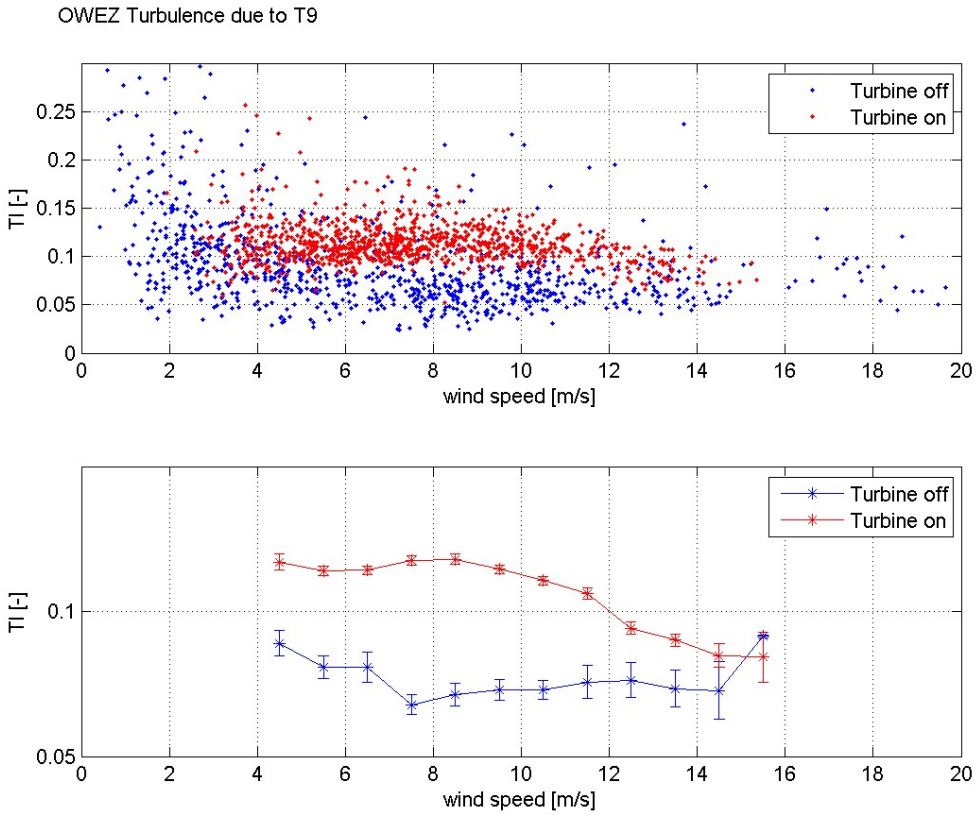

Figure 7.3 *Turbulence intensity in the wake of turbine T9 as function of the wind speed. The upper plot shows the measured data and the lower plot the binned values.*

7.4.2 Added turbulence

A power producing wind turbine adds turbulence to the ambient turbulence intensity. To what extend turbulence is added depends on the position in the wake where the turbulence is considered, i.e. measured. Therefore, not only the total turbulence intensity but also the added turbulence intensity is indicated in Figure 7.4 as function of the distance behind the wind turbine. For Figure 7.4 the following turbines are considered:

Turbine	Distance	Angle
T8	390m = 4.3D	16 degrees
T7	543m = 6.0D	102 degrees
T9	916m = 10.2D	340 degrees
T10	1536m = 17.1D	331 degrees
T11	2168m = 24.1D	327 degrees

For turbines T8 and T7 we have made sure that turbines T21 and T17 (see Figure 7.1) are off, respectively, such that multiple wakes do not occur. It is assumed that the influence of turbine T24 is negligible (see also section 7.5). It is assumed that the wake of turbine T9 is not influenced by the wakes of other turbines, when measured with the meteo mast. Because a bin sizes of 5 degrees is chosen, there is some overlap when considering turbines T10 and T11. For turbine T10 data have been selected where T11 is off and for turbine T11 data have been selected where turbine T12 is off. In the latter case also turbine T10 should be off. However, in that case the data selection becomes too tight such that hardly any data remain.

In Figure 7.4 the total turbulence intensity, the added turbulence intensity and the added standard deviation of the wind speed is shown as function of the distance for various wind speed

classes (and all wind speeds). Here, a wind speed bin of 1m/s is chosen and a wind direction window of 5 degrees. The following definitions are used:

$$\begin{aligned} TI_{added} &= TI_{total} - TI_0 \\ \sigma_{added} &= \sqrt{\sigma^2{}_{total} - \sigma^2{}_0}, \end{aligned} \qquad (9.2)$$

where TI_{added}, TI_{total} and TI_0 indicate the added, the total and the ambient turbulence intensity. This also applies for the standard deviation of the wind speed σ.

It is clearly seen that the added turbulence intensity and added standard deviation of the wind speed in a single wake decreases with increasing distance. The level of turbulence intensity depends on the wind speed.

More importantly, we see that the presence of added turbulence intensity at and beyond 20D. It has vanished at about 25D (=2250m).

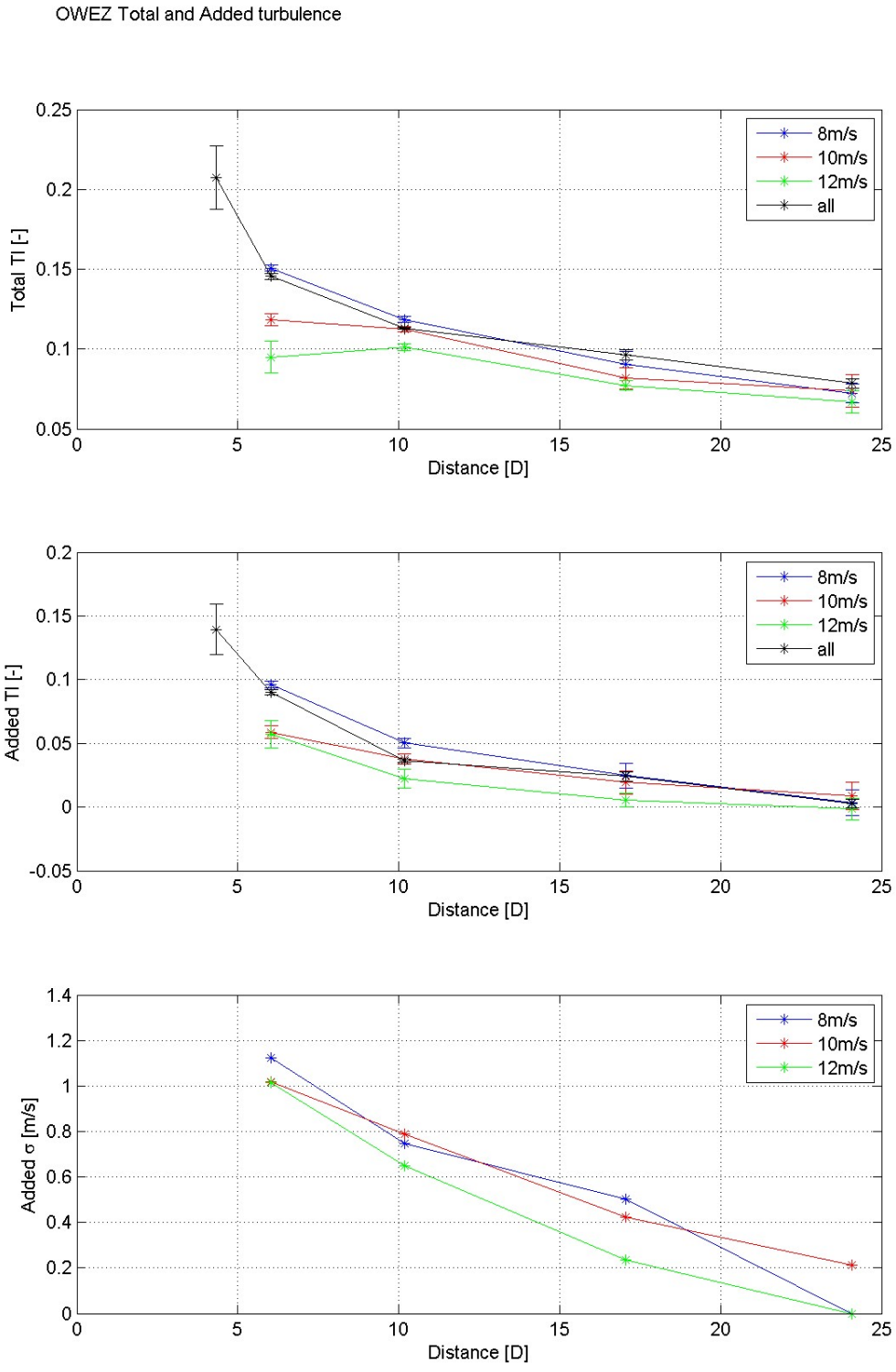

Figure 7.4 *Total and added turbulence intensity (upper and middle plot) as function of distance. The lower plot shows the added standard deviation of the wind speed as function of distance. The blue, red, green and black curves indicate wind speeds of 8m/s, 10m/s, 12m/s and all wind speeds, respectively.*

7.5 Multiple wakes

In this section the influence of multiple wakes is investigated. To do so we consider three cases for which double wakes occur. These are listed below (see also Figure 7.1):

Turbine 1	Distance	Turbine 2	Distance	Angle
T8	390m = 4.3D	T21	1579m = 17.5D	16 degrees
T7	543m = 6.0D	T17	2174m = 24.2D	102 degrees
T19	1397m =15.5D	T33	3498m = 38.9D	67 degrees

Turbines T8 and T21:

For the first situation data have been selected where the wind direction is above 356 degrees or lower than 36 degrees. Wind speeds are above 4m/s. A scatter plot of the turbulence intensity against the wind direction is shown in the upper plot of Figure 7.5; the binned values are shown in the lower plot of Figure 7.5. Here, a bin size of 2.5 degrees is chosen. The uncertainty bars are the standard deviation of the mean bin values. Different combinations of turbines being on and off are considered.

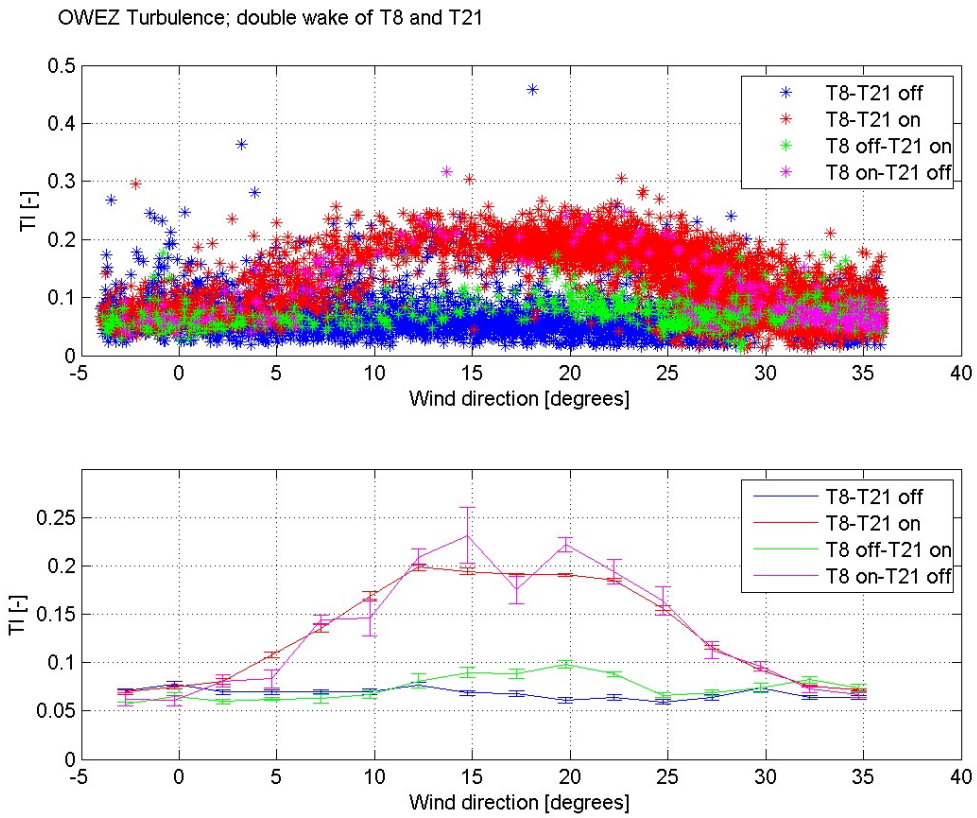

Figure 7.5 *Turbulence intensity against wind direction. Scatter data are in the upper plot and binned values are in the lower plot. Blue indicates that both turbines are off, red indicates that both turbines are on, green indicates that T8 is off and T21 is on and magenta indicates that T8 is on and T21 is off.*

At around 16 degrees a clearly increased turbulence intensity is seen when the turbines are on. The influence of turbine T21 is also seen, especially when it is on and turbine T8 is off (green). From the binned values in Figure 7.5 it seems that turbulence intensity where both turbines are on is lower than the turbulence intensity where T8 is on and T21 is off. This is most probably due to the fact that for the latter case very few data points are available.

Furthermore, we note that wind speed dependency is present, but it does not influence the presented results significantly.

Turbines T7 and T17:

For turbines T7 and T17 a similar situation applies. Here, data have been chosen where the wind direction is between 92 degrees and 112 degrees and wind speeds above 4m/s. The upper plot of Figure 7.6 shows the scatter data and the lower plot the binned values where a bin size of 2.5 degrees is chosen. The uncertainty bars are the standard deviation of the mean bin values. The different colours stand for different combinations of turbines being on and off.

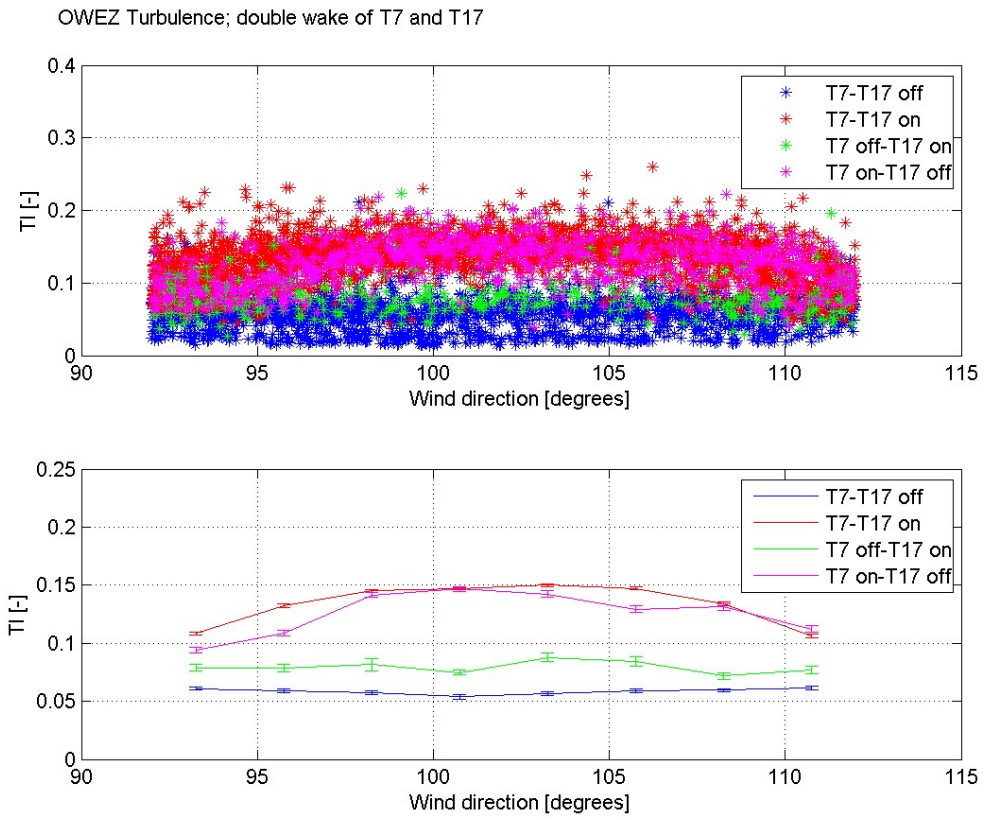

Figure 7.6 *Turbulence intensity against wind direction. Scatter data are in the upper plot and binned values are in the lower plot. Blue indicates that both turbines are off, red indicates that both turbines are on, green indicates that T7 is off and T17 is on and magenta indicates that T7 is on and T17 is off.*

An increased turbulence intensity is present when the turbines are on. Furthermore, the influence of turbine T17 on the turbulence intensity measured at the meteo mast is clearly seen, both when turbine T7 is on and off. When turbine T7 is off we see an increase of turbulence intensity when T17 is turned on and vice versa when turbine T7 is on an decrease in turbulence intensity is seen when turbine T17 is turned off.

According to IEC 61400-12-1 [1] a turbine at a distance further than 20D is not considered as a disturbance to the wind measurements. From Figure 7.6 it is clearly seen that turbine T17, being at a distance of 24.2D, is influencing the wind measurements in the sense that the turbulence intensity is affected.

Turbines T19 and T33:

To further investigate this point, the turbines T19 (15.5D) and T33 (38.9D) are considered. Wind directions are chosen between 55 and 57, where binning is applied with a bin size of 2.5 degrees. Wind speeds are all above 4m/s. For these conditions the turbulence intensity is given in Figure 7.7 as function of the wind direction. The upper plot shows the scatter data and the lower plot the binned values, where the uncertainty bars are the standard deviation of the mean bin values.

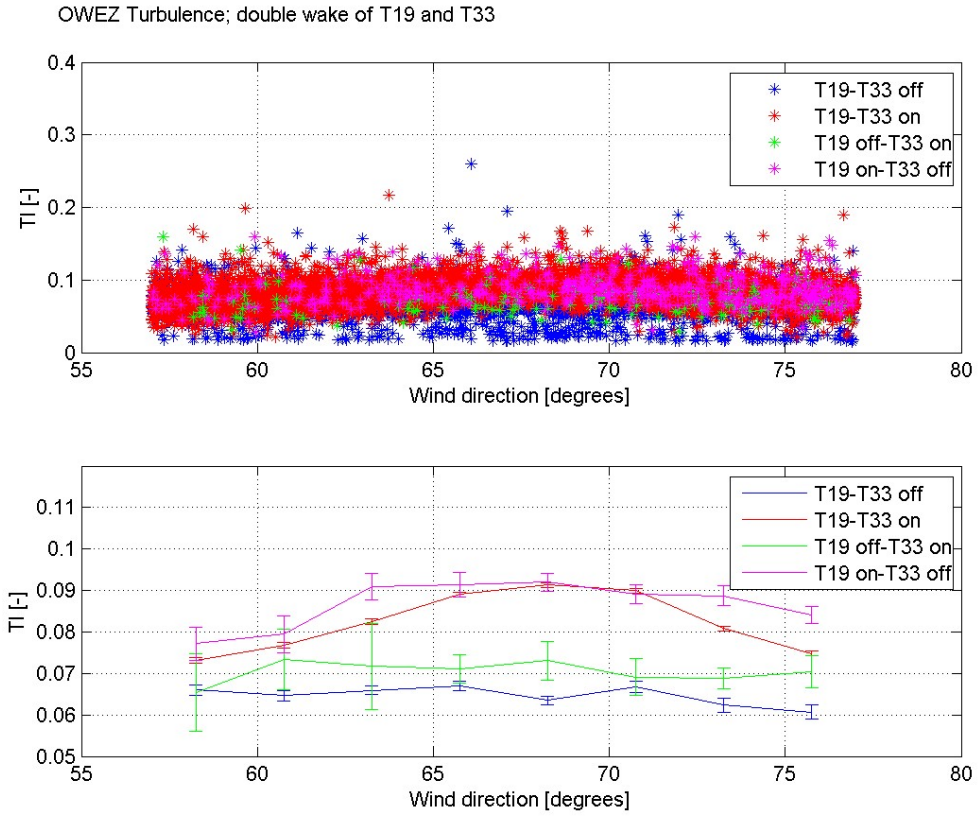

Figure 7.7 *Turbulence intensity against wind direction. Scatter data are in the upper plot and binned values are in the lower plot. Blue indicates that both turbines are off, red indicates that both turbines are on, green indicates that T19 is off and T33 is on and magenta indicates that T19 is on and T33 is off.*

As in the previous examples (Figure 7.5 and Figure 7.6) an increased turbulence intensity is seen when the turbines are on. The influence of the second turbine, i.e. the turbine in line that is furthest away, in this case turbine T33, is not as clear as in the previous examples. This is expected because the distance of this second turbine is very large (38.9D). The effect of turbine T33 is best seen when it is on and turbine T19 is off (green). The lower plot shows an increase of at most 1% when turbine T33 is turned on.

Triple wakes:

As can be seen from Figure 7.1 a triple wake situation can be identified. It involves the turbines T7, T17 and T24. Here, turbine T24 is at a distance of 3638m or 40.4D. Unfortunately, too few data points are available to make a proper analysis.

7.6 Conclusions

The main conclusions are summarized as follows:

- The total turbulence intensity in a single wake decreases with increasing wind speed. From about 9.5m/s to 15.5m/s it drops from about 11.5% to 8.5%.
- It is clearly seen that the added turbulence intensity and added standard deviation of the wind speed in a single wake decreases with increasing distance. The level of turbulence intensity depends on the wind speed. More importantly, added turbulence intensity is present at and beyond 20D. It has vanished at about 25D (=2250m).
- In double wake measurements including T7 and T17 the effect of the second turbine (T17), being at a distance of 24.2D, on the turbulence intensity is clearly seen.
- In double wake measurements including T19 and T33 the effect of the second turbine (T33, distance is 38.9D) is not as clear as in the previous example. When turbine T33 is on and turbine T19 is off the increase in turbulence intensity is at most 1%.

7.7 References

[1] IEC 61400-12-1:2005(E), Power performance measurements of electricity producing wind turbines

[2] H.J. Kouwenhoven, User manual data files meteorological mast NoordzeeWind, NZW-16-S-4-R03, October 2007

[3] J.W. Wagenaar, P.J. Eecen, Measurements of Wind, Wave and Currents at the Offshore Wind Farm Egmond aan Zee, ECN-E--09-015

[4] A. Curvers, P.A. van der Werff, OWEZ WIND FARM EFFICIENCY, ECN-E--08-092

[5] P.J. Eecen, L.A.H. Machielse and A.P.W.M. Curvers, Meteorological Measurements OWEZ, Half year report 01-07-2005 – 31-12-2005, ECN-E--07-073

8. Guideline to wind farm wake analysis

Kurt Hansen

A guideline on performing wake analysis on wind farms has been formulated as part of UpWind -WP1A2. This guideline is derived from preparing dataset and analysing data from several large offshore wind farms. The results of these wake analysis have been used to validate flow models in UpWind -WP8.

8.1 Introduction

SCADA data has shown to be of great value for flow model validation, but the quality of SCADA data is not always sufficiently high and a comprehensive validation is required before use. This Chapter summarises the experience obtained with organizing and analysing measurements from 4-5 large wind farms as part of UpWind -WP8. The Chapter has been organized as a guideline on how to establish a proper dataset for extracting wake properties; which can document the flow behaviour inside a wind farm during different flow conditions. A paper [1] has presented a general guideline for data validation, but this paper will focus on input to the UpWind WP8 model validation.
The guideline identifies six important tasks; which should be addressed before the wake flow cases can be formulated and extracted from the dataset. The data analysis is often performed by a person who have not been involved in the data acquisition process and who might not have a detailed technical knowledge on how to structure huge dataset. The data qualification process requires technical skills concerning validating meteorological data and wind turbines operational behaviour. The technical part of data organization will not be addressed in this document, but the subtask will be illustrated with examples from the data analysis performed in UpWind -WP8. The flow cases are focusing on presenting either the speed or the power deficit behind a single or a group of wind turbines in relation to the free undisturbed wind speed or wind turbine power. The dataset used in UpWind-WP8 have been organized in a MySQL® database; which enabled the use of SQL. The data queries have been organized and performed with Matlab®.

8.1.1 Purpose

The validation of wind farm flow models developed and implemented in EU-UpWind WP8 has been based on measurements from a number of wind farms. The wind farm measurements are often limited to SCADA data, recorded as part of the standard wind farm monitoring system. Unfortunately the documentation of calibration and maintenance of the sensors included in the SCADA system is not available; which influences the quality of the recorded signals and a validation is required before use.
State-of-the-art models ranging from large CFD models to engineering models like WAsP® and WindFarmer® have been included as part of UpWind-WP8 in the validation and it became necessary to formulate flow cases, which could be implemented to different kind of models. The aim was to perform wake analysis that could enable a complete model validation, taking into account combinations of flow direction, wind speed and atmospheric stability.

8.1.2 Signals

A flow case query requires access to a number of signals and a considerable number of [10 minute] statistical values from either a dedicated measurement system or from the wind turbine *Supervisory Control And Data Acquisition* [SCADA] system. The signals should as a minimum include:

- Individual wind turbine power;
- Individual wind turbine yaw position and yaw misalignment;
- Wind speed and wind direction at hub height on a free undisturbed mast (optimal).

All statistical values should be screened to:

- Identify records with turbines of line;
- Identify records with reduced power settings;
- Identify wind farm offline situations;
- Identify site specific deviations e.g. turbine size, hub height, regulation type and terrain.

8.1.3 Definitions

Some basic definitions have been adapted during the flow validation procedure. When analysing flows inside wind farms, the input refers to wind speed or [wind turbine] power and the output is expressed as the ratio between output and input values or as a deficit. The following definitions have been used:

Speed ratio: $\eta_s = U_{free} / U_{wake}$
Power ratio: $\eta_p = Power_{free} / Power_{wake}$

Speed deficit: $\eta_{sd} = 1-U_{free} / U_{wake}$
Power deficit: $\eta_{pd} = 1-Power_{free} / Power_{wake}$

Turbine spacing, unit= [Rotor] diameter

The deficit is presented according to the [ambient] flow conditions as function of distance between the [wake] object wind turbine and the wake generating turbine as function of flow direction. The power deficit distribution is illustrated in 2 different presentations below:
Figure 8.1; illustrates the power deficit distribution - as function of the normalized inflow direction where each circle represents the mean power deficit for a five degree flow sector between two turbines. The distribution is fitted with a Gaussian expression and reveals a mean wake expansion of 28°. The deficit distribution represents all atmospheric conditions in the wind speed interval 7 – 9 m/s for 7D spacing in the Horns Rev wind farm.

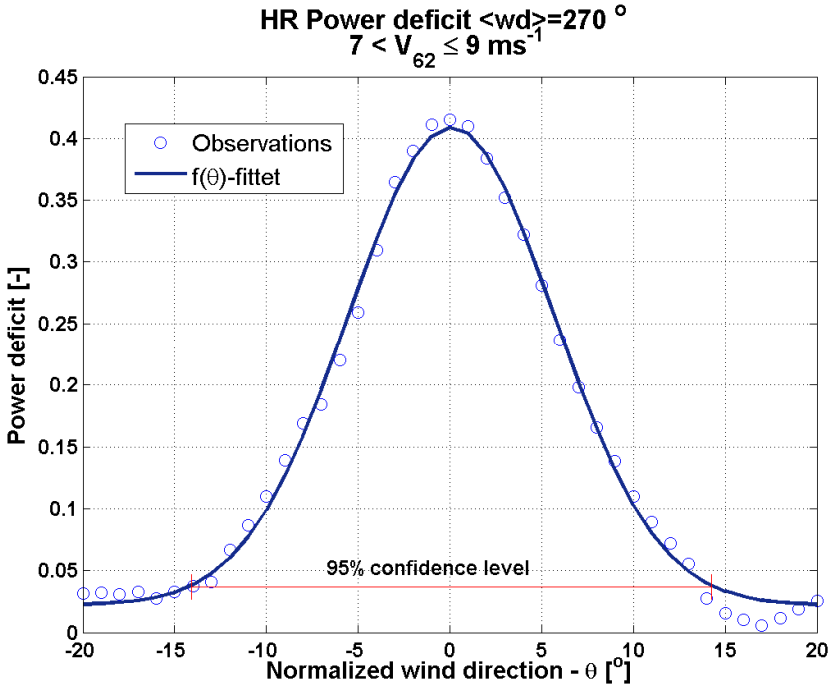

Figure 8.1: *Example of power deficit as function of normalized wind direction between two turbines with 7D spacing.*

Figure 8.2; shows the mean power deficit downstream, along rows of turbines with 7D spacing for 8 m/s wind speed and a 5 degree flow sector. The figure illustrates how the main part of deficit 30-40% occurs between the 1th and the 2th turbine. Adding some additional turbines to the row, only increases the power deficit with 10% - with reference to the first turbine. The power deficit level and shape highly depends on the wind speed, flow direction and the atmospheric stability.

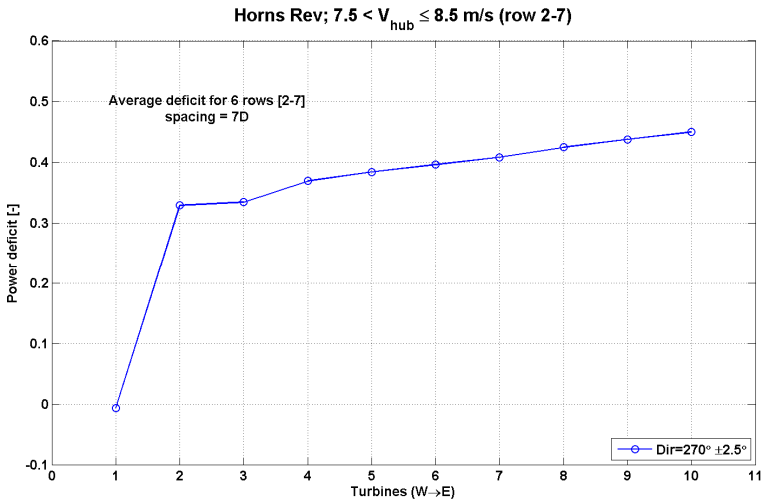

Figure 8.2: *Averaged deficit along 6 rows of turbines with reference to wt07 for a 5 degree flow sector.*

8.2 Data preparation

Before a wake analysis can be performed it is necessary to establish a high quality dataset to give confidence to the results. The recommended number of reliable observations is at least 30-60 minutes of good measurements for each flow case, which can be difficult to obtain after the data filtering. This requires a large number of "raw" observations corresponding to at least 1- 2 years of wind farm operation.
The necessary subtasks for qualifying a dataset to wake analysis are:

1. Data organization and synchronization;
2. Data qualification;
3. Wind farm layout;
4. Calculation of derived parameters;
5. Identification of descriptors and flow cases;
6. Define data filter criteria;

It is important to address all the tasks listed above; otherwise the data query will suffer from large scatter or a lack of observations.

8.3 Signals, organization and synchronization

The required data for wake flow analysis should include both primary signals like individual power values, wind speed and wind direction at hub height. Furthermore a lot of secondary signals e.g. individual values for yaw position, nacelle wind speed, pitch angle and rotor speed. The secondary values are important for validating the quality of the primary signal quality and also for validating the operational behaviour of the wind turbine. The signal statistics should include mean, standard deviation, minimum and maximum values both for primary and secondary signals.

Table 8.1: Required SCADA signals, used to qualify the wake flow properties in a wind farm

Number	Signal	Importance
1	Electric Power from all wind turbines	High
2	Wind speed from undisturbed mast(s) [2]	High
3	Wind direction at hub height	High
4	Yaw position from all individual turbines[3]	High
5	Nacelle wind speed from all wind turbines	Medium
6	Rotor speed from all turbines[4]	Medium
7	Pitch angle from all turbines	Medium
8	Temperatures	Medium

The data organization should be appropriate to avoid additional scaling or calibration during queries. Furthermore it should be possible to perform queries with a number of constraints.
The data transfers include many GB of data, stored in huge compressed [ASCII] files and a data conversion to a robust format is required. Such format can be a database or a software dedicated format. A database solution enables the use of efficient tools based on *Structured Query Language* [SQL].
The wind farm statistics are available from different sources as the *Supervisory Control And Data Acquisition* [SCADA] system or stand-alone [meteorological] logger systems. It is extremely important to facilitate a robust synchronization of the different sources of measurements, because system clocks can be unstable for stand-alone systems. The quality of the synchronization should be within 1 minute; which has to be checked throughout the whole measuring period.

8.3.1 Wind farm layout

The exact knowledge of the wind farm layout is essential, both during the data qualification and for the wake analysis. The wind turbine coordinates are available as geographical coordinates, but often it is more appropriate to use the rotor diameter as plotting unit demonstrated in Figure 8.3. This figure presents the layout of an [offshore] wind farm with 80 turbines and the position of three masts. It is important to identify free inflow sectors both for the masts observations and for wind turbines. Figure 8.4 identifies the three principal flow directions corresponding to 7D, 9.4D and 10.4 D spacing at the NW corner of the wind farm. This information is essential when validating the signal quality. The wind turbine coordinates are used to identify the wake generating turbines, according to the inflow sector.

Wind farms located in complex terrain are often installed in irregular shapes optimized to the landscape or dominants flow sectors. It can be difficult to determine a unique inflow reference due to the complexity of the terrain and the lack of undisturbed masts. This is shown in Figure 8.5, where the masts are located inside the wind farm or behind the wind farms compared to the dominant flow direction.

[2] This will require several masts, but in case such signal is not available, it is necessary to use the power values to determine the inflow conditions.
[3] This signal is equal to nacelle position, and can be a substitute to the wind direction signal.
[4] The rotor speed is important for validating the operational behavior of dual or variable speed turbines.

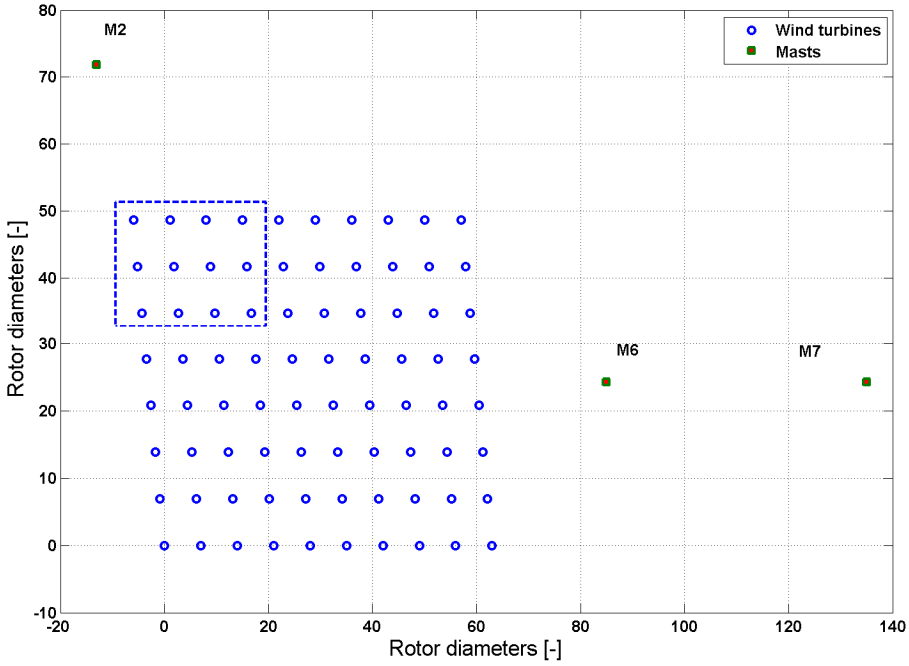

Figure 8.3: *Layout of the Horns rev wind farm, unit=rotor diameter (=80m).*

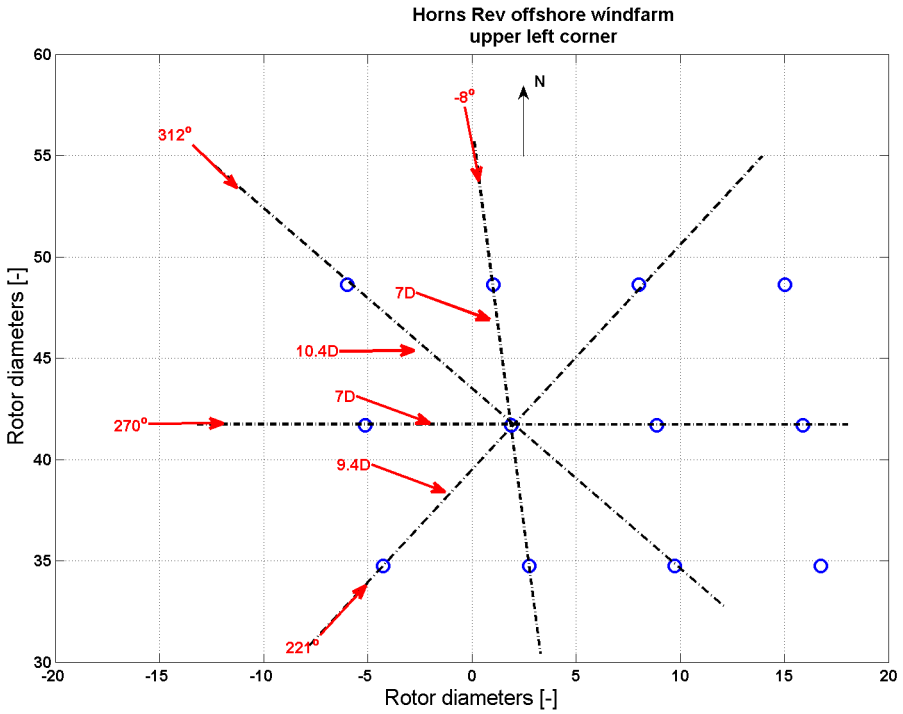

Figure 8.4: *Main flow directions and principal spacing distances at Horns Rev wind farm.*

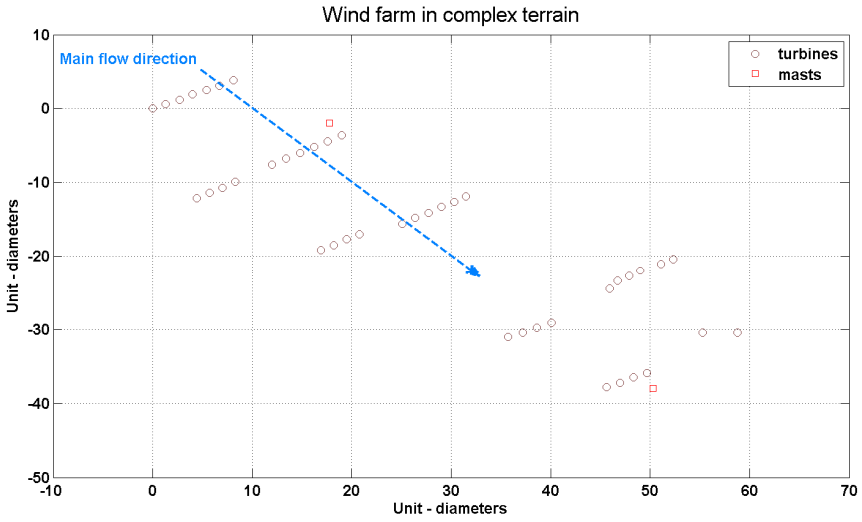

Figure 8.5: *Example of a wind farm installed in a complex terrain with a dominant flow direction.*

8.3.2 Data qualification

Before use, all data need to be quality checked while the data has been moved to another media using a transfer protocol. Furthermore data is not necessarily checked during the operational phase due to lack of time or skilled personnel. It is important to identify and exclude erroneous observations instead of using modified observations and exclusion might be implemented using a quality number as defined in [2]. Below is a list of potential error sources related to the signals in Table 8.1, which need to be verified.

Power signals can:

- include outliers, which can influence the analysis;
- include periods where the turbine is in transition mode like start, stop or emergency stop sequence;
- be limited due to power de-regulation.

The main part of deviating power observations can be identified through scatter plot of the power as function of nacelle wind speed. It can even be necessary to establish a correlation between the official power curve and the mean power curve based on the nacelle wind speed as shown in Figure 8.6.

A scatter plot of the power value as function of the nacelle wind speed can be used to identify outliers if there is a lack of undisturbed wind speed observations, especially for wind turbines located in a wind farm. A qualifying scatter plot is shown in Figure 8.7 including a disqualification line and circle. The level of the disqualification line depend a.o. on the wind turbine control and the local turbulence intensity variation.

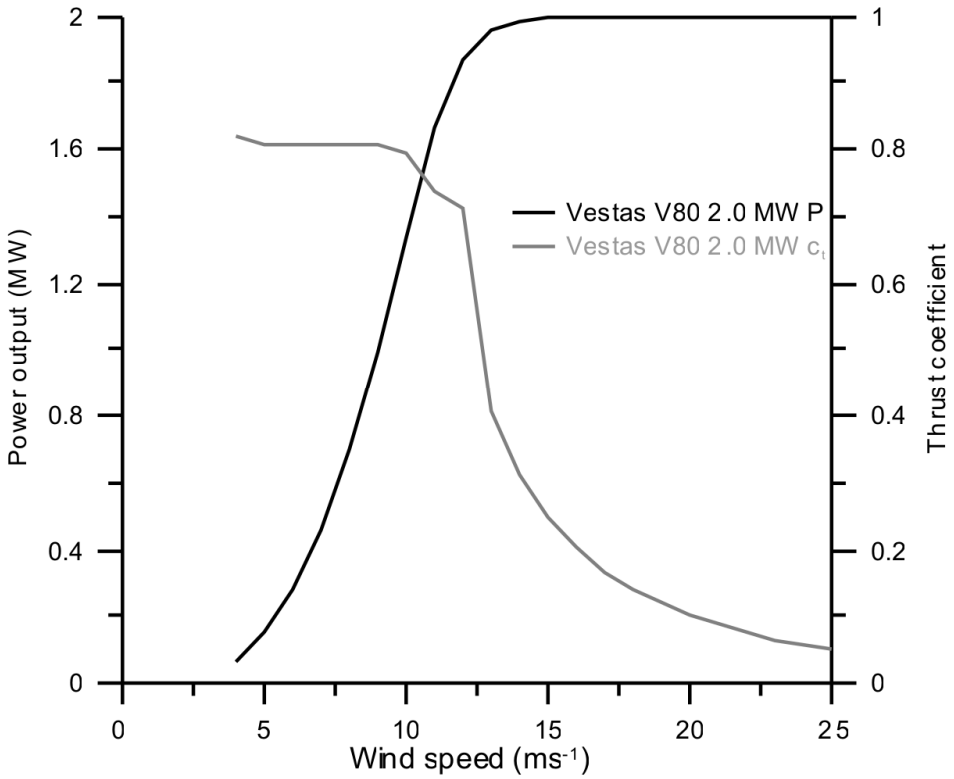

Figure 8.6: *Official power and thrust coefficient curve for VESTAS V80.*

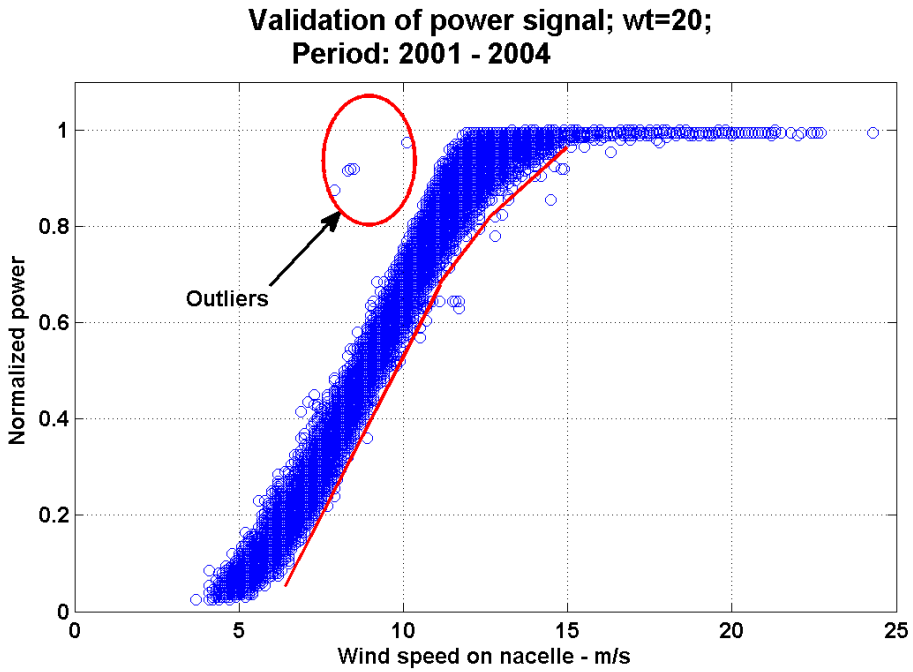

Figure 8.7: *Example of qualification of power values, all observations below the red line and inside the red circle are marked as outliers and disqualified.*

If the power values contain a high degree of scatter it is necessary to include an "acceptance" band for each wind speed interval with reference to the standard deviation of the power.

Wind speed at hub height

- could be checked for correlation with other heights;
- Could be checked for occurrence of stationarity, spikes and drop-outs through scatter plots.

The signal correlation is a robust method to identify data outliers and scatter plots of turbulence can be used but to identify signal stationarity. Unfortunately it is impossible to verify the instrument calibration due to lack of documentation.

Wind direction at hub height

- could be checked for correlation with other heights;
- Could be checked for occurrence of stationarity through scatter plots.

Yaw position of wind turbine

The wind turbine yaw position offset is often not correct or calibrated and it is necessary to perform a data analysis to determine this offset. A correlation against the wind speed direction is sufficient for a free wind sector; otherwise the signal could be verified in sectors with an expected power deficit along a line of turbines, as shown in Figure 8.8. It is sufficient to validate the yaw position for 3 – 4 reference turbines; which can represent the flows from different direction into the wind farm, if the number of masts is limited. The yaw position offset can change during the measuring period and this also need to be verified.

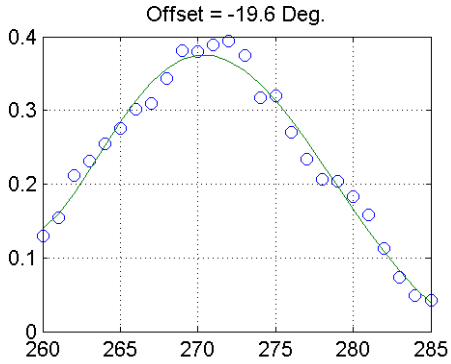

Figure 8.8: Determination of yaw position offset from Horns rev, wt02.

Each observation in Figure 8.8 is determined with a moving average technique using a window of 5 degrees. The moving window technique reduces the deficit scatter and is a robust technique to extract information from small datasets.

8.3.3 Derived parameters

The wind farm dataset does not always include the sufficient signals for wake analysis. This section identifies important signals, which should be included as constraints in the wake analysis.

Free wind direction

The wind direction signal is extremely important, while the flow deficit highly depends on the flow direction (Figure 8.8) and the spacing between the wind turbines. With a lack of direction measurements it is necessary to establish an artificial wind direction based yaw positions from 2-4 wind turbines to cover the whole wind rose. NOTE: The artificial signal is only valid for grid connected wind turbines, while the wind turbine yaw position could misbehave when the turbine is idling or stopped.

Monin-Obukhov length, L.
The M-O length can be derived either from sonic measurements or from a combination of the temperature and the wind speed gradient. To determine a robust M-O lengths in onshore and complex terrain sites, it is important to select proper observation heights and it is recommended to consult the literature on this topic.

Atmospheric stability classification
The offshore stability classification can be based on the Monin-Obukhov length L, as listed in Table 8.2

Table 8.2: *Definition of stability classes based on length, L (m).*

Class	Obukhov length [m]	Atmosperic stability class
cL=-3	-100 ≤ L ≤ -50	Very unstable (vu)
cL=-2	-200 ≤ L ≤ -100	Unstable (u)
cL=-1	-500 ≤ L ≤ -200	Near unstable (nu)
cL=0	|L|>500	Neutral (n)
cL=1	200 ≤ L ≤ 500	Near stable (ns)
cL=2	50 ≤ L ≤ 200	Stable (s)
cL=3	10 ≤ L ≤ 50	Very stable (vs)

The stability classification for Horns Rev has been based on the Bulk-Ri number with success - as demonstrated in [3,4]. The speed measurements from 15 m amsl (recorded below tip-bottom height) seem to be applicable in combination with the temperature difference between air and water. The robustness of this classification has been documented in [4] and an example from Horns Rev has been demonstrated in Figure 8.9.

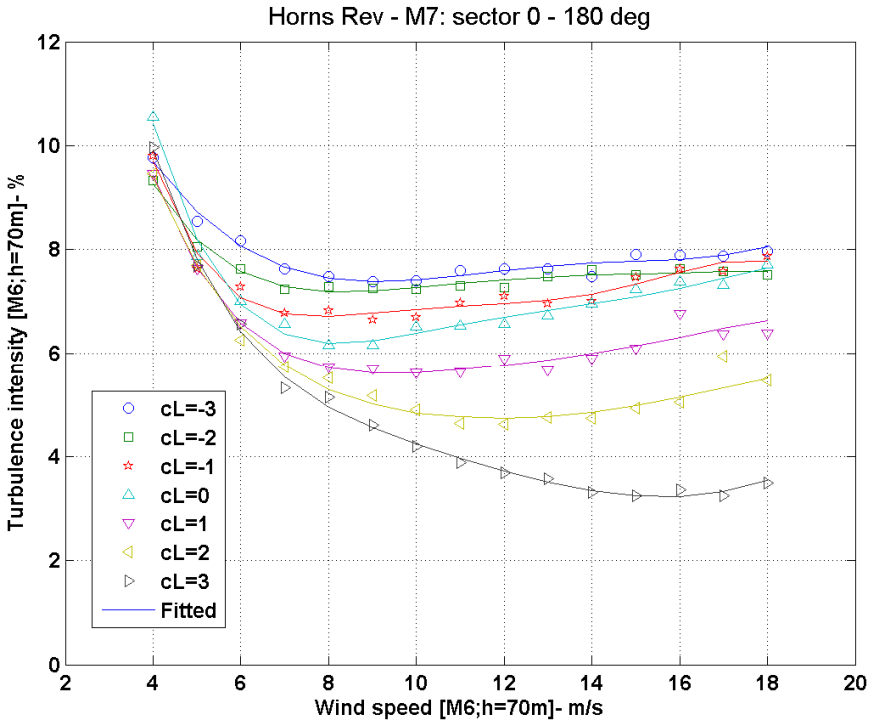

Figure 8.9: *Example of averaged turbulence intensity for different stability classifications, measured at Horns Rev offshore wind farm, Denmark.*

8.3.4 Identifications of descriptors and flow cases

The two most important descriptors for analysing the flow inside a wind farm is 1) the undisturbed wind speed and 2) wind direction at hub height measured outside the wind farm. Unfortunately such observations are not always available and another option is to use recordings from a upwind turbine, e.g. power values and yaw position as indicated in Figure 8.11.
The power range is selected according to the official power curve, Figure 8.6, for a given wind speed interval, but this method requires a signal validation as described in section 4.3 before the analysis can be performed.
The inflow sector is limited with reference to the [upwind] free wind turbine yaw position as illustrated in Figure 8.12. Using the wind turbine yaw position increases the directional uncertainty, while the wind turbine yaw misalignment averaging procedure is not documented, but a |yaw misalignment| > 0 can be expected[5]. Many observations are required to reduce the scatter in the measurements compared to wind vane signals.
Other descriptors can be the ambient turbulence intensity and/or the stability classification as listed in the section 4.4.
The flow case is defined together with the users who are validating flow models; which is could either be the code developers or the end-users who need the flow model performance.
The flow cases are defined in steps; ranging from simple [flow] cases to very complicate [flow] cases and a list with increasing complexity is given in Figure 8.10:

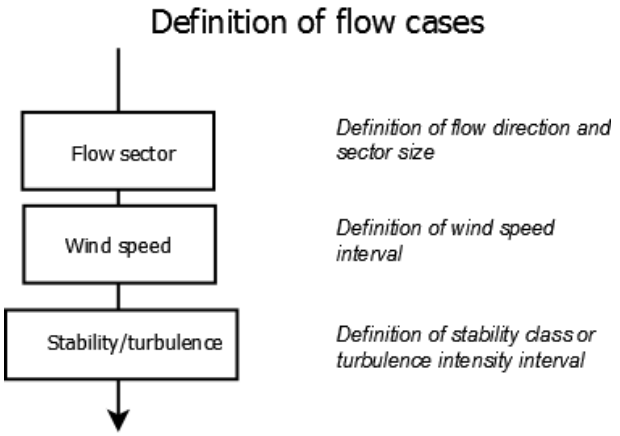

Figure 8.10: *Definition of flow cases with increasing complexity.*

i) Flow within a limited sector, along a line of wind turbine;
ii) Flow within a limited sector, along a line of wind turbines and a limited wind speed interval;
iii) Flow within a limited sector, along a line of wind turbines, a limited wind speed interval and a stability class.

The simple flow case i) is applicable for a limited number of observations and depends only on the selected sector size. Increasing complexity requires much more observations and flow cases from class iii) can only be fulfilled with a limited number of combinations of wind speed, flow sectors and stability classes.
The number of flow cases derived from class iii) could include 18 flow sectors x 12 wind speeds interval x 7 stability classes – in total 1512 flow cases[6]. Such amount of cases requires a proper verification and planning before the queries can be performed. The size of the flow sector should be applicable for the flow model verification and may vary between 5 and 30 degrees.

[5] Caused by a hysteresis, in the yaw misalignment.
[6] Many flow cases can be eliminated due to symmetry, depending on the wind farm layout and inflow complexity.

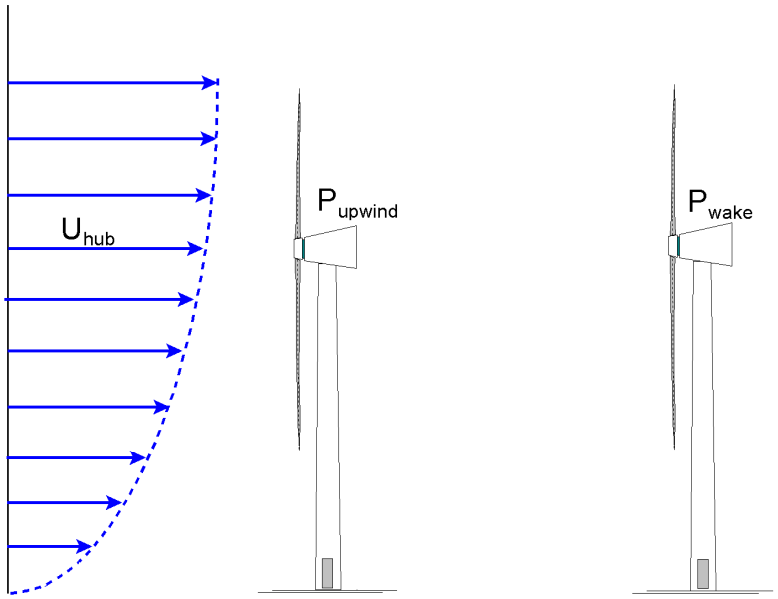

Figure 8.11: *Wind farm inflow conditions*

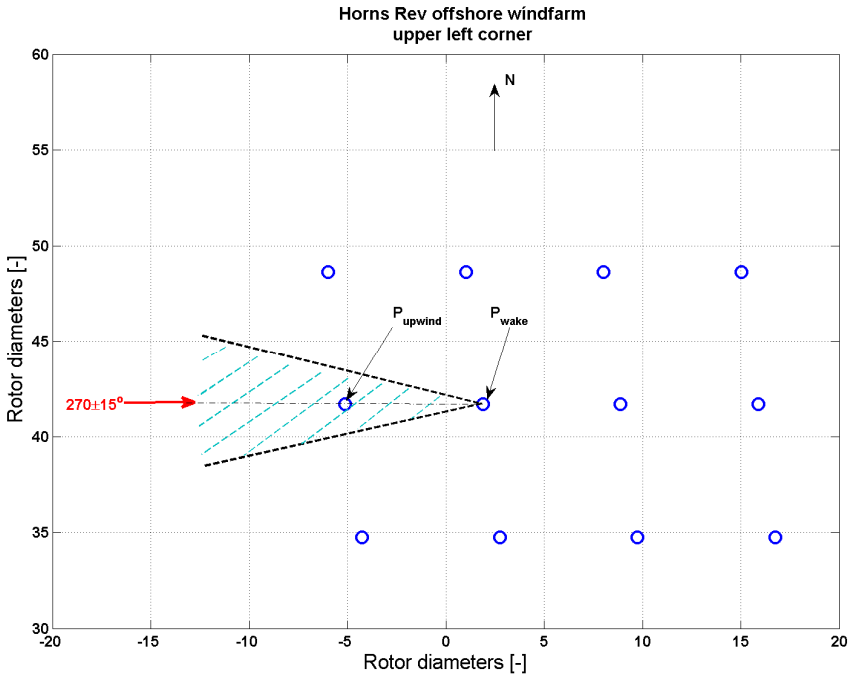

Figure 8.12: *Definition of 30 degrees flow sector along a row of turbines.*

I

8.3.5 Data filtering

The purpose of using data filtering is to identify the exact flow conditions in the wind farm. The simple flow case includes only two turbines, a free turbine and a turbine operating in the wake of the free turbine Figure 8.11. Increasing inflow complexity results in more than 2 turbines, and it necessary to include the operational conditions of all upstream turbines; which can influence the operational behaviour of the turbine operating in the wake. The filtering process consists of a number of subtasks with reference to Figure 8.11 and Figure 8.12 and according to the list of conditions below:

i) The free [upwind] wind turbine is grid connected 100% during each 10 minute period;
ii) The object [wake] wind turbine is grid connected 100% during each 10 minute period;
iii) All wake generating wind turbines should be grid connected 100% during each 10 minute period;
iv) Flow stationarity through the whole wind farm is required.

Rule iii) requires a detailed mapping of the wind farm with reference to the actual flow sector. It is required that all wind turbines inside the flow sector are grid connected as shown in Figure 8.12. This criterion could involve 5-10 turbines depending on the inflow sector, but turbines at a distance larger than 40-50 diameters can be neglected.

Figure 8.13 illustrates an inflow sector equal to 263±2.5° for turbine E03. The wake generating turbines; which have to be taken into account are A05, B04, B05 & C04 when using an offshore wake expansion coefficient 0.05.

Rule iv) on flow stability throughout the wind farm has been included to identify and exclude situations where the wind farm is partly covered by a weather front[7]. The size of a wind farm determines whether it is necessary to implement these criteria.

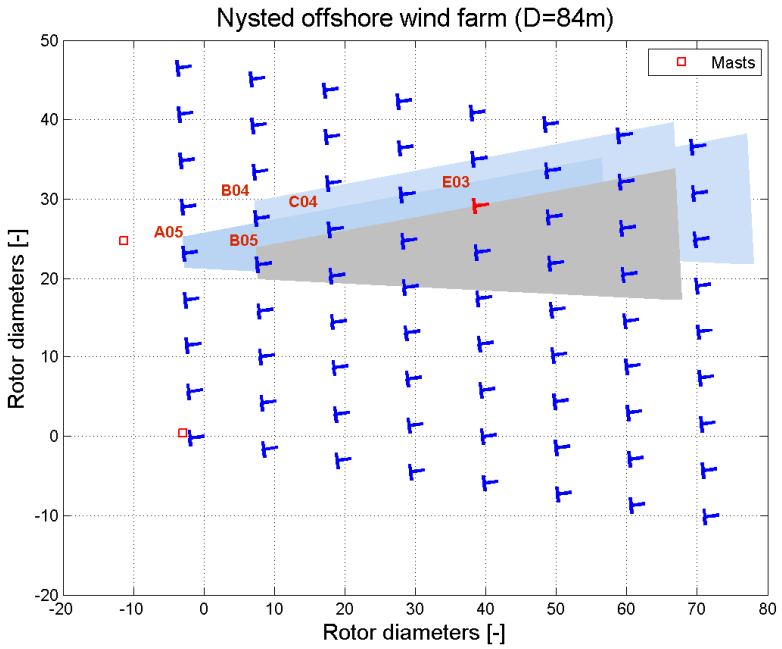

Figure 8.13: *Wake generating wind turbines located upwind to the turbine E03 for a westerly inflow sector of 263±2.5°.*

[7] Flow stability can be obtained by only selecting the second of two consecutive records.

8.4 Data query and wake analysis

The complexity of data query depends on the amount of available turbines ranging from 1) small wind farms with 10 - 40 turbines distributed in irregular patterns (complex terrain and complex inflow conditions) and low availability; to 2) large wind farms consisting of 30 – 100 wind turbines and requires more than 1 complete year of operation distributed in regular patterns (offshore and regular inflow conditions). Both types of wind farms or a combination can be analysed; but wind farms situated in a complex terrain is a big challenge due to the complex inflow conditions and even varying hub heights caused by the topography. Such analysis requires more than 1 year of observations to establish a robust estimate of the power deficit distributions.

The wake analysis can be formulated according to the complexity of the flow conditions and the purpose:

i) Deficit for pairs of turbines as function of wind direction;
ii) Deficit for pairs of turbines with different spacing;
iii) Maximum deficit as function of turbulence intensity and spacing;
iv) Deficit along rows of turbines;
v) Deficit for partly covered turbines as function of flow direction;
vi) Deficit variations at different atmospheric conditions;
vii) Park efficiency.

These analyses require a well-organized and quality controlled dataset according to the guidelines given in the previous section.

i) Deficit for a pair of turbines.

This basic query requires a pair of [identical] turbines with spacing between 2-10D. The purpose of this analysis is to determine the deficit distribution a function of wind direction - as illustrated in Figure 8.1. Refined analysis can reveal the dependence due to wind speed level, rotor speed, pitch angle or turbulence intensity, because the angular deficit distribution depends on the actual operational turbine condition.

ii) Deficit for a pair of turbines with different spacing.

The deficit distribution for some distinct spacing can be derived from a group of turbines located in a wind farm. With turbines arranged in an ordinary grid; this enables at a number of spacing to be validated when taking into account the diagonals directions. Figure 8.4 defines three distinct spacing 7D, 9.4D and 10.4D for the Horns Rev wind farm.

iii) Maximum deficit as function of turbulence intensity and spacing.

The maximum deficit is determined for a narrow flow sector as function of turbulence intensity and spacing as shown in Figure 8.14. The flow sector size depends on the number of available observations, but increasing the flow sector decreases the maximum deficit value. Figure 8.14 illustrates a clear correlation between deficit, turbulence intensity and spacing. This query can furthermore be applied for more than two turbines and will then result in a multiple wake deficits estimate.

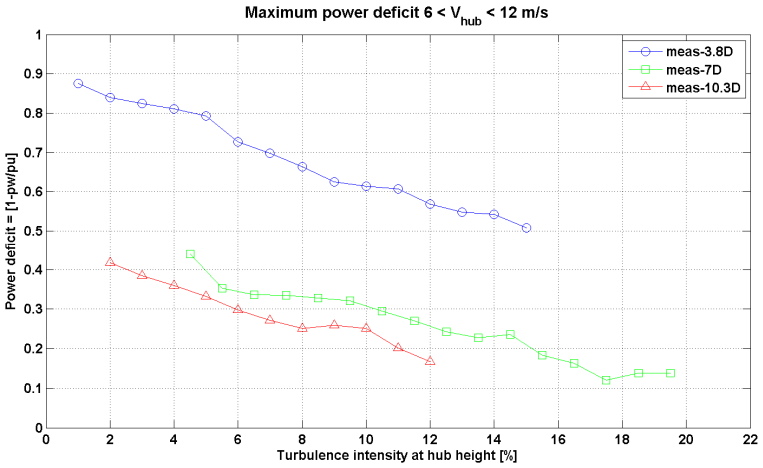

Figure 8.14: *Maximum power deficit for three different spacing - as function of turbulence intensity.*

iv) Deficit along row of wind turbines.

The state-of-art wake analysis has been focusing on the power deficits along row of turbines. The query sequence consists of a "guided walk" from wt01 to wt98 with reference to the "up-wind turbine" including the filtering constraints as defined in the previous section .

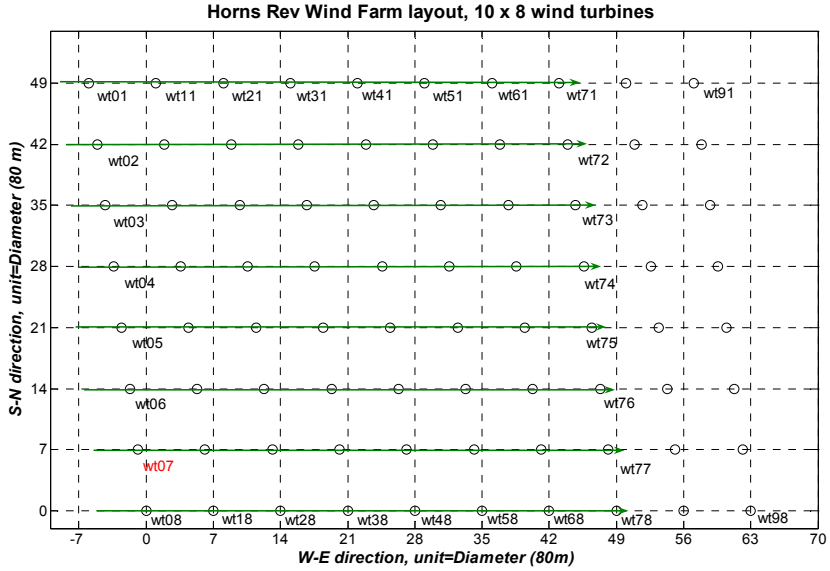

Figure 8.15: *Horns Rev offshore wind farm, with an indication of 270^o flow direction along the rows of wind turbines. The reference turbine for this flow analysis is wt07.*

A flow case from the Horns Rev wind farm, Figure 8.15 estimates the deficit for a narrow flow sector along the lines of turbines in a small sector (270 ±2.5°). The power deficit is presented in tables (Table 8.3) with reference to wt07. Each number in the table represents approximately 6 hours of measurements after data filtering. Reducing the data filtering criterion will result in more observations and increased scatter, where the scatter is defined as the standard deviation of the power deficit values. The flow direction is perpendicular to the first column (Col 1) of turbines and the findings indicate a small lateral power gradient for this flow case; which represents 3-4 km distance. A lateral power gradient is often observed in large offshore wind farms and depends on local inflow conditions like fetch distance. The power deficit is visualized in Figure 8.16 and indicates a scatter between the rows, partly due to the lateral gradient. The deficit for row 1 and 8 has been excluded in the averaged deficit due to partly free inflow.

Table 8.3: *Mean power deficit at Horn Rev for flow direction = 270±2.5° and V_{hub}=8±0.5m/s*

Flow case 8: Power deficit [filters: wake & stationarity]										
	Col 1	Col 2	Col 3	Col 4	Col 5	Col 6	Col 7	Col 8	Col 9	Col 10
row 1	1.02	0.74	0.73	0.71	0.72	0.68	0.65	0.63	0.61	0.59
row 2	1.01	0.72	0.71	0.69	0.65	0.65	0.63	0.58	0.57	0.57
row 3	1.02	0.69	0.69	0.64	0.63	0.61	0.61	0.58	0.57	0.56
row 4	1.02	0.69	0.67	0.65	0.63	0.61	0.57	0.59	0.58	0.57
row 5	0.99	0.67	0.67	0.62	0.62	0.60	0.60	0.59	0.59	0.55
row 6	1.01	0.64	0.64	0.60	0.60	0.59	0.58	0.58	0.55	0.54
row 7	1.00	0.63	0.62	0.58	0.56	0.55	0.55	0.53	0.52	0.51
row 8	0.99	0.64	0.63	0.61	0.60	0.58	0.60	0.61	0.63	0.62

The park efficiency is calculated with reference to wt07 to 66%. The inflow condition for this number is an inflow sector: 270±2.5° and a wind speed, V_{hub} = 8±0.5 m/s and the number has been calculated as the average of all individual wind turbine deficit numbers from in Table 8.3.

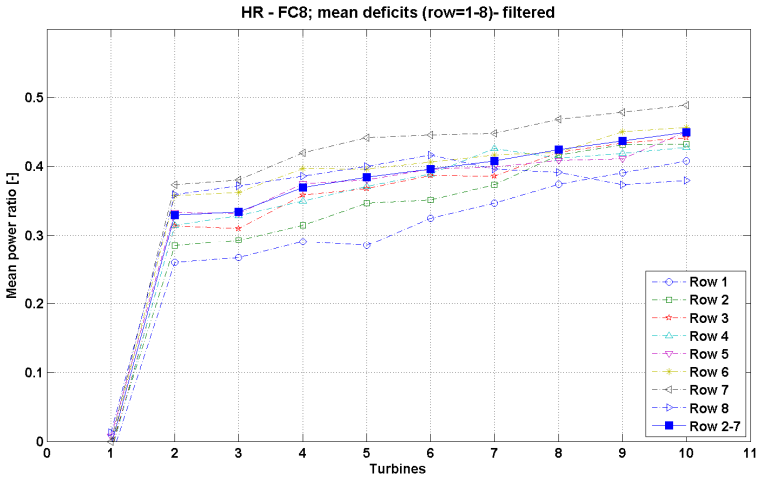

Figure 8.16: Horns Rev Flow Case 8, power deficit along wind turbine rows.

v) Deficit of turbines operating partly in wakes.

When the flow direction deviates from the line of turbines the turbines are operating partly in wake and a query process identical to case *iv)* can be used. The results are organized in tables' analogue to the example given in Table 8.3. Figure 8.17 defines the inflow sector with turbines, operating partly in wake, divided in 5 degree sectors. The averaged power deficit curves are shown for in Figure 8.18 for 7 different sectors ranging from sector 255, 265, .., 285° and the curves clearly illustrates how the power deficit depends of the wake coverage.

When the flow direction deviates from the turbine row direction a speed-up effect is visible on the outer row, because this row is partly facing the wind. This is illustrated in Figure 8.19 for an inflow deviation of 15°, compared to the direction of the row, and the power deficit is reduced considerably.

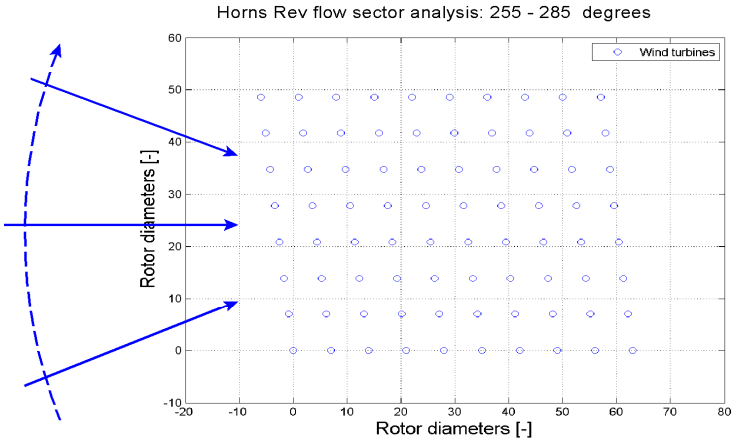

Figure 8.17: *Example of wind farm flow sector analysis for Horns Rev wind farm*.

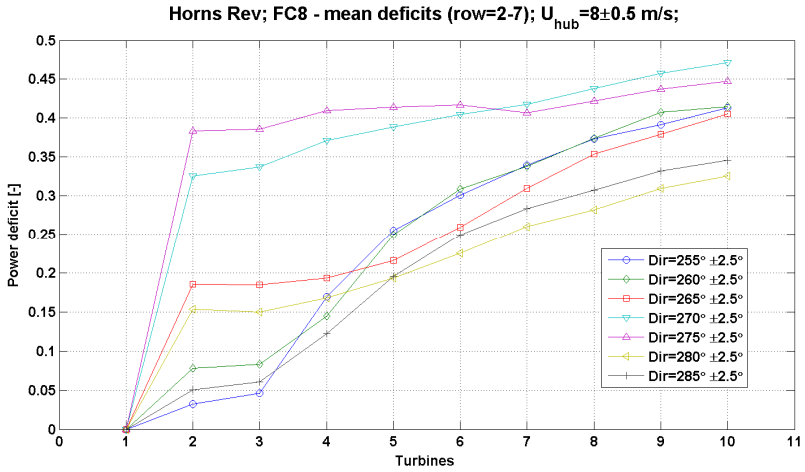

Figure 8.18: *Mean deficit for turbines operating partly in wake*.

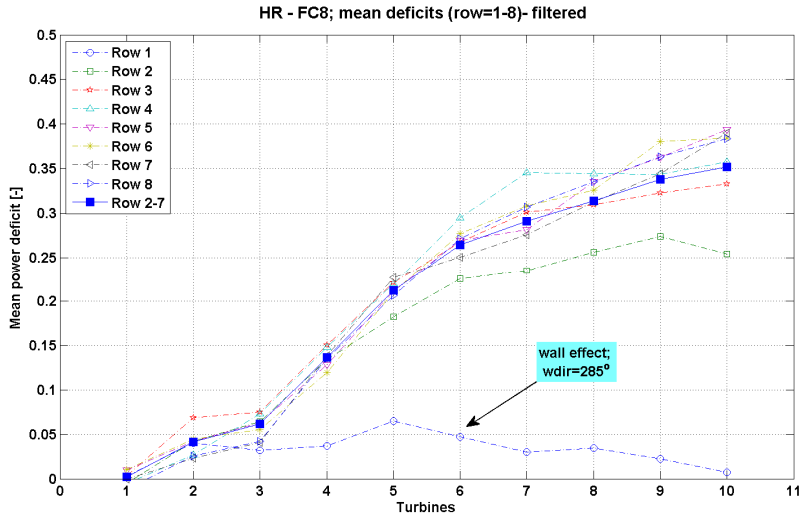

Figure 8.19: *Power deficit at Horns Rev wind farm for V_{hub}=8 m/s, WDIR=285±2.5°.*

vi) Deficit sensitivity due to stability.

Adding an additional constraint in terms of stability in the data query, reduces the number of available observations but reveals an important correlation between the deficit and the stability classification. To obtain a recent amount of data for this query, both the wind speed interval and flow sector has been increased considerably. The previous 1 m/s wind speed interval combined with 5 degree flow sectors requires a huge amount of data when including the stability constraint. Large wind speed intervals results in averaged wind turbine operational conditions; which are difficult to interpret and evaluate afterwards. The power deficits distributed according to the classification are shown in Figure 8.20 and indicates a distinct correlation to the atmospheric stability.

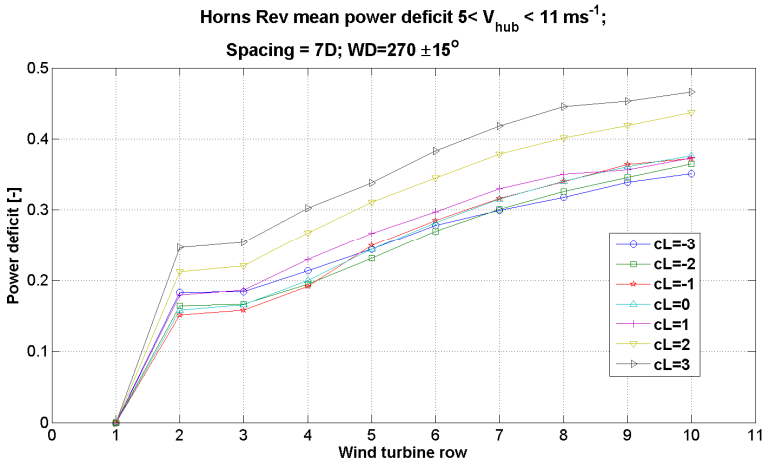

Figure 8.20: *Power deficit along rows of wind turbines for different atmospheric stability conditions.*

vii) Wind farm efficiency.

The efficiency of the wind farm deviates from an isolated wind turbine due to the wake deficit as determined above. The determination of the wind farm efficiency requires access to a free, undisturbed reference wind speed for all flow directions; which can be difficult - at least for offshore wind farms. If there is a lack of free, undisturbed inflow signals, one or two validated [corner] turbines can be used as reference in the problematic flow sectors. This method has been used with limited success to validate park model with the Dutch Egmond aan Zee wind farm park production. The layout of the wind farm is visualized in Figure 8.21 and illustrates the lack of free wind and instead two corner turbines have been included as reference.

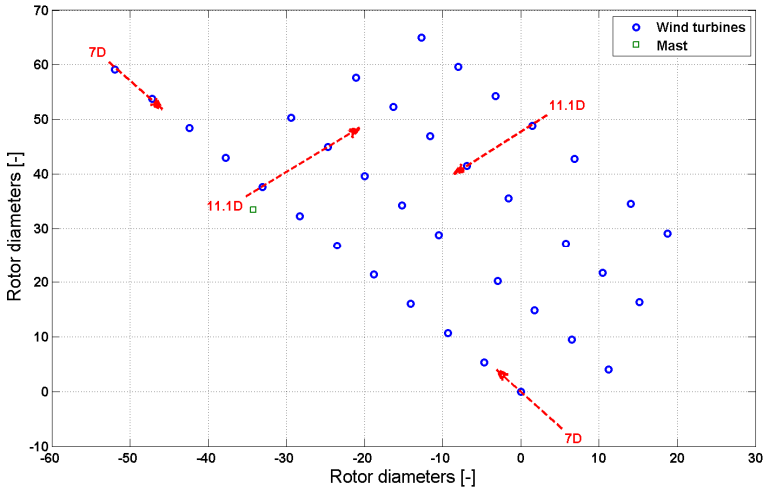

Figure 8.21: *Layout of the Egmond aan Zee(NoordZeeWind) wind farm including an indication of 7D and 11.1D spacing directions.*

The query has been performed for U_{hub}=8 m/s using the mast as reference for the SW sector and two turbines for the remaining sectors. The wind speed interval is transferred to a power interval when using the wind turbines as reference. The analysis has been divided into 5 degree flow sectors where the normalized, averaged park power is shown in Figure 8.22 with an indication of problematic sectors where park production decreases.

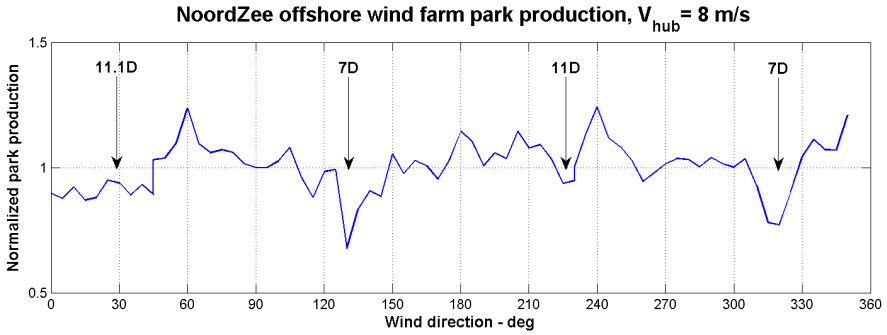

Figure 8.22: *Example of a normalized, directional park power production from the Egmond aan Zee offshore wind farm.*

The process of determining the park production as function of wind direction and wind speed is the final step for a complete park model verification.

8.5 Conclusion

As part of the UpWind WP8 code validation, a number of procedures to facilitate wind farm wake analysis have been formulated to improve and verify the data quality. A number of steps for data filtering have been formulated, which enabled a robust determination of the power deficit as function of direction, wind speed, spacing and atmospheric stability. Many power deficit results inside wind farms have been identified and used in the flow model validation during the UpWind-WP8 flow model verification.
Large offshore wind farms with a simple geometrical layout seems to be straight forward to analyse with a fair amount of high quality data (1-2 years). Wind farms with irregular layout can be more difficult to analyse, due to a lack of a robust references (mast or turbines). Wind farms located in complex terrain is difficult to analyse due to both lateral gradients and complex inflow. The most important lesson learned is that the quality of the wake analysis correlates very much on quality and the amount of data.

8.6 Acknowledgement

Horns Rev offshore wind farm: We would like to acknowledge VESTAS A/S, Vattenfall AB and DONG Energy A/S for data from the Horns Rev wind farm.
Nysted offshore wind farm: We would like to acknowledge Siemens Wind Power, DONG Energy A/S and E.On Sweden for data from the Nysted wind farm.
NoordZee/Egmond Aan Zee offshore wind farm: We would like to acknowledge VESTAS A/S and NoordZeeWind B.V. for data from the NoordZee wind farm.

8.7 References

[1] Réthoré et al. “Systematic Wind Farm Measurement Data Filtering Tool for Wake Model Calibration”, Presented at the European Offshore Wind Conference (EOW2009)
[2] Database of Wind Characteristics; http://www.windata.com/
[3] Larsen, G.C. et.al. ” The dependence of wake losses on atmospheric stability characteristics. To be submitted in 2011.
[4] Hansen,K.S.;Barthelmie,R.;Jensen,L.E.;Sommer,A. ” The impact of turbulence intensity and atmospheric stability on power deficits due to wind turbine wakes at Horns Rev wind farm”, submitted to Wind Energy, Wiley in 2010.

9. Recommendation to IEC61400-12-2 Wake sector analysis

May 18th 2006. To the members of the IEC 61400-12-2 expert working group
From P.J. Eecen

9.1 Introduction and background

Data from the ECN 2.5MW research turbines have been analysed in order to characterise the effect of wakes on nacelle anemometer power performance verification.

The ECN Wind turbine Test site Wieringermeer (EWTW) is located in the Netherlands, 35 km East of ECN, Petten. The test site consists of:

- 4 locations with a 100m and a 108m high meteorological mast for testing of prototype wind turbines up to 6MW,
- a wind farm of five research 2.5MW wind turbines equipped for experimental research with another 108m high meteorological mast (MM3),
- and a measurement pavilion with offices and computer center for the measurements.

Several ECN research projects are carried out at the EWTW. The collected data comprise:

- Meteorological data measured in the 108m masts
- SCADA data (134 signals, ten-minute statistics) from each of the five research turbines, obtained from Nordex by e-mail on a daily basis
- Measured SCADA data (8 signals, 25Hz) from each of the five research turbines
- Measured condition monitoring data from five research turbines
- Measured loads from one research turbine
- Maintenance reports of the research turbines

Data from the research turbines and the meteorological mast MM3 at EWTW are collected and are stored in the Wind Data Management System (WDMS) since September 2004. The Wind Data Management System is a database developed by ECN for storage of data at the signal dependent sample rates together with 10-minute statistic values (average, minimum, maximum and standard deviation). For the analysis shown here, 1-minute statistic values have been created. The test site and its surroundings are characterised by flat terrain, consisting of mainly agricultural area, with single farmhouses and rows of trees. The lake IJsselmeer is located at a distance of 2 km east of meteorological masts 1 and 3.

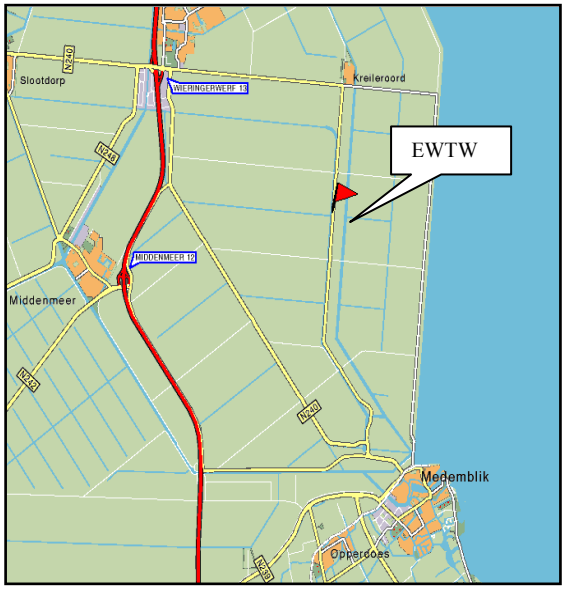

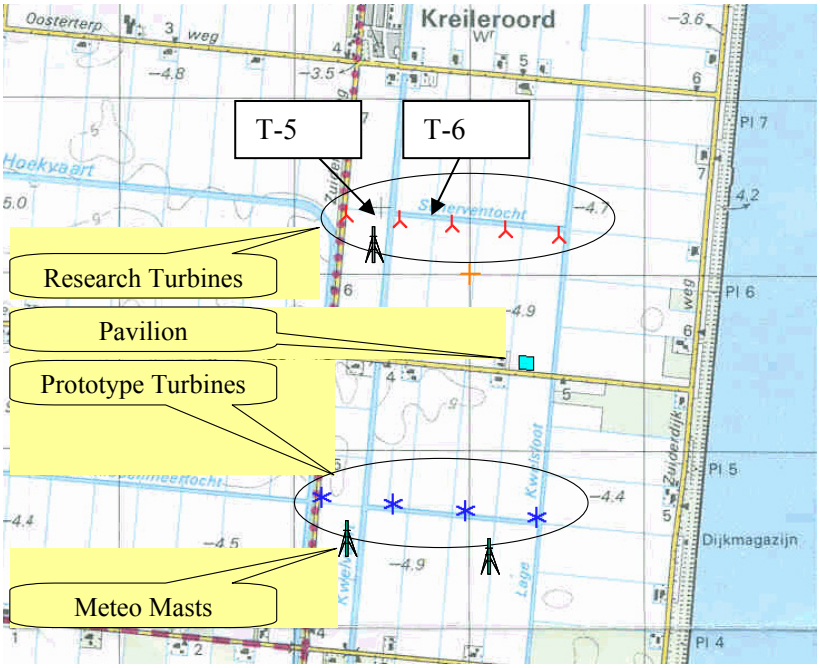

Figure 9.1 *The research turbines are installed in a line which has an angle with respect to North of 95 degree. The distance between successive turbines is 305m. In the present analysis, turbine 6 is investigated, which is in the wake of the undisturbed turbine 5. The research turbines have hub height of 80m, rotor diameter of 80m and nominal power of 2500 kW.*

One-minute averaged data are made and selections are made for the wind direction between 200 and 320 degrees (from the West) and for 'normal' operational modes of the turbine. At these wind directions, turbine 5 is operating in undisturbed wind conditions, while turbine 6 is operating in the wake of turbine 5. For sectors of 2 degrees wide data are selected and with this data nacelle power performance is calculated. The power curves are quite similar and the largest differences are found in the power coefficient. The largest differences in the power coefficient inside and outside the wake are found at nacelle wind speeds of 6 to 8m/s.

The wind direction reference is chosen to be the nacelle direction of turbine 6, which is in the wake of turbine 5. The nacelle direction of turbine 6 would also be used when nacelle power performance verification would have been applied. To show the effect of the wake of turbine 5 on the produced power by turbine 6 the power deficit is indicated in Figure 9.2: the ratios of the power produced by turbine 5 (free) and turbine 6 (in the wake) are plotted in wind direction bins of 2 degree where turbine 5 produced between 1000 and 2000 kW. From the power deficit, it is clear that the wake is centred around 270 degrees. (from geometry the wake should be at 275 degrees).

The (normalized) average power coefficient between 6 and 8m/s based on nacelle power performance is also indicated as function of nacelle direction. This is done both for turbine 5 as turbine 6, where turbine 5 indicates the accuracy of the applied method, since there should be minimal effect of wind direction. The normalized power coefficient correlates with the wake of turbine 5. This analysis clearly shows that the power performance analysis is influenced by nearby turbines in a wind direction sector ±15 degrees with respect to the direction of the disturbing turbine.

Note 1: discussions at the Glasgow meeting expected a hat-like behaviour of the nacelle power performance analysis inside a wake. This behaviour cannot be found in the data analysed of the research turbines.

Note 2: similar results are obtained using 10-minute averages.
Note 3: according IEC 61400-12 the following numbers apply for the sector to be excluded due to wakes of neighbouring and operating wind turbines: (Ln = 305m, Dn = 80m, Ln / Dn = 3.8) and disturbed sector is 60 degrees. The disturbed sector described in IEC 61400-12 is roughly two times larger than we can derive from our analyses.

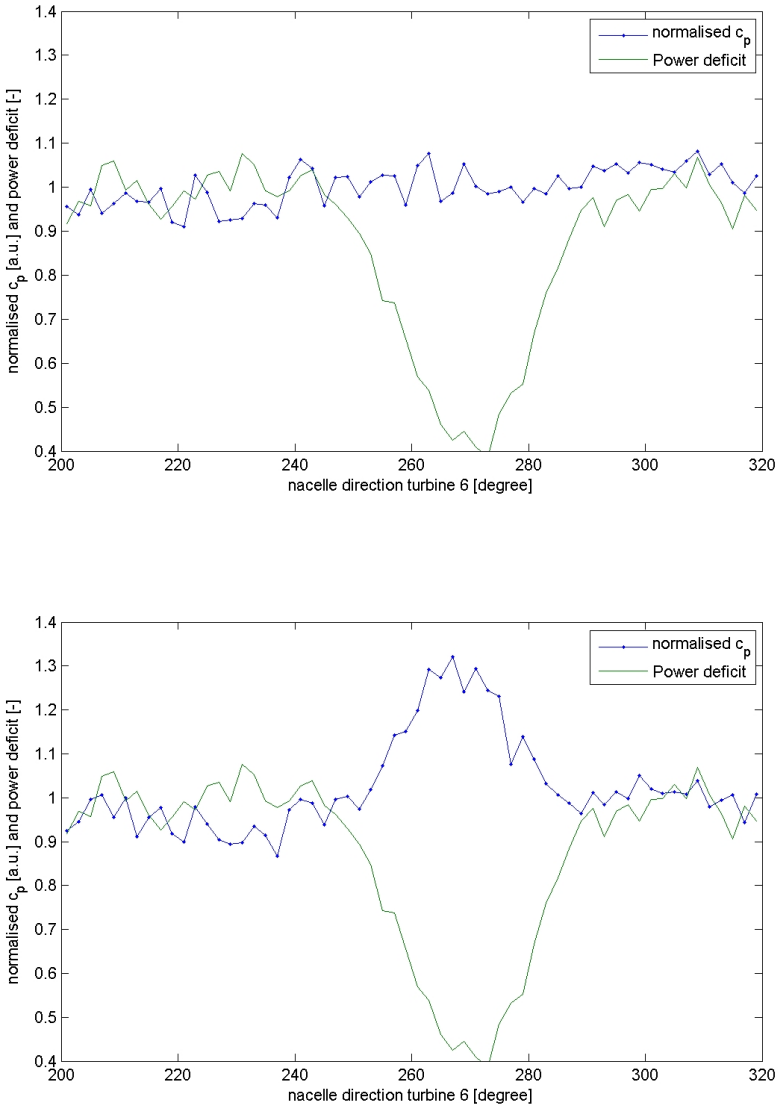

Figure 9.2. *In the upper figure the power deficit of turbine 6 due to the wake of turbine 5 is indicated (green) together with the (normalized) power coefficient for turbine 5 averaged over 6 to 8m/s (blue). The power deficit is depicted to indicate the angles at which power is influenced by the wake. For turbine 5 the (normalized) power coefficient should be independent of wind direction. In the lower figure the power deficit of turbine 6 due to the wake of turbine 5 is indicated (green) together with the (normalized) power coefficient for turbine 6 averaged over 6 to 8m/s (blue). The (normalized) power coefficient is clearly different within the wake.*

9.1.1 Additional analysis turbulence dependency

For the analysis above it would be interesting to know whether the effect of increased cp is dominated by added turbulence due to the wake or due to the nacelle anemometer method. Therefore, the same data of the above analysis (10-minute averaged) have been used to determine the dependency on turbulence. We disregarded the data within the wake. We calculated a normalized cp averaged over 6 to 8m/s and plotted the results. The (normalized) power coefficient increases with increasing turbulence. However, the effect of the wake on the nacelle power performance analysis is significantly larger.

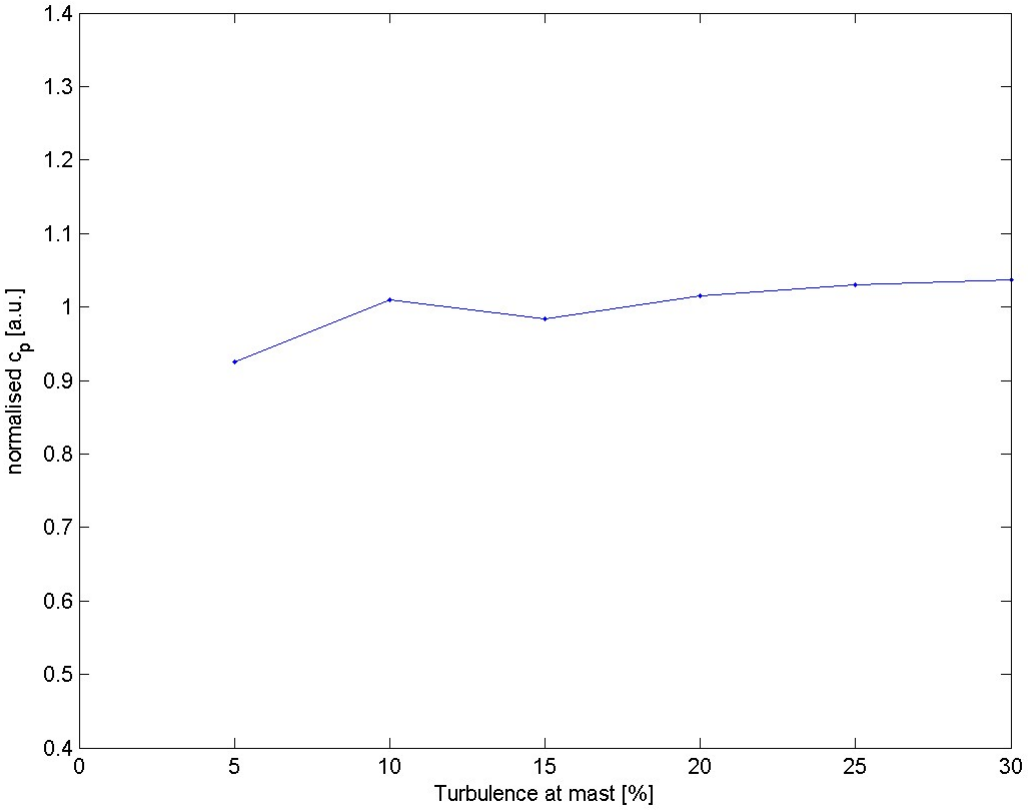

Figure 9.3. *This figure illustrates the (normalized) power coefficient for turbine 5 averaged over 6 to 8m/s. The (normalized) power coefficient increases slightly with increasing turbulence.*

10. Classification of atmospheric stability for offshore wind farms

Kurt S. Hansen, Department of Mechanical Engineering, DTU

Validation of power deficit and structural wind turbine fatigue loads on turbines in wind farms requires knowledge of the stability conditions. As part of the wake analysis performed on the Horns Rev offshore wind farm, a robust classification of the atmospheric stability has been established, based on the Bulk Richardson number.

10.1 Introduction

Determination of power deficit and structural wind turbine fatigue loads on turbines operating in wind farms requires knowledge of the stability conditions. As part of the wake analysis at Horns Rev offshore wind farm, it has been necessary to develop, implement and verify a classification method for the atmospheric stability.
The Horns Rev Wind farm consists of 80 wind turbines, arranged in a regular shape together with three offshore masts as shown in Figure 10.1. The wind farm includes one mast NW to the wind farm and two masts E east to the wind farm. The wind farm operation has been recorded during 4 years (2005 – 2008) and the wake analysis has been performed on a merger of wind turbine SCADA data and meteorological data.

10.1.1 Instrumentation

The Horns Rev wind farm includes three masts M2, M6 and M7. M2 was erected prior to the wind farm installation and has been used to determine the offshore wind resources and wind conditions, which was [partly] used to establish the wind farm design specification. Mast M2 is located approximately 2 km NW of the wind farm and is measuring free, undisturbed wind speeds more than 75% of the time. The instrumentation includes cups, vanes, thermometers and a sonic anemometer, as sketched in Figure 10.2. All measurements from these masts have been stored as 10-minute statistics in terms of mean, standard deviation, minimum and maximum values. M2 has been operational in the period 1999-2006 [1], but unfortunately there has only been one year overlap between mast and wind farm operation. Furthermore the instrumentation was not maintained well during 2005, which resulted in a lack of quality data.

M6 & M7 were installed in 2003, as part of the offshore wake measurement program and are located 2 and 6 km east of the wind farm as indicated in Figure 10.1. The mast instrumentation is identical and is located between 20 to 70 m above mean sea level - as indicated in Figure 10.2. The mast setup and the measurements representing the first period of operation have been reported in [2]. The purpose was to measure the wake properties and the masts are located inside the wind farm wake more than 60% of time.
M2 was equipped with a sonic anemometer, 50 m above sea level and a huge amount of time series has been stored in a wind repository [3]. Unfortunately the sonic anemometer was mounted on a boom pointing towards SW; which reduced the free, undisturbed inflow sector considerably 225±45°.

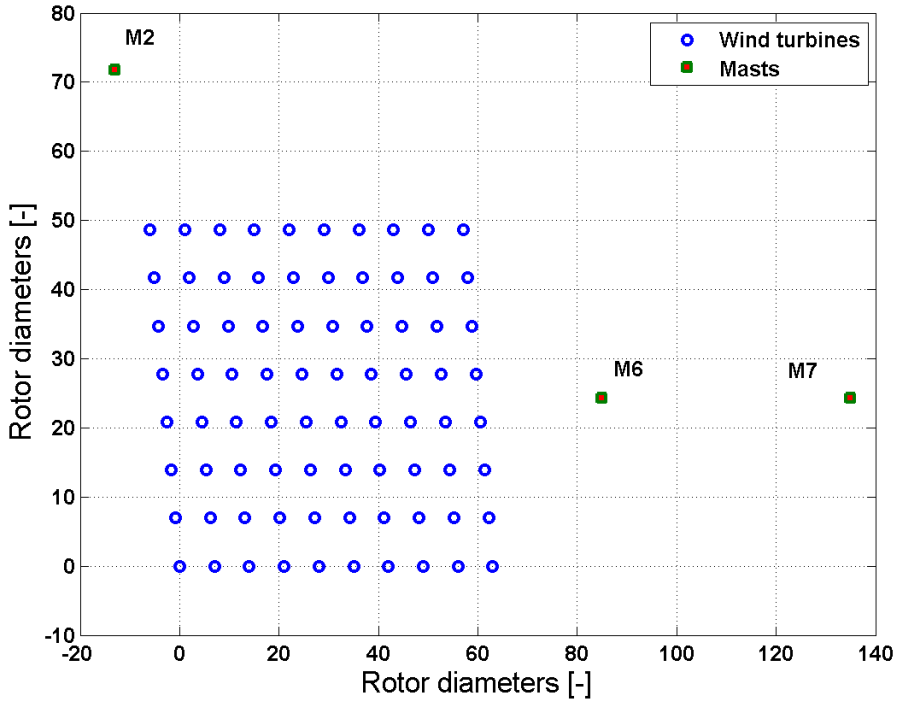

Figure 10.1: *Layout of Horns rev wind farm, including 3 offshore masts.*

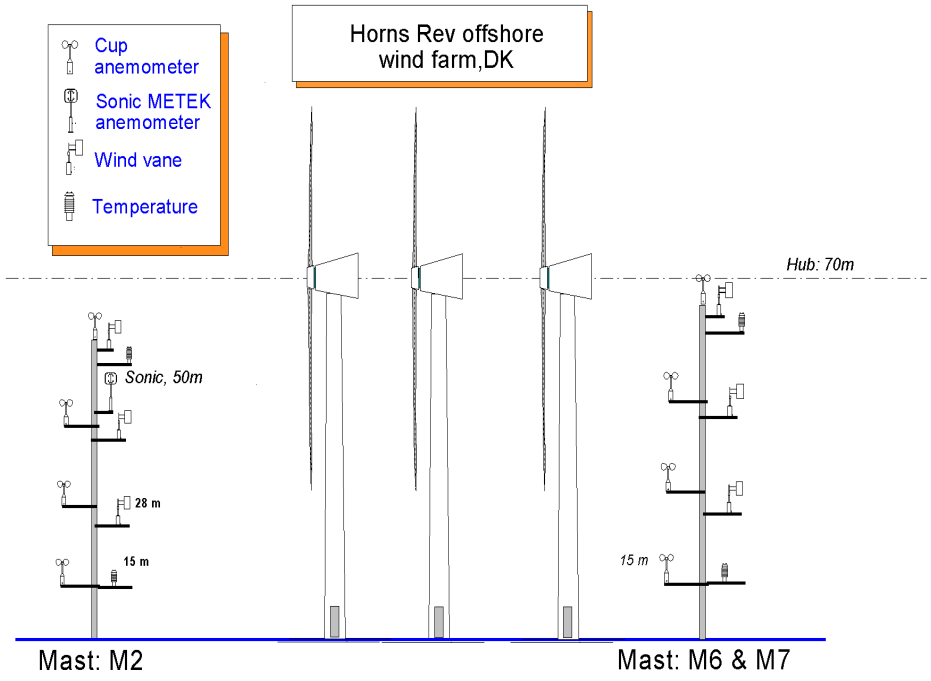

Figure 10.2: *Horns Rev offshore wind farm mast instrumentation.*

10.2 Determination of atmospheric stability.

The atmospheric stability can be expressed with the stability parameter z'/L where L is the Monin-Obukov length L and z' is a reference height. Previously the stability parameter has been determined as part of several research project mainly focusing on onshore locations with success. The wake analysis in UpWind WP8 required a stability classification and during this project three different methods have been evaluated with respect to the available signals from the Horns Rev site. Different solutions have been presented during the recent years to establish a classification and the most promising is based on the temperature gradient [4, 5]. A short description is given below, including a short summery of the main findings and problems. The problems were caused by the limited data coverage, poor data quality and the wake conditions.

10.2.1 Gradient method.

The atmospheric stability parameter z'/L has been calculated according to the gradient method applied on year 2005 measurements and was based on either the difference between 1) water and air or 2) air and air temperatures, from the wake mast M7; which had a very good signal quality and a high availability. The Richardson number (*Ri*) is calculated with (eq. 1):

$$Ri = 9.81/\left(273.15 + t_u\right) \times \left(\left(t_u - t_l\right)/\Delta h_T\right)/sqr\left(\left(U_{70} - U_{20}\right)/\Delta h_V\right) \qquad (10.1)$$

The signals from M7, used in the stability calculation are listed in Table 10.1, but situations with reduced wind speed at hub height caused by the wind farm wake were not been eliminated.

Table 10.1: *Sensors used to determine the atmospheric stability parameter*.

Sensor	Air/water	Air/air
t_u - degC	h = 64 m (asl)	h = 64 m
t_l - degC	h = -3 m (bsl)	h = 64 m
U_{70}	h = 70 m	h = 70 m
U_{20}	h = 20 m	h = 20 m
z'	31 m	37.5 m

The stability parameter z'/L has been derived from the Ri number according to (10.2), (10.3) and (10.4):

z'/L=Ri;	for Ri≤0;	(10.2)
z'/L=Ri/(1-5Ri);	for 0<Ri<0.2	(10.3)
z'/L=2×z'×Ri;	for Ri≥0.2;	(10.4)

The relation between speed ratio and the stability parameter are plotted in Figure 10.3 and demonstrates a clear correlation for negative stability parameters, while positive stability results in a large scatter.

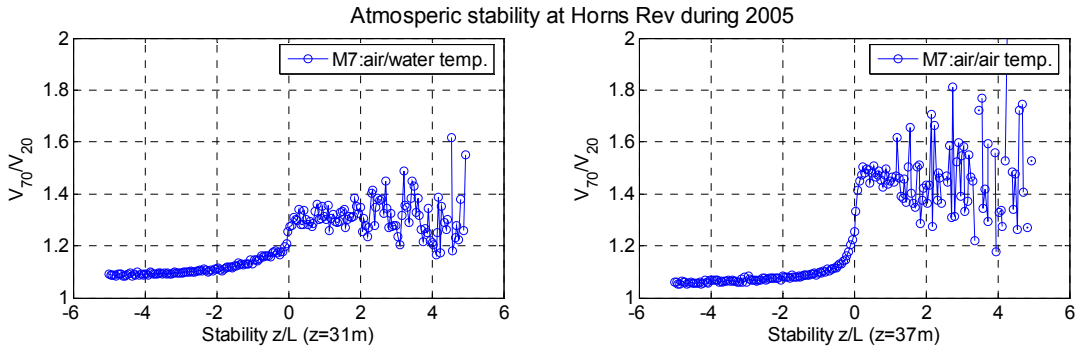

Figure 10.3: *Distribution of atmospheric stability measured at Horns Rev during 2005; a) air/water difference and b) air/air temperature difference.*

8.606 hours of measurements, recorded during 2005 were classified in 4 stability classes in Table 10.2. The main part of observations demonstrates (slightly) unstable atmospheric stratification (-12 <z'/L <-2) with reference to air/air stability.

Table 10.2: *Stability classes for Horns Rev measurements during 2005, based on air/air temperature measurements.*

Very unstable; z/L < -12	1920 hours
Unstable, -12< z/L<-2	1881 hours
Near neutral, -2 < z/L < +2	2618 hours
Stable; z/L> 2	2187 hours
Total	8606 hours

All temperature signals from Horns Rev are recorded with thermometers without calibration[8] and with a low resolution; the resolution of the derived temperature difference is low as well.

Discussion
The quality of the stability parameters, with respect to the wake analysis, have been difficult to validate, while large part of the observations represent situations where M7 is situated in the wind farm wake. The signals from M7 were selected because only a limited amount of observations exist from M2. The implementation of the stability parameter to the wake analysis is difficult, mainly due to the absence of reliable, undisturbed wind speeds.

10.2.2 Sonic measurements

A huge amount of sonic time series was recorded during 2000-2005, partly with an overlap to the wind farm operation in 2005. The Monin-Obukhov length L is derived from (10.5)

$$L = -(273+t)\times u^{*3} \Big/ (9.81\times 0.4\times w't') \qquad (10.5)$$

Where u^* and $w't'$ are derived from the time series.
The stability parameter z'/L is determined from (10.2), (10.3) and (10.4).

[8] The calibration is not documented and the maintenance is performed irregularly.

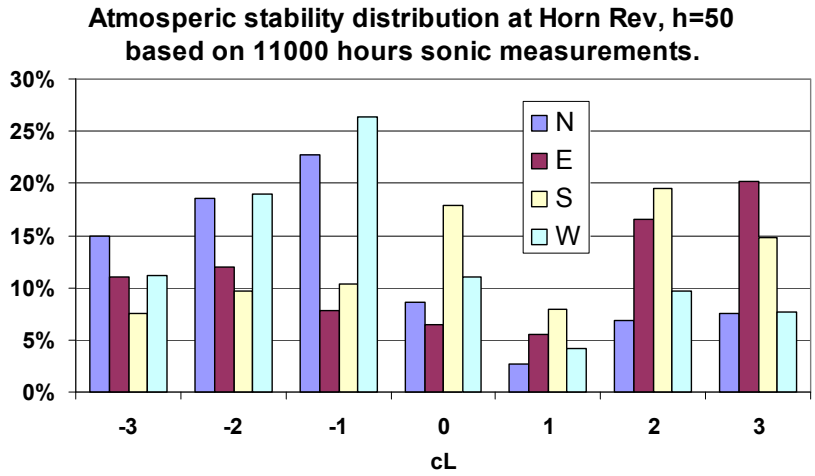

Figure 10.4: *Stability classification based on sonic measurements.*

The huge amount of stability parameters have been classified according to the classification scheme in Table 10.3 and the classification distribution for the 4 main directions (N, E, S & W) are shown in Figure 10.4.

Discussion
The quality of the calculated stability parameters seems to be fine and the distribution seems to be applicable. Unfortunately a very limited overlap between sonic measurements and the wind farm operation exist and this is not sufficient for a proper validation of this method. It needs to be verified whether the sonic height of 50 m is applicable for offshore locations or a lower offshore measuring height should be recommended.

10.2.3 Bulk-Richardson number

The flow conditions, expressed in terms of atmospheric stability classes, have been established with reference to a Bulk-Richardson approach evaluated in [4, 5, 6]. The Ri_b number is derived from a single wind speed observation (U_h), measured at 15 - 20 m height above mean sea level combined[9] with the air and water temperature difference (Δt) from (10. 6). The Obukhov length, L is derived from the Ri_b number (10.7) and (10.8) as described in [6] including the classification of the atmospheric stability.

$$Ri_b = -9.81 \times (\Delta t / \Delta h - 0.01) / (T \times (U_h / h)^2) \qquad (10.6)$$

$$z'/L = 10 \times Ri_b \qquad \text{for unstable stratification} \qquad (10.7)$$

$$z'/L = \frac{10 \times Ri_b}{1 - 5 \times Ri_b} \qquad \text{for stable stratification} \qquad (10.8)$$

The stability parameter has been derived for all available measurement (M2, M6 and M7); which were recorded before, during and after the wind farm installation. The wind speed signal at the lowest available height has been selected[10] to minimize the wake reducing effect from the wind farm.

[9] A zero wind speed at sea level is assumed.
[10] The lowest blade-tip position is 10-14 m above the measuring height but still the wake expansion could influence the recorded wind signal.

The stability classification has been adapted from a previous onshore classification [7] with reference to the Obukhov length L and is listed in Table 10.3.

Table 10.3: *Classification of atmospheric stability at Horns Rev, based on Obukhov length L.*

Class	Obukhov length [m]	Atmosperic stability class
cL=-3	-100 ≤ L ≤ -50	Very unstable (vu)
cL=-2	-200 ≤ L ≤ -100	Unstable (u)
cL=-1	-500 ≤ L ≤ -200	Near unstable (nu)
cL=0	|L|>500	Neutral (n)
cL=1	200 ≤ L ≤ 500	Near stable (ns)
cL=2	50 ≤ L ≤ 200	Stable (s)
cL=3	10 ≤ L ≤ 50	Very stable (vs)

The use of the air-water temperature difference to define stability classes tends to limit the number of observations in the near-neutral class. A further issue at Horns Rev is that temperatures are measured to a precision of 0.1 ºC. At moderate temperatures and at moderate/high wind speeds this inaccuracy will lead to minor differences (e.g. observations being placed in the very stable class rather than the stable class). However when temperature differences are small, the measurement precision could lead to erroneous classification. Hence the neutral and near-neutral classes (c_L=-1, 0, 1) should be seen as a broad grouping. The classification has been validated for four flow directions and Table 10.4 lists the amount of available hours. The validation is performed for a wind speed interval of 5.5 – 10.5 m/s at hub height (70m); which was used in the wake analysis, performed in UpWind WP8.

Table 10.4: *Number of hours representing wind speeds interval of 6 - 10 m/s, representing a 60° inflow sectors.*

5.5 - 10.5 m/s	M2	M6	M7
	hours	hours	hours
N (partly free)	1829	1773	6821
E (wake)	1701	1604	6811
S (partly free)	2458	2149	7881
W (wake)	2548	2254	8053

Validation for northern wind direction

The free M2 wind speed measurements, recorded 15m above mean sea level, have been used to classify the stability. A northern flow direction 0±30° has been validated according to the recorded number of hours in Table 10.4, with an operating wind farms.

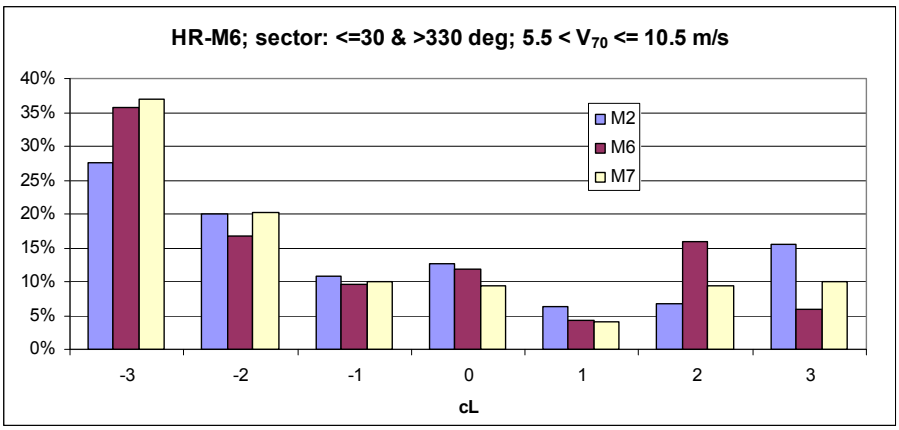

Figure 10.5: *Comparison of classification results, based on measurements from M2, M6 & M7 at Horns Rev recorded in the northern sector.*

Discussion
Figure 10.5 demonstrates a fair agreement between the stability classifications, derived from the [free] mast M2 compared to the derived results from mast (M6 & M7). The agreement is less for the vu, s and vs classes, compared to the results obtained in the western sector.

Validation for eastern wind directions
The free M6 wind speed measurements, recorded 20m above mean sea level, have been used to classify the stability. An eastern flow direction 90±30° has been validated for the measurements listed in Table 10.4.

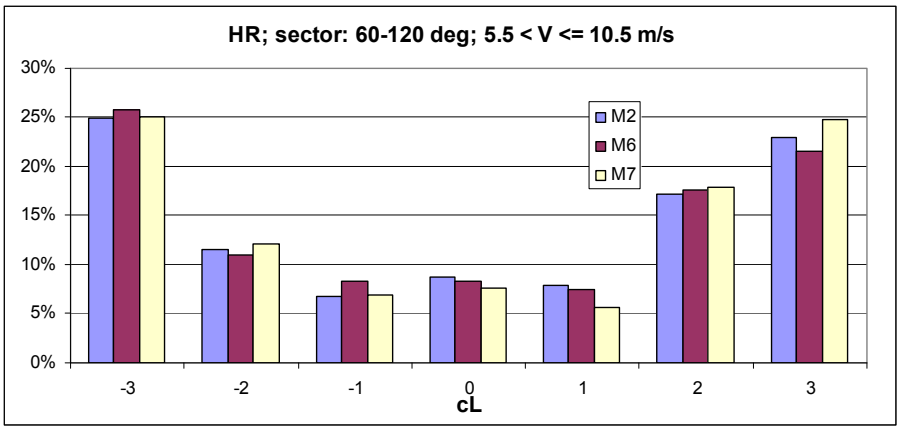

Figure 10.6: *Comparison of classification results based, on measurements from M2, M6 & M7 at Horns Rev recorded in the eastern sector.*

Discussion
Figure 10.6 demonstrates a very high agreement between the stability classifications derived from the free mast M6 compared to the derived results from the wake mast M2 and the other free mast M7.

Validation for southern wind directions
The partly free M6 wind speed measurements, recorded 20m above mean sea level, have been used to classify the stability. A southern flow direction 90±30° has been validated according to the recorded numbers of hours in Table 10.4, with an operating wind farms.

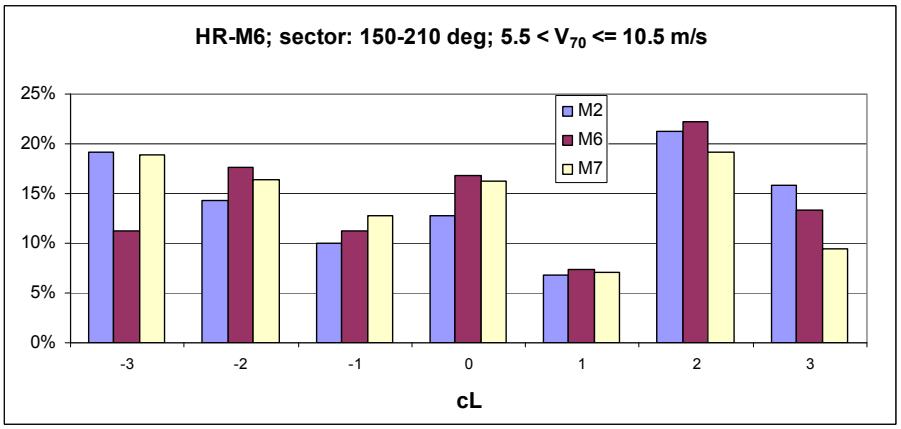

Figure 10.7: *Comparison of classification results, based on measurements from M2, M6 & M7 at Horns Rev recorded in the southern sector.*

Discussion
Figure 10.7 demonstrates a good agreement between the stability classifications derived from the free mast M6 compared to the derived results from the partly free mast M2 and the other

free mast M7 for a southern flow sector. The agreement is less for the vu and vs classes, compared to the other sectors.

Validation for western wind directions
The free M2 wind speed measurements, recorded 15m above mean sea level, have been used to classify the stability. A westerly flow direction of 270±30° has been validated according to the recorded numbers of hours in Table 10.4, with an operating wind farms.

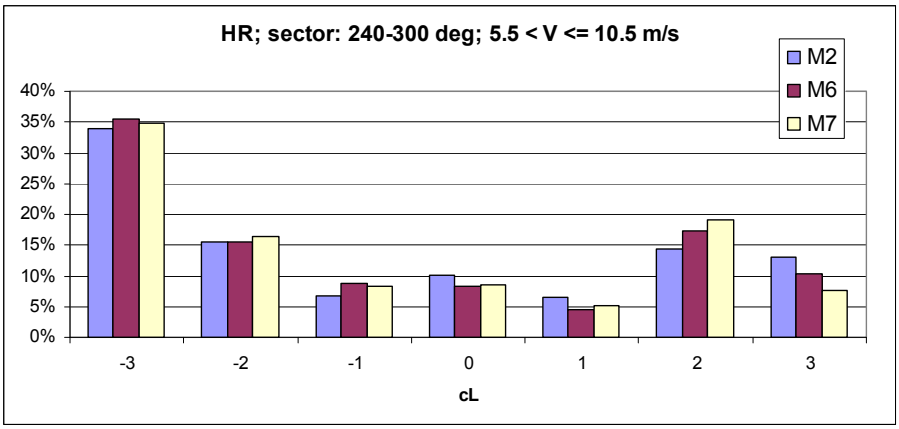

Figure 10.8: *Comparison of classification results, based on measurements from M2, M6 & M7 at Horns Rev recorded in the western sector.*

Discussion
Figure 10.8 demonstrates an very good agreement between the stability classifications derived from the free mast M2 compared the derived results from the wake masts (M6 & M7) for a western flow sector. This is the most important flow sector for the wake analysis and the deviations related the stable and very stable classes complement each other.

Conclusion:
The validation reveals a high level of confidence between the different atmospheric stability classifications when using measurements recorded at low heights. The main difference is probably related to the quality of the measurements and seems to be isolated within the stable or the unstable classes. This enables us to use the most appropriate measurements, when categorizing the flow deficits near wind farms. A sector-wise validation of the stability classification shows no large discrepancy between “wake” and “no-wake” situation.

10.3 Site classification

This sector-wise site classification of stability is performed for three wind speed intervals 5-10 $ms^{-1,}$ 10-15 ms^{-1} and 15-20 ms^{-1} in relation to the wind turbine inflow speed. As shown in Figure 10.9 - Figure 10.11, the frequency of stability classes is similar for the first two wind speed intervals, but differs for high wind speeds. For the 5-10 ms^{-1} grouping, the frequency of stable conditions tends to be higher. All three wind speeds intervals demonstrate a similar directional distribution of the stability including a larger number of near-neutral and unstable classes from the south and west and higher numbers of stable conditions from the east and south. This is broadly in line with the distribution of stability classes shown previously. Figure 10.9 - Figure 10.11 shows the sector-wise distribution of the stability classes for these three wind speed intervals. Approximately 30% of all observations are categorized as stable or very stable at low wind, but this number decreases with increasing wind speed.

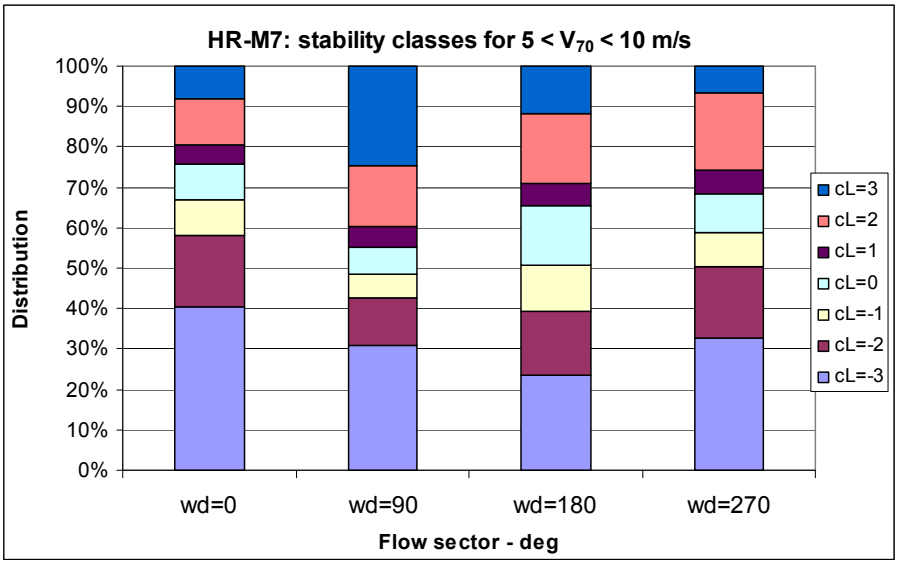

Figure 10.9: *Sector wise stability distributions for wind speed interval 5 – 10 m/s at 70 m level.*

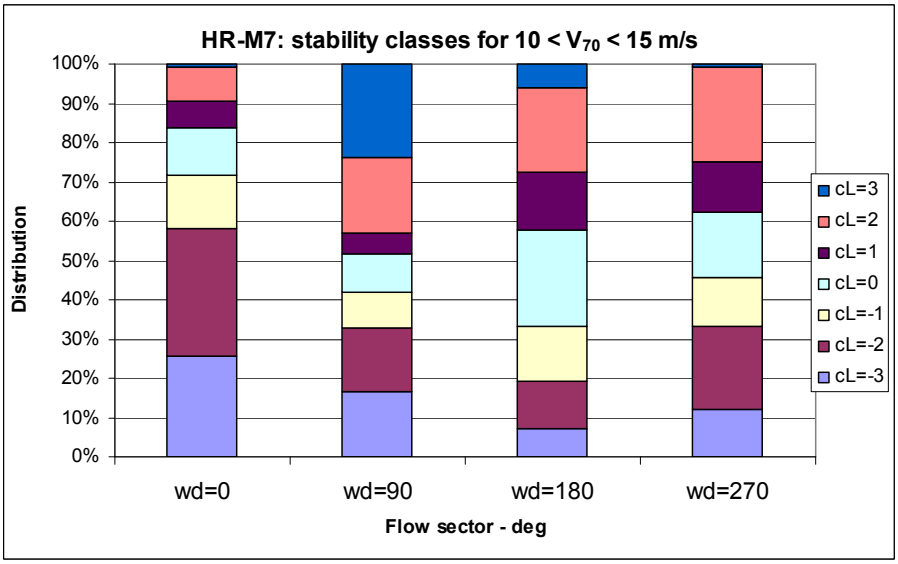

Figure 10.10: *Sector wise stability distributions for wind speed interval 10 – 15 m/s at 70 m level.*

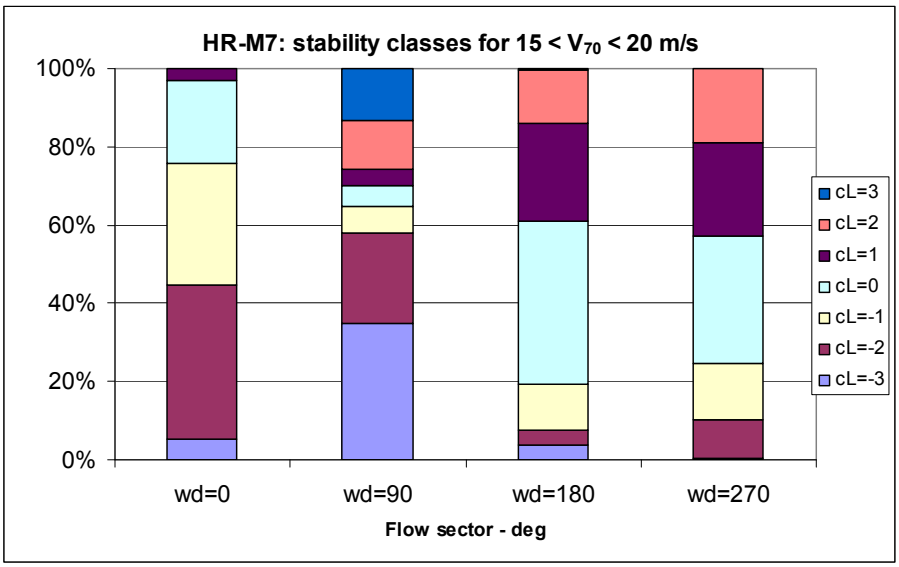

Figure 10.11: *Sector wise stability distributions for wind speed interval 15 – 20 m/s at 70 m level.*

10.3.1 Turbulence intensity correlated to atmospheric stability.

Combining the turbulence intensity with the stability classification enables a determination of the turbulence intensity as function of wind speed, grouped according to the stability classification. The turbulence intensity is bin-averaged as function of wind speed for each stability classes and illustrated in Figure 10.11. The figure reveals very low turbulence intensity for stable conditions and a distinct correlation between intensity and stability. As shown, the differences between unstable and neutral conditions are relatively small and stable conditions can be associated with low turbulence levels.

The stability classification is derived with reference to M7 measurement; where the wind speed is chosen at the lowest level ($U_{surface} \equiv 0$) to avoid the potential wake effects and T_{air}: Absolute temperature is chosen at the lowest level.

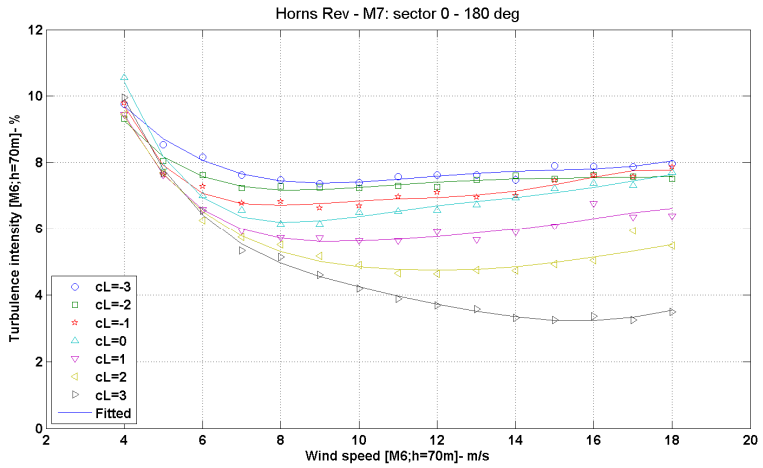

Figure 10.12: *Three years of average turbulence intensity measurements (2005-2007) for easterly winds - grouped on stability.*

Discussion

Figure 10.12 demonstrates a strong correlation between the bin-averaged turbulence intensity as function of wind speed for the stable stratification, while the distribution for neutral to unstable stratification is almost equal.

10.4 Wake analysis

The previous section demonstrates a correlation between turbulence intensity level and the atmospheric stability. Due to lack of free, undisturbed turbulence measurements at offshore locations it is not possible to perform a wake analysis for different turbulence levels. Instead a wake analysis has been performed according the stability classification. Wake analysis [8, 9] is performed for different flow cases defined with the wind speed interval, flow sector, flow direction and turbine spacing. Furthermore all wake generating turbines need to be in grid connected. Results from wake analysis are presented as power deficit along rows of turbines with fixed spacing.

10.4.1 Power deficits for 7D spacing.

The averaged power deficit along 6 rows has been extracted for different stability classes based on wind speed in the range 5 – 11 m/s and for a narrow, 5 degree flow sector.
Figure 10.13 shows the deficit along a row of turbines with 7D spacing for a narrow flow sector. The figure demonstrates a strong correlation between the deficit level and the stability, where very stable and stable stratification results in the largest deficits.
Figure 10.14 shows the deficit along a row of turbines with 7D spacing, for a 30 degrees flow sector. The figure demonstrates a strong correlation between the deficit and the stability, where stable and very stable stratification results in the largest deficit. The remaining deficit curves are grouped and represent all other stability classes.

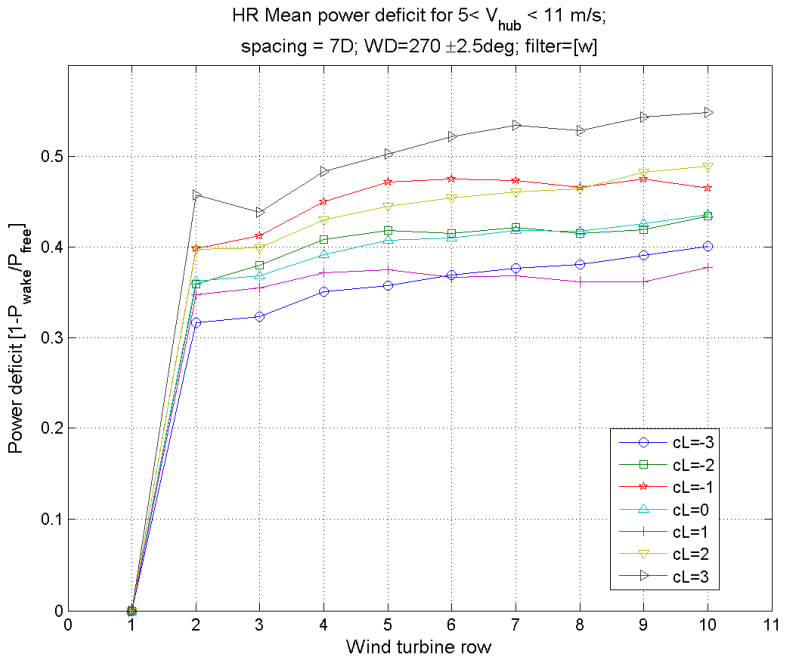

Figure 10.13: *Averaged power deficit along 6 rows with 10 turbines grouped in stability classes, for a small inflow sector of 270 ±2.5°.*

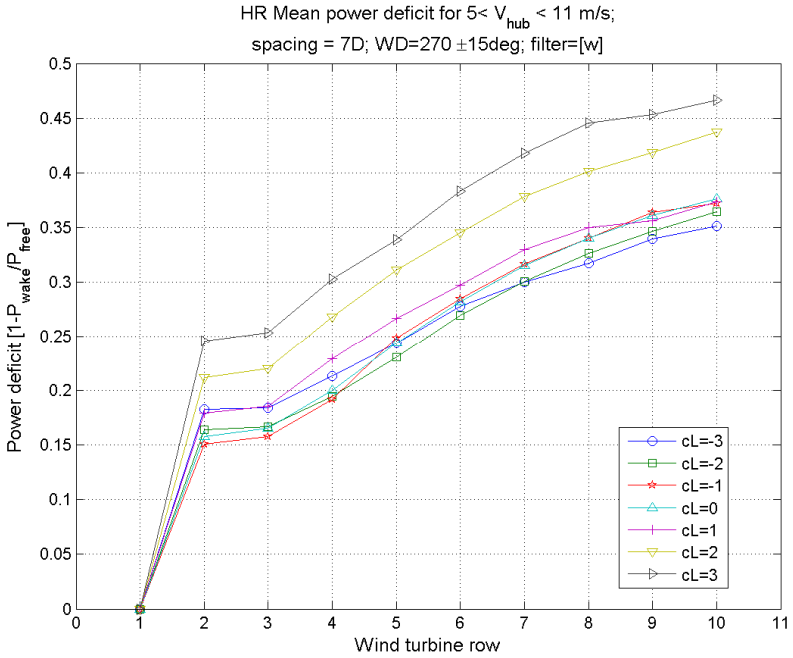

Figure 10.14: *Averaged power deficit along 6 rows each of 10 turbines, grouped in stability classes, for an inflow sector of 270 ±15° and 7D spacing.*

10.4.2 Power deficit for 9.4D spacing.

The averaged power deficit along 5 rows has been extracted for different stability classes based on wind speed in the range 5 – 11 m/s and for a 30 degree flow sector.
Figure 10.15 shows the deficit along a row of turbines with 9.4D spacing for a 30 degrees flow sector. The figure demonstrates a strong correlation between the deficit level and the stability, very stable stratification results in the very large deficit. The remaining deficit curves are almost equal and represent all other stability classes.

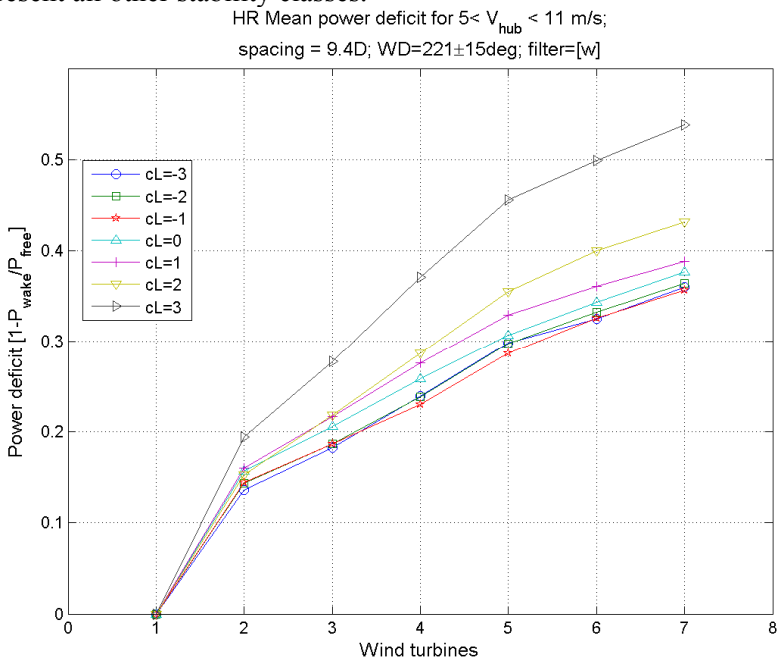

Figure 10.15: *Averaged power deficit along 6 rows each of 7 turbines, grouped in stability classes, for an inflow sector of 221 ±15° and 9.4D spacing.*

10.4.3 Power deficit for 10.4D spacing.

The averaged power deficit along 5 rows has been extracted for different stability classes based on wind speed in the range 5 – 11 m/s and for a 30 degree flow sector.
Figure 10.16 shows the deficit along a row of turbines with 10.4D spacing for a 30 degrees flow sector and are identical to the result for 9.4D spacing.

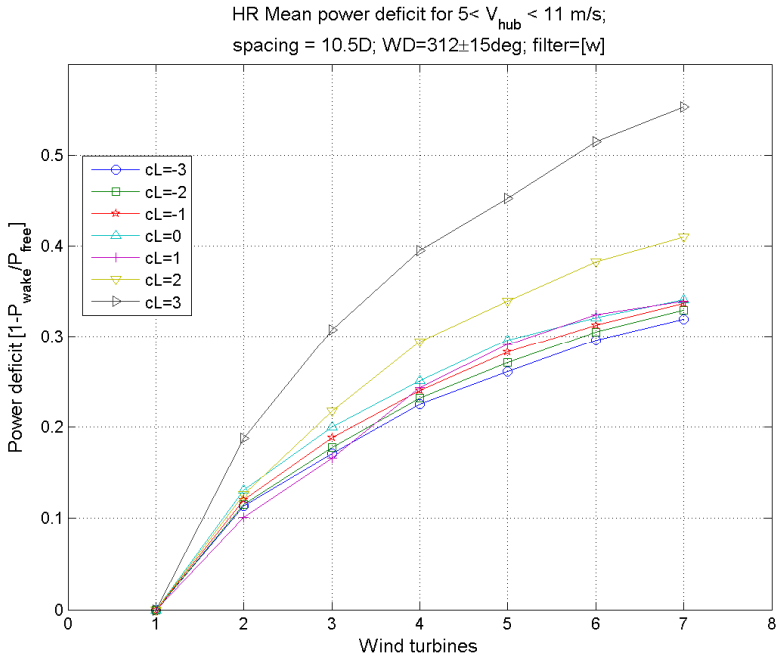

Figure 10.16: *Averaged power deficit along 6 rows each of 7 turbines, grouped in stability classes, for an inflow sector of 312 ±15° and 10.4D spacing.*

Discussion
All the deficit curves display a distinct correlation between atmospheric stability and power deficit and increases downstream to the wind farm.

10.5 Conclusion

A robust method to classify the atmospheric stability at an offshore wind farm site from the Bulk-Richardson number has been developed. The method limits the influence from wake generating wind turbines, while it is based on observations, recorded at low heights. The classification, which has been validated with offshore measurements, demonstrates a high correlation between the turbulence intensity. Finally a strong correlation between stability and power deficit inside the wind farm has been identified. Unfortunately, an additional constraint in the wake analysis requires more observations.

10.6 Acknowledgement

We would like to acknowledge VESTAS A/S, Vattenfall AB and DONG Energy A/S for using data from the Horns Rev offshore wind farm.

10.7 References

[1] Sommer,A.;Hansen,K.S. “Wind Resources at Horns Rev. 2002”, Techwise:Eltra PSO-2000 Proj. nr. EG-05 3248. DK-7000 Fredericia.

[2] Sørensen,P.B.;Hansen K.S. “Wake effect east of the Horns Rev offshore wind farm.” 2002, Elkraft System:PSO-F&U 2002/FU 2103. DK-7000 Fredericia.

[3] Database of Wind Characteristics; http://www.windata.com/

[4] Lange, B. et.al. "Modelling the vertical wind speed and turbulence intensity profiles at prospective offshore wind farm sites" In: Proceedings CD-ROM. 2002 global wind-power conference and exhibition, Paris (FR), 2-5 Apr 2002

[5] Jens Tambke et.al. "Offshore Meteorology for Multi-Mega-Watt Turbines" presented at EWEC 2006

[6] Larsen, G.C. et.al. ” The dependence of wake losses on atmospheric stability characteristics. To be submitted in 2011.

[7] Penã, A.,et.al. "Extending the wind profile much higher than the surface layer", presented at EWEC2009 in Marseille, FR 16-19 March 2009.

[8] Hansen,K.S.;Barthelmie,R.;Jensen,L.E.;Sommer,A. ” The impact of turbulence intensity and atmospheric stability on power deficits due to wind turbine wakes at Horns Rev wind farm”, submitted to Wind Energy, Wiley in 2010.

[9] Barthelmie,R. et.al. "Flow and wakes in large wind farms:Final report; Appendix 6: Guideline to wind farm wake analysis"; Report number Risø-R-1765(EN), January 2011

11. Quantification of Linear Torque Characteristics of Cup Anemometers with Step Responses

Troels Friis Pedersen

11.1 Introduction

The standard IEC61400-12-1 on power performance measurement [1] requires cup anemometers to be classified according to the normative Annex I. An informative Annex J proposes methods for determination of physical characteristics such as aerodynamic torque characteristics. The described method uses wind tunnel measurements where a thin rod is attached to the cup anemometer rotor and extended to the outside of the flow. Here a torque sensor and a motor are connected with the rod. The torque is then measured for typical wind speeds and rotational speeds of the cup anemometer. The torque measurements are normalized to obtain a generalized torque coefficient curve that is normally not linear. Meanwhile, if the torque coefficient above and below equilibrium speed ratio (tunnel calibration condition) both can be approximated to linear curves going through the equilibrium speed ratio point, then it might be possible to determine the linear curves with two step responses, one starting from below and one from above tunnel wind speed. This paper describes an investigation of the consequences of making classification of cup anemometers with such partial linearised torque coefficient curves. The investigation is described in further detail in the report [5].

11.2 Basic torque characteristics of cup anemometers

The generalised torque coefficient curve of a cup anemometer [1, annex J] is defined as the torque coefficient versus the speed ratio. The torque coefficient is related to the aerodynamic rotor torque as:

$$C_{QA} = Q_A/(\frac{1}{2}\rho A R u^2) \qquad (11.1)$$

The speed ratio λ is defined as:

$$\lambda = \frac{\omega R}{U - U_t} \qquad (11.2)$$

In case the torque coefficient curve can be assumed linear on either side of the equilibrium speed ratio the torque coefficient can be expressed as:

$$\begin{cases} \lambda \leq \lambda_0 : C_{QA} = \kappa_{low}(\lambda - \lambda_0) \\ \lambda > \lambda_0 : C_{QA} = \kappa_{high}(\lambda - \lambda_0) \end{cases} \qquad (11.3)$$

Where $\lambda_0 = R/A_{cal}$ is the equilibrium speed ratio.
When determining the torque relations we consider the friction in bearings being negligible. Thus the calibration coefficients relates to the speed ratio as:

$$U = A_{cal}\omega + B_{cal} = \frac{A_{cal}N}{2\pi}f + B_{cal} = \frac{R}{\lambda_0}\omega + U_t \qquad (11.4)$$

11.3 Linearized torque characteristics of a typical cup anemometer

The analysis is based on measurements of torque coefficients made in the FOI wind tunnel by Jan-Åke Dahlberg in the ACCUWIND project [2]. The cup anemometers that were considered are shown in Table 11.1 with some details.

Table 11.1 *Main data of cup anemometers analysed in ACCUWIND project [2]*

	NRG	RISØ	THIES-FC	VAISALA	VECTOR
Cup diameter (mm)	51	70	80	54	51
Projected cup area A (mm^2)	2000	3850	5030	2290	2040
Rotor diameter (mm)	191	186	240	184	155
Radius to cup centre R (mm)	70	58	80	65	52
Pulses/rev	2	2	37	14	25
Rotor inertia I (kg m^2)	$1.01 \cdot 10^{-4}$	$0.992 \cdot 10^{-4}$	$2.8888 \cdot 10^{-4}$	$0.6141 \cdot 10^{-4}$	$0.441 \cdot 10^{-4}$

The torque coefficient curves from [2] were linearized on either side of the equilibrium speed ratio, forced through the point of equilibrium speed ratio. The linearized torque coefficient data are shown in Table 11.2 together with derived time constants from inertia in table 1 and with a standard air density of 1.23kg/m^3.

Table 11.2 *Linearized torque coefficient data from linearization of Main data of cup anemometers analysed in ACCUWIND project [2]*

	NRG	RISØ	THIES-FC	VAISALA	VECTOR
Equilibrium speed ratio λ_0	0.28461	0.29653	0.28022	0.28964	0.26177
Slope at low speed ratios κ_{low}	-6.5282	-4.9590	-4.6520	-4.8867	-6.6914
Slope at high speed ratios κ_{high}	-6.3595	-6.2140	-5.6901	-4.7652	-6.3128
Ratio $\kappa_{low}/\kappa_{high}$	1.0265	0.7980	0.8176	1.0255	1.0600

11.4 Classification of cup anemometers with linear torque

The torque coefficient curves from the ACCUWIND project [2] were applied for classification according to the standard IEC61400-12-1 [1]. The results with the full torque coefficient curves and tilt response data measured in the FOI wind tunnel were compared with the results using the linear torque coefficient data from Table 11.2. The results are shown in Table 11.3.

Table 11.3 *Classification of Risø P2546a using Cm curves or two linearized curves*

	Class A	Class A linearized	Class B	Class B linearized
Risø P2546	1.39628	1.39404 (-0.16%)	5.09301	5.0887 (-0.09%)
Thies First Class	1.78074	1.76010 (-1.17%)	3.87461	3.89775 (+0.59%)
Vector	1.82939	1.84430 (+0.81%)	4.48396	4.26761 (-5.07%)
Vaisala	2.22558	2.14491 (-3.63%)	11.9380	11.8207 (-0.98%)
NRG Max40	2.41664	2.52689 (+4.36%)	8.28358	7.98579 (-3.73%)

The comparison of classification results from Table 11.3 shows very good results. The largest deviation is 5.07% on the classification value. Considering that other uncertainties are significant in the whole classification process, this is an indication that linearized torque coefficient curves can be considered sufficient for classification.

11.5 Step response measurement procedures

There are two standards that consider step response measurements.
The recommended practice document IEA-11 [3] considers step response measurements in order to determine the time constant and the distant constant. The step response model used in the IEA-11 document is described as:

$$u(t) = u_0 + \Delta u\left(1 - \exp\left(-\frac{t - t_0}{\tau}\right)\right) \qquad (11.5)$$

In IEA-11 a linear fitting of a conversion of the step response function is proposed:

$$\ln\left(1 - \frac{u(t) - u_0}{\Delta u}\right) = -\frac{t - t_0}{\tau} \qquad (11.6)$$

The standard ISO 17713-1 [4] on wind tunnel test methods for rotating anemometer performance describes step response measurements in order to determine the distance constant. The model used is described as:

$$U_t = U_f\left(1 - \exp\left(-\frac{t}{\tau}\right)\right) \qquad (11.7)$$

And the distance constant is determined from:

$$L_U = U\tau \qquad (11.8)$$

The standard requires 10 step response measurements made at 5m/s and 10m/s. The time constant τ is determined from data measured between 30% and 74% of the tunnel wind speed, and the distance constant is determined by multiplying the tunnel wind speed with the time constant.

When we want to determine torque coefficient characteristics from step response measurements we have to find an appropriate method for determination of the slopes of the torque coefficient curves below and above the equilibrium speed ratio. Theoretical considerations documents and derive such a procedure [6]. The result is that the slopes can be derived as:

$$\kappa = -\frac{2I(u_0 + \Delta u - U_t)}{\rho A R^2 (u_0 + \Delta u)^2 \tau} \qquad (11.9)$$

11.6 Step response measurements – an example

An example of a step-up response made by WindGuard is shown in Figure 11.1. The cup anemometer is a Risø P2546 and the tunnel wind speed is 5m/s. Using the IEA-11 fitting procedure we get the logarithmic expression as function of time as shown in Figure 11.2.

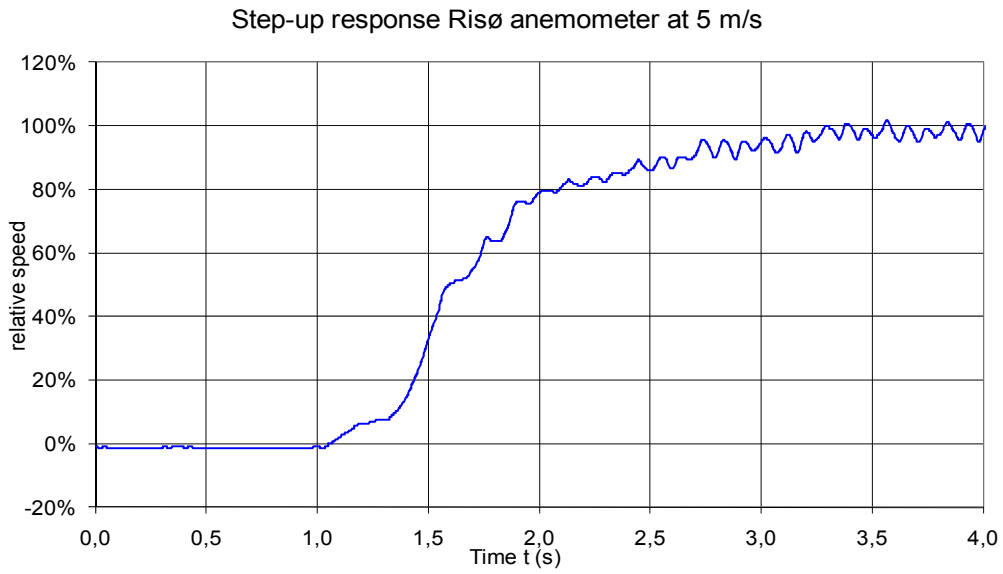

Figure 11.1 *Step-up response of Risø P2546 cup anemometer at 5m/s tunnel wind speed.*

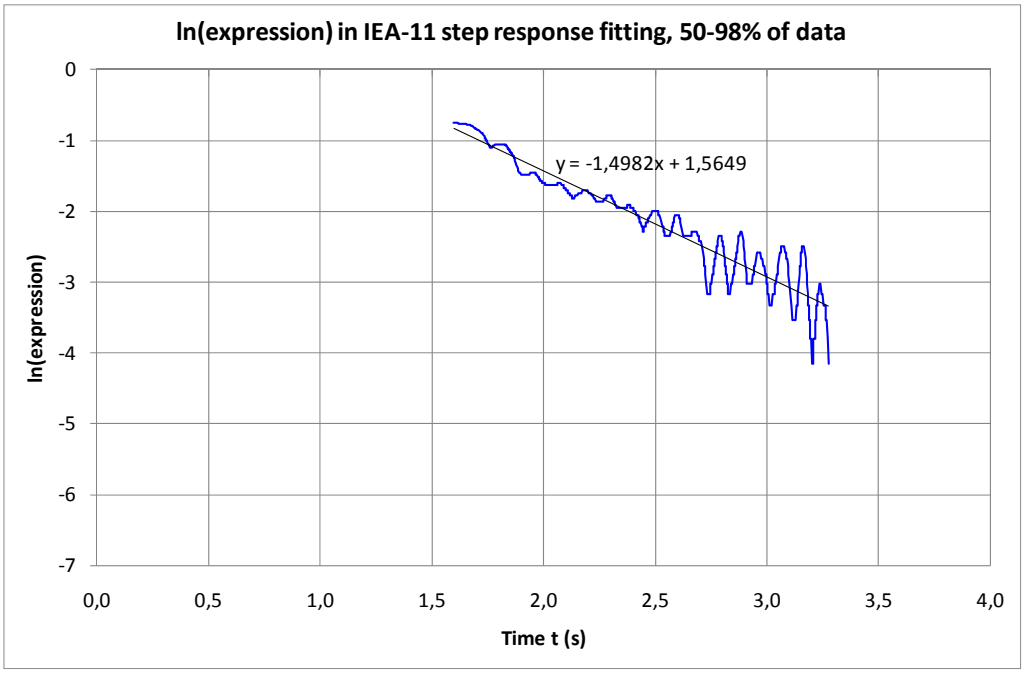

Figure 2

Figure 11.2 *ln-expression from IEA-11 step response fitting procedure using 50-98% of step-up data*

Figure 11.3 shows a speed-down response of the same Risø cup anemometer, first speeded up to 200%, and Figure 11.4 shows the ln-expression for a relative speed range of 150-102%, which seems to cover quite well the essential part of the step response.

Figure 11.3*Step-down response of Risø P2546 cup anemometer at 5m/s tunnel wind speed.*

Figure 11.4*ln-expression from IEA-11 step response fitting procedure using 150-102% of step-down data.*

The step responses were performed more than once. Table 11.4 shows the results, where they are compared with the values from linearization of the torque curves from the ACCUWIND project.

Table 11.4 *Slopes of linear torque coefficient curves for Risø P2546 cup anemometer determined with torque measurements according to [2] and with step responses*

Risø torque coefficient slopes	Torque measurements ACCUWIND linearised	Torque measurements step responses	Ratio step/ACCUW
Equlibrium speed ratio λ_0	0.29653		
Slope at low speed ratios κ_{low}	-4.9590	-3.493	0.704
Slope at high speed ratios κ_{high}	-6.2140	-4.088	0.658
Ratio $\kappa_{low}/\kappa_{high}$	0.7980	0.8545	1.071

From Table 11.4 it is seen that the step response method gives about 30% lower torque coefficient slopes than the linearized torque from the measurements in the ACCUWIND project. The torque coefficient slope values are proportional to the rotor inertia and the slopes of the ln-expressions, but reverse proportional to the time constants. The reason for the difference might be due to additional inertia in the rotating test equipment during the tests, but the cause has not been identified. The deviation is slope ratios is only 7%. It can be shown that the maximum overspeeding (at high frequencies) is only dependent on the ratio between the slopes of the torque coefficient curves. In this case it might be satisfactory for the classification only to know the ratio with a good accuracy.

11.7 Conclusions

The step response model of the IEA-11 document intrinsically leads to linear torque coefficient curves for step responses from low or high speed ratios. The slopes of the linear torque coefficient curves can thus be determined from the step response time constants. The intercept of the linear torque coefficient curves, which is the equilibrium speed ratio, is determined from the normal wind tunnel calibration gain value. The standard ISO 17713-1 recommends step response data in the speed ratio range 30-75% to be used. This seems to be in a range that is outside of the usual range being used in classification according to IEC61400-12-1. In practice, a range closer to equilibrium speed ratios should be used; 50-98% for speed-up step responses and 150-102% for speed-down step responses. The step response measurements can satisfactorily determine linear torque coefficient characteristics of cup anemometers with the only assumption that the friction in bearings is negligible with respect to determination of aerodynamic torque characteristics. Meanwhile, slope values were found to be about 30% too low. The step response method may be improved by adding more inertia to the rotor to extend the data and to reduce torque ripples due to the cups, and by determining the rotor inertia with high accuracy.

11.8 References

[1] IEC 61400-12-1, 2005 Wind turbines – Part 12-1: Power performance measurements of electricity producing wind turbines

[2] Pedersen TF, Dahlberg J-Å, Busche P, "ACCUWIND – Classification of Five Cup Anemometers According to IEC61400-12-1", Risø-R-1556(EN), May 2006

[3] IEA-11 Wind Speed Measurement and Use of Cup Anemometry, Recommended Practices for Wind Turbine Testing and Evaluation, 1999

[4] ISO 17713-1, 2007 Meteorology – Wind Measurements – Part 1: Wind tunnel test methods for rotating anemometer performance

[5] Pedersen TF, "Quantification of Linear Torque Characteristics of Cup Anemometers with Step Responses", Risø-I-3131(EN), February 2011

12. Generics of nacelle anemometry

Troels F. Pedersen

12.1 Introduction

The generic influence of the flow induction on nacelle anemometry was studied lately by Sten Frandsen. He published a paper at the EWEC conference 2009 in Marseille [1] with five co-authors, including the author of this article. The paper was the last work of Sten Frandsen on nacelle anemometry, which was a dedicated topic in his large variety of research. He sadly passed away autumn 2010. This article is an extract from his paper.
Nacelle anemometry is the state of the art wind measurement method for turbine regulation and performance verification. The option of using the nacelle anemometer when determining the power curve of a wind turbine is attractive since it is much cheaper than erecting a separate meteorological mast and simpler since all data signals are already recorded in the wind turbine's control and data recording system. In particular, the consequences of the effect of rotor flow induction must be dealt with, but also the local flow distortion over the nacelle where nacelle anemometry is positioned is necessary to consider in turbine regulation and performance verification. Thus, if the power changes it must a priori be expected that the rotor flow speed changes, even if the free wind speed is unchanged. In that case the calibration of the nacelle anemometer is changed, effectively introducing an error to the test. In the paper of Sten Frandsen [1], previous investigations of nacelle anemometry is reviewed, the relevance of Betz theory is investigated by means of CFD computations, and the generic errors caused by the rotor flow induction is evaluated, estimated and exemplified.

12.2 Review of nacelle anemometry

Nacelle anemometry as an option for power performance verification was identified in the beginning of the 1990'ies, where some developers and manufacturers started to apply nacelle anemometry in the context of commercial contracts. The method included the calibration of the nacelle anemometer, already installed on the top of the nacelle of the wind turbine, against an unobstructed met mast at a reasonably flat location in the wind farm. The method was first mentioned in 1994 [2], which deals with trends in power performance measurement techniques and recommendations with respect to positioning of the wind sensor on the nacelle is presented. In the mid 1990'ies the concept was assessed in several European research projects. Antoniou [3,4] investigated nacelle anemometry on a 1MW wind turbine by positioning the nacelle anemometer at different height above the nacelle and he made conclusions on the technique when the anemometer was in the wake of the blade root and behind the profiled blade. Another investigation [5,6,7] considered basic problems with nacelle anemometry and stipulated the uncertainty of the method. Yet another project [8] considered measurements on several different turbines throughout All assessments of the method have so far concluded that the method was acceptable when carefully addressing all aspects of the procedure. In 2007 an alternative wind measurement concept to nacelle-mounted anemometry, the spinner anemometer, was proposed, [9], the concept taking advantage of the less complicated flow field in front of the rotor. The international standardization organisation International Electrotechnical Commission decided in 2006 that the nacelle anemometry method was ripe and the decision resulted in a draft in 2008 [10], where past experience are condensed and the procedure to apply is given in detail. Following international review and revisions the standard is expected to be issued ultimo 2009.

12.3 Specific background

By convention, the power curve is the electric power plotted against the wind speed at hub height, measured at a location undisturbed by the wind turbine itself. Partly also by convention data are pre-averaged over 600 sec. The mentioned upcoming IEC standard [10] gives detailed directions for the procedure to employ, including specifications on how to calibrate the nacelle

anemometer so that the free flow speed can be deduced from the reading of the nacelle anemometer. Obviously, the nacelle anemometer is mounted on top of the nacelle at some vertical distance from the nacelle and some distance from the wind turbine rotor. In short, the calibration of the nacelle based-anemometer is made by correlating the reading from the nacelle anemometer in fairly flat, non-complex terrain with the free-flow wind speed measured in a met mast 2-3 rotor diameters upwind of the wind turbine.
However, the effect rotor induced flow is a priori correlated to the effect we want to estimate, namely rotor power. According to simple Betz theory [11] the speed of the flow passing through the rotor is the average of the free wind speed and the wind speed in the wake some distance downwind of the rotor. And further, the rotor flow speed is linked closely to the power output. Therefore, if the power changes it must a priori be expected that the rotor flow speed changes, even if the free wind speed is unchanged. In that case the calibration of the nacelle anemometer is not the same as it were beforehand. In the following we try to shed light on the generic effect rotor induction.

12.4 Flow induction at rotor

Most often, the end product of the performance test is the annual energy output of the wind turbine, conditioned on specific characteristics of the wind speed climate,

$$E_{AEP} = 8760 \cdot P_m \quad \text{where } P_m = \int_0^\infty p(u) f(u) du \qquad (12.1)$$

where $f(u)$ is the frequency distribution of wind speed at hub height at the specific wind turbine site. The number 8760 is the number of hours per year.

The purpose of the field test of the power curve by means of nacelle anemometry is to identify and quantify possible deviations relative to the warranted power curve, $\delta_p(u) = p(u) - p_{warranted}(u)$. However, when determining δ_p, the principle itself of nacelle anemometry affects the result so that the deviation has an error attached to it, $\delta_p^* = \delta_p + \delta_{p,error}$. In the following, we quantify the error in the deviation, $\delta_{p,error}$, introduced by nacelle anemometry.

12.4.1 Betz and nacelle anemometry

In the formulation of the theory for an ideal, infinitely fast rotating propeller, Betz (1920) finds that the wind speed in the wake of the rotor is $(1-2a)u$ and in the rotor plane

$$v = (1-a)u \qquad (12.2)$$

where u is the undisturbed free wind speed and a is a quantity denominated induction factor. Thus, v is the mean of upwind and downwind wake wind speed.

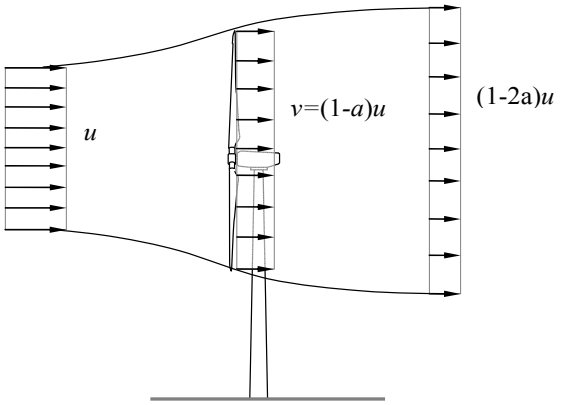

Figure 12.1 *Stream tube of wind turbine rotor.*

Further, Betz deduces that the power curve and power coefficient of the rotor is related to the undisturbed wind speed and induction factor by

$$C_P = 4a(1-a)^2 \qquad (12.3)$$

$$p = \tfrac{1}{2}\rho u^3 A_R 4a(1-a)^2 \qquad (12.4)$$

Consider now the scenarios outlined in the following. A specimen of a wind turbine series is tested in terrain complying with the appropriate standard, and the *reference* power $p_0(u)$, corresponding to the free wind speed u, and the corresponding nacelle anemometer wind speed v are measured and an induction factor a is determined,

$$v = (1-a)u \Rightarrow \quad a = 1 - \frac{v}{u} \qquad (12.5)$$

Next, another specimen of the wind turbine series is sold and installed at a *field site*. In order to check its productive capacity relative to the reference turbine, a *met tower* is erected to measure the free wind speed and together with measured power and nacelle wind speed, these determine a power curve point and an induction factor:

$$p(u) = p_0(u) + \delta_p = p_0\left(1 + \frac{\delta_p}{p}\right) \qquad (12.6)$$

$$v_1 = \left(1 - (a + \delta_a)\right)u \;\Rightarrow\; a_1 = a + \delta_a = 1 - \frac{v_1}{u} \qquad (12.7)$$

where u is the free wind speed (same as in the reference case), δ_p is the increase in power relative to the reference case, v_1 is the wind speed in the rotor plane and δ_a is the change in the induction factor relative to the reference case. With fixed free wind speed *u,* the change in power may be related to the change in induction factor:

$$\delta_p \approx \frac{\partial p}{\partial a}\cdot\delta_a + \frac{\partial p}{\partial u}\cdot 0 = \frac{\partial p}{\partial a}\cdot\delta_a, \qquad (12.8)$$

where

$$\frac{\partial p}{\partial a} = 6\rho u^3 A_R (\tfrac{1}{3} - a)(1-a) \quad .$$

Thus, the change of the power curve relative to the reference power curve is

$$\delta_p \approx 6\rho u^3 A_R (\tfrac{1}{3} - a)(1-a)\delta_a \quad . \qquad (12.9)$$

Now, assume that during the field test the wind speed is determined *only by means of the nacelle anemometer*. The reading of the nacelle anemometer is still v_1 and with no new information available on the calibration of the nacelle anemometer, the induction factor is assumed to be the one deduced previously from the reference test. Thus, the free wind speed will be estimated as

$$u_1 = \frac{v_1}{1-a} \qquad (12.10)$$

The estimate of power output is unchanged, $(p_0 + \delta_p)$, and therefore the PC estimate at wind speed u_1 is

$$p_1(u_1) = p_0 + \delta_p \quad . \qquad (12.11)$$

In order to compare directly with the field test result, where a met mast was available, the immediate result must be extrapolated from the presumed free wind speed u_1 to the actual free wind speed u,

$$p_1(u) = p_1(u_1) + \delta_{p,error} = p_0 + \delta_p + \delta_{p,error} \qquad (12.12)$$

By differentiating for fixed nacelle wind speed v and by assuming the change in induction "small", the extrapolation distance $\delta_u = u_1 - u$ is found:

$$\delta_u \approx \frac{\partial u}{\partial a}\delta_a = -\frac{u}{1-a}\delta_a \quad \text{since} \qquad (12.13)$$

$$\frac{\partial u}{\partial a} = \frac{\partial}{\partial a}\left(\frac{v}{1-a}\right) = -\frac{v}{(1-a)^2} = -\frac{u}{1-a}$$

For a specific wind turbine the test assumption is that power is solely a function of hub height free wind speed, and therefore also the induction factor is a function of wind speed only, $a = a(u)$. Therefore, the error introduced by the nacelle anemometry technique may be estimated as

$$\delta_{p,error} \approx \delta_u \frac{dp}{du} \quad , \qquad (12.14)$$

where

$$\begin{aligned} \frac{dp}{du} &= \frac{d}{du}\left(\tfrac{1}{2}\rho u^3 A_R 4a(1-a)^2\right) \\ &= 6\rho u^2 A_R \left[a(1-a)^2 + (\tfrac{1}{3} - a)(1-a)u\frac{da}{du} \right] \end{aligned} \qquad (12.15)$$

The derivative $\frac{da}{du}$ can in principle only be estimated from the measured complete power curve. However, it appears from a typical power curve, that the second term in the hard bracket of (12.15) is insignificant compared to the first term. Therefore,

$$\frac{dp}{du} \approx 6\rho u^2 A_R a(1-a)^2 \quad . \qquad (12.16)$$

Thus, combining eqs. (12.13), (12.14) and (12.16) we get

$$\begin{aligned} \delta_{p,error} &\approx 6\rho u^2 A_R a(1-a)^2 \frac{u}{1-a}\delta_a \\ &= 6\rho u^3 A_R a(1-a)\delta_a \end{aligned} \qquad (12.17)$$

It seems appropriate to relate the error to the real deviation δ_p of the field power curve from the reference power curve:

$$r_{p,error} = \frac{\delta_{p,error}}{\delta_p} \approx \frac{6\rho u^3 A_R a(1-a)\delta_a}{6\rho u^3 A_R (\frac{1}{3}-a)(1-a)\delta_a} \Rightarrow$$

$$r_{p,error} \approx \frac{a}{\frac{1}{3}-a} \quad . \qquad (12.18)$$

Thus, if by means of the nacelle anemometry technique a deviation from the reference power curve is measured, then the technique itself exaggerates the deviation by $100 \cdot \frac{a}{\frac{1}{3}-a}\,\%$. The exaggeration increases dramatically when the induction factor approaches its optimal value $\frac{1}{3}$. The consequences of this result are illustrated in Figure 12.2.

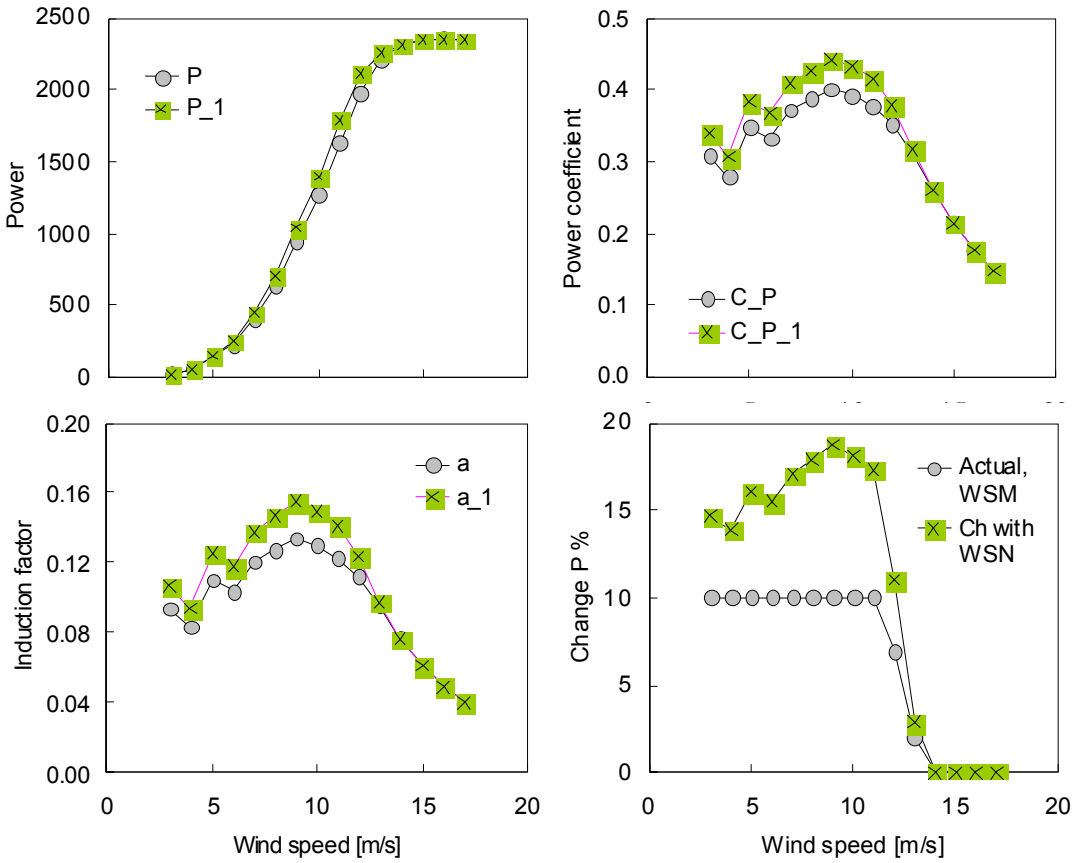

Figure 12.2 *Illustration of reference measurement and measurement at a field site, indexed "1". top left) power curves measured with met tower; top right) corresponding power coefficient curves; bottom left) corresponding induction factor, and bottom right) difference in power from the reference measurement to the field site with standard technique (including met mast WSM and with only the application of nacelle anemometry, respectively – the difference between the two curves corresponds to (12.22).*

The paper [1] relates the theoretical derivations of the influence of the induction to CFD computations on a 500kW Nortank and a 2MW turbine. It is here remarked that the 1-D Betz distributions largely correspond to the computed values using averaged interference factors. This strongly supports the idea that (12.18) is a relatively exact measure of the overall bias error.

12.5 Conclusions

The generic problems related to the use of the nacelle anemometer for determination of the power curve of a wind turbine was investigated. The following was noted:

- The flow induction caused by the rotor depends on wind speed *and* power and thus a problem concerning the nacelle anemometer's calibration persists, being increasingly worse with increasing rotor efficiency.
- The error related to the flow induction is by nature a bias error and may be estimated by means of a combination of the data recorded for the power curve and of 1-D Betz theory adjusted and thereby enhanced by more comprehensive aerodynamic calculations
- The rotor induction close to the hub is most often significantly less, which counter the induction error

- The radial transient in induction factor close to the hub – and therefore potentially close to the position of the nacelle anemometer – is high and may make it difficult to determine the error to be compensated for.
- In all, it is believed that nacelle anemometry is a viable option, given that careful investigation of and correction for the error caused by induction is made *in addition* to the directions made in the present draft of the standard for nacelle anemometry power curve measurements.

12.6 References

[1] Frandsen S, “The Generics of Wind Turbine Nacelle Anemometry”, EWEC2009 Marseille

[2] Pedersen TF, "Trends in power performance measurement standards", AWEA'94

[3] Antoniou I, Pedersen TF, "Nacelle Anemometry on a 1MW Wind Turbine: Comparing the power performance results by use of the nacelle or mast anemometer", Risø-R-941(EN), August 1997

[4] Frandsen, S. (ed.); Antoniou, I.; Chaviaropoulos, T.; Dahlberg, J.A.; Derrick, A.; Douvikas, D.; Dunbabin, P.; Hansen, J.C.; Hunter, R.; Kanellopoulos, D.; Kapsalis, G.; Kristensen, L.; Aagaard Madsen, H.; Mortensen, N.G.; Ruffle, R., “Power performance assessment. Final report”. (Risø National Laboratory, Roskilde, 1999) 205 p

[5] Dahlberg, J.-A.; Frandsen, S.; Aagaard Madsen, H.; Antoniou, I.; Pedersen, T.F.; Hunter, R.; Klug, H., “Is the nacelle mounted anemometer an acceptable option in performance testing?”. In: Wind energy for the next millennium. Proceedings. 1999 European wind energy conference (EWEC '99), Nice (FR), 1-5 Mar 1999. Petersen, E.L.; Hjuler Jensen, P.; Rave, K.; Helm, P.; Ehmann, H. (eds.), (James and James Science Publishers, London, 1999) p. 624-627

[6] Dahlberg, J.-A.; Frandsen, S.; Aagaard Madsen, H.; Antoniou, I.; Pedersen, T.F.; Hunter, R.; Klug, H., “Is the nacelle mounted anemometer an acceptable option in performance testing?”. In: Wind energy for the next millennium. Proceedings. 1999 European wind energy conference (EWEC '99), Nice (FR), 1-5 Mar 1999. Petersen, E.L.; Hjuler Jensen, P.; Rave, K.; Helm, P.; Ehmann, H. (eds.), (James and James Science Publishers, London, 1999) p. 624-627

[7] Frandsen, S.; Antoniou, I.; Hansen, C.J.; Kristensen, L.; Aagaard Madsen, H.; Chaviaropoulos, B.; Douvikas, D.; Dahlberg, J.A.; Derrick, A.; Dunbabin, P.; Hunter, R.; Ruffle, R.; Kanellopoulos, D.; Kapsalis, G., "Redefinition power curve for more accurate performance assessment of wind farms", Wind Energy (2000) 3 , 81-111

[8] Frandsen, S.; Antoniou, I.; Hansen, C.J.; Kristensen, L.; Aagaard Madsen, H.; Chaviaropoulos, B.; Douvikas, D.; Dahlberg, J.A.; Derrick, A.; Dunbabin, P.; Hunter, R.; Ruffle, R.;

[9] Albers A, Klug H, Westermann D, "Power Performance Verification", EWEC'99

[10] Pedersen TF, et.al. "Spinner Anemometry - An Innovative Wind Measurement Concept", EWEC2007 Milan

[11] IEC CD 61400-12-2 “WIND TURBINES – Part 12-2: Power performance of electricity producing wind turbines based on nacelle anemometry”, 88/325/CD, 2008-07-18

[12] Betz, A. „Der Maximum der theoretisch möglichen Ausnützung des Windes durch Windmotoren“, 1920, Zeitschrift für das gesamte Turbinenwesen, Heft 26, Sept. 26, pp. 307-309

13. Spinner anemometry as an alternative to nacelle anemometry

Troels Friis Pedersen

13.1 Introduction

The state of the art of measuring wind on wind turbines is based on nacelle anemometry. In nacelle anemometry wind speed and wind direction are measured with sensors mounted on the upper side of the nacelle behind the rotor. Typically the sensors comprise a redundant pair of cup anemometers and wind vanes or a couple of 2D sonic sensors, see Figure 13.1. Nacelle anemometry provides input to the control system for yaw control, for start up and shut down, and is also used for power performance verification. Meanwhile, nacelle anemometry is hampered by the fact that it is positioned behind the rotor [1]. Nacelle anemometry measures wind that is influenced by: the wakes of the blade roots, the blade root vortices, the boundary layer over the nacelle, and the mounting arrangement of the nacelle anemometry. These effects can be calibrated for to a certain extent, but nacelle anemometry is also dependent on accurate adjustment at mounting. If the effect is significant, as indicated in Figure 13.2, it leads to losses in electric power and increased loads.

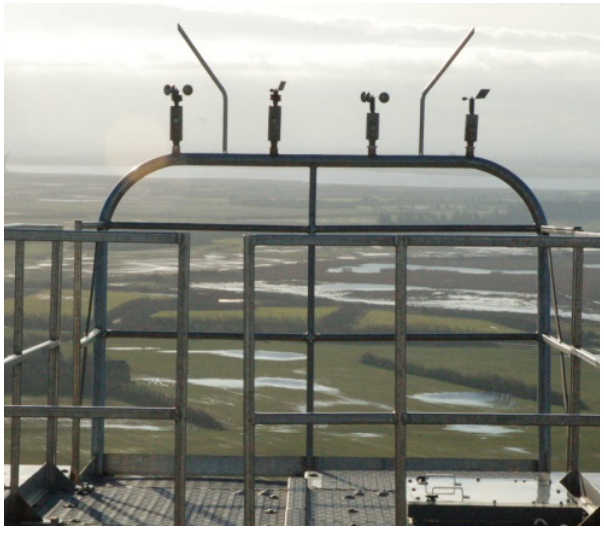

Figure 13.1 *Arrangement of nacelle anemometry on the back of the nacelle of modern wind turbines. The instruments are typically mounted on a reasonably solid support structure with lightning protection covering the instruments and with redundant mounting of instruments*

Figure 13.2 *Often seen in the landscape: wind turbines that deviate significantly in yawing direction*

13.2 Wind measurement in front of the rotor

With the so-called “spinner anemometer” the wind is measured on the wind turbine spinner in front of the rotor. Measurement of wind in front of the rotor avoids most of the flow distortion effects that is inherent in nacelle anemometry. Due to the rotation, the flow angle wind mea-

surements also become insensitive to mounting inaccuracies. In front of the rotor, the wind is almost undisturbed by the rotor and the nacelle. The spinner does distort the wind flow, but in this case the distortion of the flow is an integrated part of the measurement principle, and cannot therefore be considered a disturbance. A flow distortion is, on the other hand, due to the blade roots, but thanks to the almost potential flow regime in the nose of the spinner and around the blade roots, the influence is considered an integrated part of the concept in the same way as the spinner itself.
The concept of the spinner anemometer was first presented at EWEC2007 [2]. The idea to use the spinner arose from the shape of the nose of a pitot-tube, which is often spherical. Instead of measuring flow speed with differential pressure measurements directional wind speed is measured with sonic sensors, which has the advantage that flow components due to rotation are cancelled out. A spinner anemometer thus typically consists of three 1D sonic wind speed sensors mounted on the spinner as shown in Figure 3.
The flow over the spinner was investigated by CFD (Ellipsys code) [3]. Directional wind speeds were determined in the three fixed positions above the boundary layer over the spinner surface, see Figure 13.3. When the wind angle of attack on the spinner changes, the three wind speeds at the sensors change. This systematic change is used to measure the wind angles of attack. The principle can be easily understood by studying Figure 13.4 for a 10º upwards inflow angle.

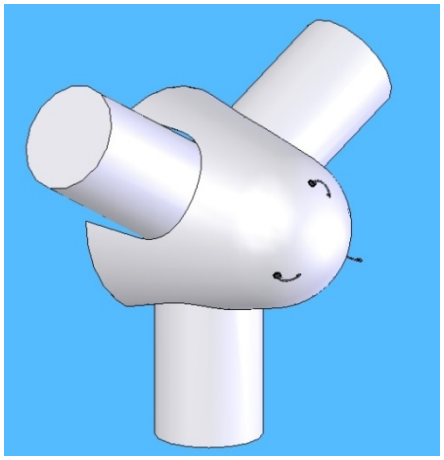

Figure 13.3 *The concept of a spinner anemometer with three 1D sonic sensors mounted on the front part of the spinner. The spinner is in this figure shown with a spherical nose and a conical part.*

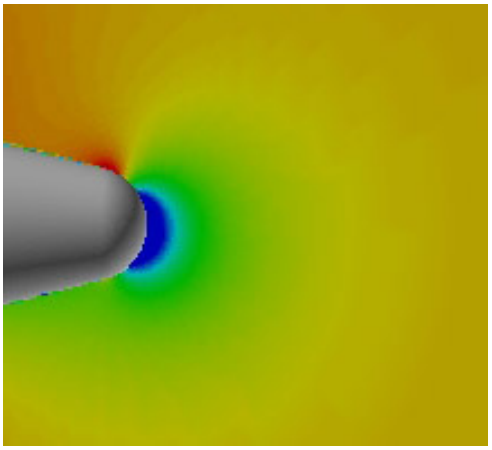

Figure 13.4 *Wind speed contours around a rotational symmetric spinner without rotation (wind from the right). Wind is from the right and the air inflow angle is 10º from below. Notice the zero wind speed at the stagnation point at the nose (blue), the "free" wind speed (yellow-red) far in front of the spinner and at about 50º position over the surface of the spherical part, and the "overspeeding" (red) after the transition from spherical to conical part.*

At an axial inflow to the spinner all three wind sensors measure the same wind speed. The “free” flow can then easily be determined by applying a constant to the average of the three measurements. When an off-axis wind speed is applied the three sensors experience a cosine shaped variation during a rotation, with each sensor offset by 120°. The flow wind speed over a small spinner, (S300), with the shape shown in Figure 13.4, was calculated with the ELLIPSYS code, showing the results as smooth curves in Figure 13.5.
The sensor wind speeds shown in Figure 13.5can be found theoretically from derivation of the flow over a sphere. The signal of one sonic sensor can be expressed as a function of the inflow

angle α and the inflow azimuth position φ at the location of the stagnation point on the spinner and the free wind speed U and two constants K_1 and K_2:

$$V_S = U(K_1 \cos\alpha + K_2 \sin\alpha \cos\varphi) \qquad (13.1)$$

As seen in Figure 13.5, the average sensor wind speed over one rotation decreases with increasing inflow angle while the amplitude increases. In fact the average sensor wind speed is reduced with the cosine to the yaw setting angle while the amplitude increases with the sine.
The ELLIPSYS calculated curves (smooth) in Figure 13.5 correspond very precisely to the theoretical curves (open dots) up to inflow angles at 60°. Only at 80° there is a significant deviation. In fact the analysis shows that the deviations decrease with the inflow angle. This is a characteristic that is in line with the purpose of the instrument; the smaller the yaw error, the more accurate the yaw error measurement.

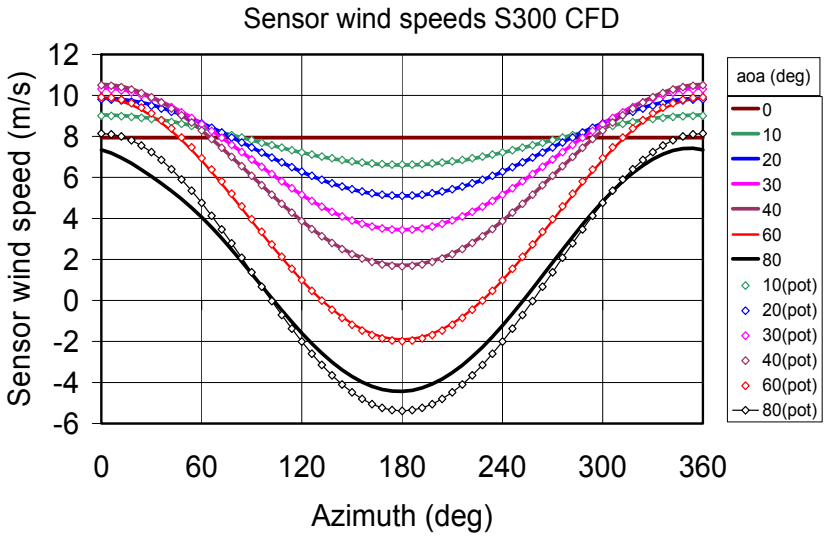

Figure 13.5 *ELLIPSYS computed velocity distribution around the S300 spinner for 10m/s off-axis inflow at 0°, 10°, 20°, 30°, 40°, 60°, and 80°, smooth curves. Open dots represents theoretical values from formula 1.*

With the expression in formula (13.1) for one sensor an expression can be found for each of the three sensors positioned at equidistant angles on the spherical nose. The inverse solution, to find the wind values from the sensor path air speeds, can then easily be derived. The yaw error and the flow inclination angle can be determined with only two instrument constants K_1 and K_2. K_1 is mostly connected to determination of the wind speed and K_2 is mostly connected to the flow angles. This makes calibration of the instrument just as simple as the gain and offset of a cup anemometer.

13.3 Free field comparison to 3D sonic anemometer

The S300 spinner anemometer was tested under field conditions at the Risø test site using the simple spinner anemometer algorithm with two constants, and with a rotational speed of 15rpm. A 3D Gill Windmaster sonic anemometer was mounted at same height and about three meters to the side of the spinner anemometer. The spinner anemometer and the sonic anemometer are shown in Figure 13.6. Figure 13.7 to Figure 13.9 show 100 seconds of time traces of the two wind sensors. The two sensors signals show quite comparable results.

Figure 13.6 *Arrangement of the S300 spinner anemometer with "new" sensors in comparison with the sonic anemometer at Risø test site*

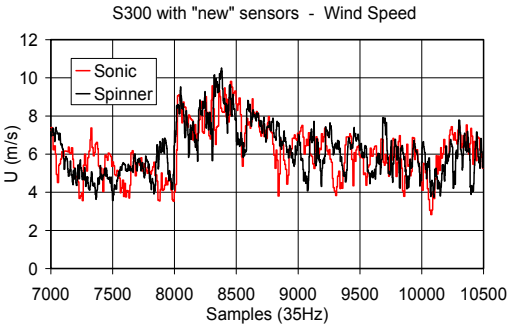

Figure 13.7 *Comparison of measured wind speed at 35Hz sampling rate (100sec of data) of spinner anemometer and 3D sonic anemometer*

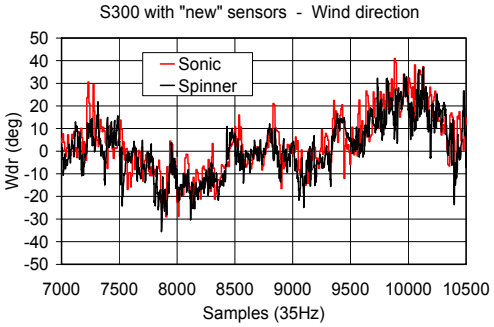

Figure 13.8 *Comparison of measured horizontal inflow angle at 35Hz sampling rate*

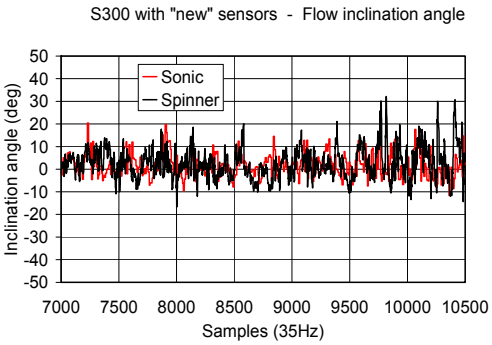

Figure 13.9 *Comparison of measured vertical inflow angle at 35Hz sampling rate*

13.4 Calibration of the spinner anemometer

There have been developed calibration procedures for the spinner anemometer. The key calibration factors of the spinner anemometer are the K_1 and K_2 factors, which are calibrated with a stopped rotor without rotor induction. The calibration can be made by CFD calculations or by field measurements. This calibration can be supplemented with an accredited traceable wind tunnel calibration and an internal spinner anemometer calibration to compensate for geometry deviations of the spinner and for sensor mounting.

13.5 Tests of spinner anemometers on wind turbines

The spinner anemometer has been tested on a 3,6MW wind turbine [4, 5], see Figure 13.10. Yaw error measurements are shown in Figure 13.11. In this case the level of yaw error might lead to power losses in the order of 2%. The spinner anemometer has also been tested on turbines of different sizes.

Figure 13.10 *The three 1D sonic wind sensors mounted on the 3,6MW wind turbine spinner at Risø DTU Høvsøre test site.*

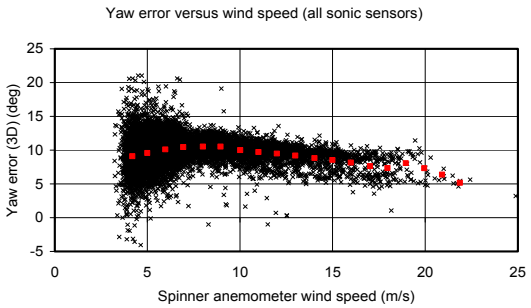

Figure 13.11 *Yaw error of 3,6MW wind turbine (10min averages).*

Further work

The spinner anemometer can be used for yawing of wind turbines, power performance verification, and for flow inclination measurements in complex terrain. A new project (EUDP Spinnerfarm) has been started in 2009 which has the purpose to study yaw statistics of offshore wind turbines, to determine potential power losses due to yaw errors, and to verify power performance by nacelle/spinner anemometry.

13.6 Conclusions

The idea of using the spinner of a wind turbine for wind measurements has been investigated theoretically and experimentally. A spinner anemometer with a small spinner has been investigated in detail by wind tunnel tests and CFD, and the investigations confirm the ideas of the wind measurement concept. Spinner anemometers were tested on a 3,6MW wind turbine, and on a number of other wind turbines of different size, and the tests confirm that yaw errors can be measured accurately, and that wind turbine yawing can be improved.

13.7 References

[1] Frandsen S, Sørensen JN, Mikkelsen R, Pedersen TF, Antoniou I, Hansen K, 2009: The generics of wind turbine nacelle anemometry, EWEC2008 Marseille

[2] Pedersen TF, Madsen HA, Møller R, Courtney M, 2007: Spinner anemometry – an innovative wind measurement concept, EWEC2007 Milan

[3] Pedersen TF, Sørensen NN, Enevoldsen P, 2008: Aerodynamics and characteristics of a spinner anemometer, The Science of Making Torque from Wind

[4] Pedersen TF, Vita L, Sørensen NN, Enevoldsen P, 2008: Operational experiences with a spinner anemometer on a MW size wind turbine, EWEC2008 Marseille

14. Long term stability of cup anemometer operational characteristics

14.1 Identification of the problem

Anemometer calibration is of fundamental importance for every wind energy related measurement activity. For this reason, international standardization bodies, apart from the usual metrological confirmation methodologies used in all measurement equipment (traceable calibration, proper maintenance, documented life long history) require additional measures for anemometers used in wind energy applications. The aim is to assure that any possible degradation of the operational characteristics of anemometers during their operational period is kept within known limits, to allow for a reliable estimation of the measurement uncertainty. **Recalibration of the primary anemometers** is proposed as the preferred method, while in-situ comparison is accepted as a second solution.
Detailed presentation of method used to approach the above problem and results obtained are given in [1] (recalibration) and [2] (insitu comparison). In the following main features from both studies are briefly presented.

14.2 Method of approach

Recalibration
The Laboratory for Wind Turbine Testing of CRES applies as a standard procedure the recalibration of cup anemometers after operation in the field, a common practice among Testing Laboratories. A large data base of recalibrations of cup anemometers has evolved through the Laboratory's operation in the last years. In the present work, statistical analysis of the differences seen in the response characteristics of cup anemometers before and after their use is made. The differences were compared to the overall uncertainty of the calibration procedure, and the effect of operation duration was examined. The statistical analysis aims at providing a sound base for the decisions related to the determination of the recalibration interval of cup anemometers.
To get a measurable value for the effect of usage on the operational characteristics, the difference in wind velocity (DV) corresponding to the same frequency output as estimated from the calibration characteristics before (a1, b1) and after the use (a2, b2) is calculated, as in the following equations

$$DV = V_1 - V_2$$

where

$V_1 = a_1 * f + b_1$

$V_2 = a_2 * f + b_2$

f selected frequency

α1, b1, response characteristics as defined by the calibration before use

α2, b2, response characteristics as defined by the calibration after use

In-situ comparison

As an alternative to recalibration the procedure of "In situ comparison" is proposed. In this case a secondary anemometer is installed close to the main anemometer. A comparison of the relative readings of the two anemometers is made for a period at the begging of the measurement campaign and for a period at the end of the measurement campaign. No change in the relative readings between the two periods is considered as an indication that no serious degradation on the anemometers is seen. The assumption underlying is that the possibility of both anemometers degrading in a identical pattern is very low.

A combined statistical analysis of in situ comparisons of anemometers was made using data available at CRES. Sensitivity effects of parameters like time of operation on site, local wind flow characteristics and meteorological conditions are analysed.

As a measure of "anemometer degradation" the square sum of the Systematic deviation and the Statistical Deviation (SSD) between the two operating periods is used. For the in situ comparison to be considered as successful SSD must be less than 0,1 m/s for each wind speed bin in the range of 6 to 12 m/s.

14.2.1 Results

Recalibration

A representative number of recalibrations of VECTOR A100K cup anemometers after operation on site were examined. The traceability and repeatability of the calibration procedure were assured by the strict implementation of the requirements IEC61400-12-1:2005/Annex F and MEASNET Cup Anemometer Measurement Procedure.

The differences in the response characteristics of the anemometers were kept within the calibration typical error interval for the majority (>90%) of cases studied for all usage class up to 540 days (18 months). The deviation indexes examined show a week trend for increasing deviation for usage more than 18 months (540 days). This is demonstrated in Figure 14.1 where the recalibration cases per usage class that exceed the error margins of calibration uncertainty are presented. A low drop out rate (below 10%) is seen for classes up to 540 days of use. For the usage class greater than 540 days a trend to increase the rate of recalibrations with deviations exceeding the calibration uncertainty is clearly seen.

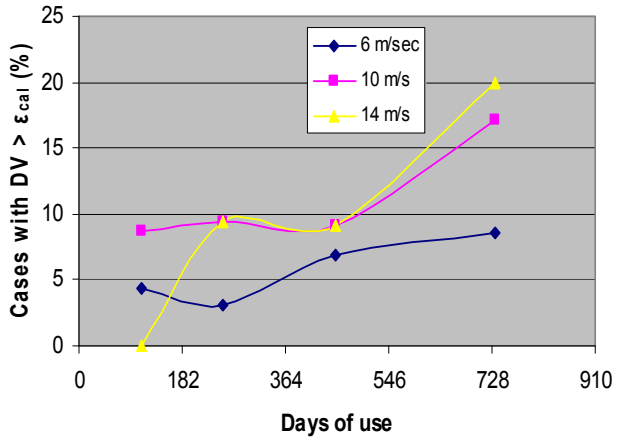

Figure 14.1 *Cases of anemometer recalibration per usage class where the velocity deviation exceeds calibration uncertainty error margins.*

In-situ comparison

A sensitivity analysis of the In situ comparison results, using as an index the SSD values estimated by the procedure was made. The operation time on site, the annual mean wind speed, the mean turbulence intensity and the annual mean temperature where examined.

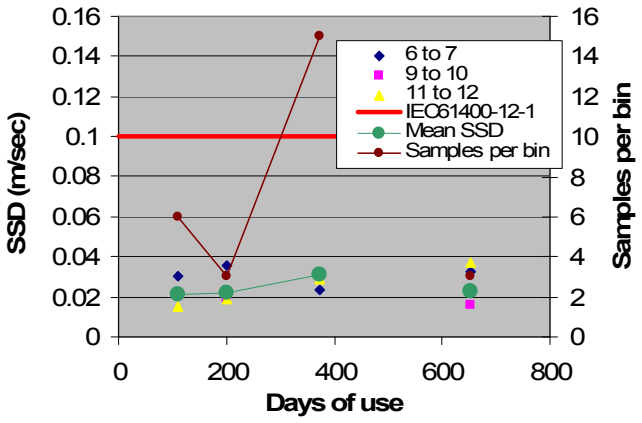

Figure 14.2 : Binned SSD values as a function of operation time on site (only cases with Vector A100 series anemometers)

A weak dependence of averaged SSD values to operation time was seen (see Figure 14.2), as should be expected, since increased operation time on site may increase anemometer bearing wear.

No obvious effect on SSD from site annual mean wind speed, mean turbulence intensity, and mean air temperature were detected for the range of the parameters covered.

In situ comparison was successful for 90% of cases examined. Acceptable results where found even for anemometers operating more than 18 month on site. Where available, recalibrations of anemometers in the wind tunnel after the end of the measurement campaign, were in full accordance with in situ results.

14.2.2 Discussion

The differences in the response characteristics of the anemometers are kept within the calibration typical error interval for the majority (>90%) of cases studied for all usage class up to one year, while, of the limited data available in higher usage classes (up to 18 months) similar trend is observed. The above is confirmed by both methods applied (recalibration of anemometers after use and in-situ comparison).

The above results suggest that, at least for the type of instruments mainly examined in the present study (VECTOR A100K series anemometers) the calibration interval could be increased up to 18 months with out affecting the reliability or the uncertainty of the measurements.

Additionally, the good agreement in the results of both recalibration and in-situ comparisons support the position that the “in situ comparison” as described in IEC 61400-12-1:2005 provides a reliable tool for the verification of anemometer calibration integrity.

Further work on the effect of anemometer type, and operating conditions – temperature range, air salinity, and dust etc- could provide important information to the manufacturers and users of cup anemometers that could help in improve the reliability of wind speed measurements.

14.3 Applicability of current power performance measurement recommended practices in various types of terrains.

14.3.1 Identification of the problem

During the first years of the wind power expansion in Europe, the easily accessible flat terrain sites with good wind potential were the first to be developed in the wind pioneering countries such as Denmark, Holland, and Northern states of Germany. Wind turbines today can be seen operating all over the world in various terrain types. Since the power performance verification is considered a vital tool in the development of an efficient wind farm, an intense discussion is under way, considering how reliable power performance verification measurements are in complex terrain sites are. Spatial variations in wind speed (terrain induced distortion in the flow field, wind shear), flow inclination relative to the wind turbine rotor, and large differences in air density are some of the parameters that are pointed out as having an effect on the power performance of a wind turbine operating in complex terrain sites.
Considerable efforts by both the scientific community and the industry have been made to assess the above issues, but the actual physical problem is not yet addressed in full. Furthermore the urgent need to have workable tools to make power performance verification in complex terrain sites, have led standardization organizations and expertise networks (namely IEA, IEC and MEASNET) to include in their recommendations special guidelines aiming at reducing uncertainties associated to complex terrain sites.

14.3.2 Method of approach

Some sample cases of power curve verification of passive and active power control wind turbines w/t operating in various terrains (from semi-flat to very complex) were examined. It should be note that the machine examined were in the low to medium range with nominal power 500 kW to 1.5 MW) and with rotor diameters from 50 to 70 m.
The difference between the Annual Energy Production (AEP) measured in the actual sites compared to the guaranteed AEP (ΔAEP) was used as a measure of terrain dependency of the power performance of a wind turbine and therefore as an index for the suitability of the recommended procedures in various terrains.
A sensitivity analysis, using the ΔAEP as an index, was made for some of the parameters expected to influence the power performance (magnitude of site calibration correction factors, turbulence intensity, distance of reference mast, air density, etc). Detailed presentations of the analysis, methods and results were presented in [3].

14.3.3 Results and discussion

The available results from the comparison of the power performance characteristics measured in complex terrain compared to flat terrain, in general supports the suitability of the methods proposed for medium sized wind turbines, and also underlines the influence of both terrain and machine related parameters in the uncertainty of the measurement results. Deviations from the warranted power curve were within the typical error of measurement, and comparable to overall statistical scatter seen in the AEP of wind turbines operating in flat terrain..
Possible correlations between parameters characterizing the flow field in complex terrain sites and the deviations from the warranted AEP were subsequently investigated. The effect of the terrain on the evolution of the wind flow around the wind turbines was evident in all cases, as quantified by the impact of altitude difference between the reference mast and WT on the site calibration correction factors, by wide variations in shear profiles, as well as the differences in the site mean air density. A sensitivity analysis, using the ΔAEP as an index, showed small dependence of ΔAEP to increasing site calibration correction factors, as also to increasing directional sensitivity of the site calibration factors and turbulence levels. No effect was observed for other parameters such as terrain inclination, distance of reference mast from the WT, air density difference, sector width etc. Considering this, the differences in ΔAEP are smaller than the estimated measurement error, hence it can be concluded that the application of the current proce-

dures successfully reduced the influence of complex terrain parameters on the results for both pitch and stall regulated medium sized wind turbines.
Some weaknesses of the site calibration procedure proposed, especially in very complex terrain are revealed. Current standards propose the use of a unified correction factor for a very wide wind speed range (4-16m/s). As it is proved in the present work [3], this procedure works very well in most cases, but can lead to additional errors in extreme cases, since in very complex terrain sites, the flow field strongly depends on the wind speed magnitude. The above further stresses the importance of a thorough verification of site calibration results.
Shear profiles were also examined in some of the sample cases. The analysis of the shear profiles revealed a wide variation of profiles among the cases studied, while strong direction dependence was also seen in some of the cases. More detailed parametric analysis of shear effect on the power curve is necessary.
As the above approach showed, for medium, sized wind turbines, the application of the current recommended procedures, the power performance of WTs in various terrains can be successfully evaluated and produce coherent and accurate results.

14.4 Definition of reference wind speed for power curve measurements of large wind turbines (>2.0 MW).

14.4.1 Identification of the problem

Modern wind-industry history has shown a constant trend towards the development of significantly larger, not only in hub height (H_{hub}), but also in rotor diameter, Multi-MW Wind Turbines (WTs). At the same time, power performance tests are being implemented by measuring the wind speed at H_{hub} assuming that the wind speed is uniform over the rotor area. This is a fair assumption as far as small scale WTs are concerned, while being by far simplistic for the large scale ones. Wind speed, turbulence and wind direction do vary with height, in respect to the meteorological regime and / or the terrain morphology. Consequently, the uncertainty related to the representative wind speed is increased, affecting the reliability of power performance and load predictions. The evaluation of the wind speed in over the whole rotor area is an issue open since a long time.

14.4.2 Method of approach

Sample power curve measurement campaigns, meeting the IEC 614000-12-1:2005 requirements are examined involving wind turbines with nominal power output in the range of 800 - 1500 kW and operating in a variety of terrain types, from semi flat terrain to highly complex terrain. Additionally to the current standard requirements, wind speed was measured at heights below hub height also, allowing the wind shear to be estimated. On two of the cases studied, power curve data were analysed applying a new definition for the reference wind speed as proposed by Antoniou et all in [5].
The swept area of the rotor is divided to eight horizontal zones, assuming constant wind speed along each zone and the energy flux through each “constant speed zone” is calculated. The “equivalent wind speed” is defined as the wind speed giving the same total energy flux, as the sum of the energy fluxes by each “constant speed zone”, as detailed in Equation (14.1), where $\overline{U_i}$ is the wind speed along i-th “constant speed zone” and A_i the area of the i-th “constant speed zone” and A the rotor’s swept area.

$$U_{eqM1} = \frac{1}{A} \cdot \sum \overline{U_i} \cdot A_i \qquad (14.1)$$

If turbulence is taken into account then the equation giving the equivalent wind speed U_{eqT1} becomes,

$$U_{eqT1} = \frac{1}{A} \cdot \sum \sqrt[3]{\overline{U_i^3}} \cdot A_i \qquad (14.2)$$

where, $\overline{U_i^3}$ is the average energy flux defined as,

$$\overline{U^3} = \overline{U}^3 \cdot \left(1 + 3\frac{\sigma^2}{\overline{U}^2}\right) = \overline{U}^3 \cdot \left(1 + 3I_T{}^2\right) \qquad (14.3)$$

where σ is the standard deviation and I_T is turbulence intensity.

Differently, the equivalent wind speed can be expressed as the wind speed which results in the same energy flux through the rotor area as the varying wind speed over the integration period.

$$U_{eqT3} = \sqrt[3]{\frac{1}{A} \cdot \left(\sum \overline{U_i^3} \cdot A_i\right)} \qquad (14.4)$$

Direct measurement of wind speed at the complete rotor area requires either a mast high enough to reach upper blade tip position or a lower mast in combination with remote sensing systems (Lidar or Sodar). Both configurations are well in excess of the budget of a typical commercial power curve verification campaign. As a less expensive alternative, conventional masts used for site calibration and power curve campaigns were equipped with additional anemometers at two to four levels below hub. This configuration gives instantaneous velocity measurements at various heights up to H_{hub} allowing the estimation of shear profiles. Thereupon, the wind speed along the rotor surface can be estimated, based on the assumption that the shear profile in the upper half of the rotor is same as the one below. This assumption is definitely a drawback of this approach, since discontinuity in the shear profiles has been observed in various cases. On the other hand, such an approach allows the use of data from conventional measurement campaigns in complex terrain with the view to investigating alternative methods for the definition of the reference wind speed.
For the estimated wind shear profile, total energy flux through the rotor is calculated, and an equivalent uniform wind speed value is defined. The measured power curves derived when using the "hub-height wind speed" and the "equivalent wind speed" are compared to the warranted power curves, with the aim of evaluating whether this approach improves measurement reliability.
Additionally on one of the cases, short term wind speed shear measurements were being obtained using a Lidar system and were compared with these of an adjacent met mast equipped with cup anemometers.
Detailed description of the approach followed and of the results obtained were presented in [4].

14.4.3 Results and discussion

Data from sample cases involving commercial power performance measurements in complex terrain sites were analysed. Alternative method for the definition of the reference wind speed involving an "equivalent rotor averaged wind speed" as described above was applied. The wind

speed shear along the rotor disk was estimated using cup anemometer measurements corresponding to heights at the lower part of the rotor. In the following graphs (Figure 14.3), results from one of the cases studied are presented.
Differences in the power curve and AEP when using different definitions for the reference wind speed are given. Small differences between conventional H_{hub} wind speed and "rotor averaged wind speed" were observed. Assuming the local wind speed at each rotor "constant speed zone" to be proportional to the area of the zone, the zones close to hub were over- weighted (having larger area due to the fragments' width) relative to the outer zones. On the outer constant speed zones, the torque increment for a given wind speed is larger than for an inner segment (closer to hub) due to the larger torque arm (distance of zone to the axis of rotor rotation. This effect is not weighted in the approach followed.

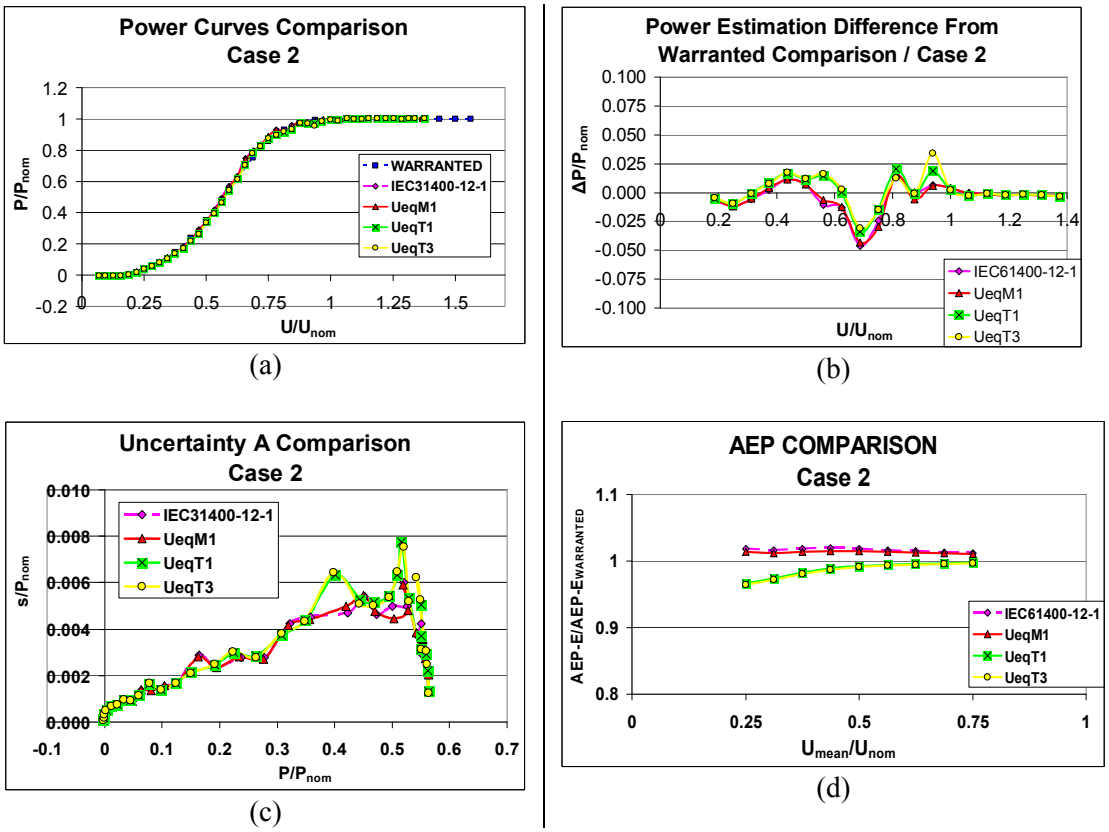

Figure 14.3CASE 2: Effect of Reference Wind Speed Definition on Power Curve

(a) P-U Curves
(b) Difference from Warranted
(c) Type A Uncertainty
(d) AEP comparison

Still the differences between the H_{hub} wind speed and rotor averaged wind speed are small either seen as average power output or as Type A uncertainty in the binning procedure or as differences in the AEP. Therefore, in the cases studied which correspond to small to medium sized wind turbines (hub height 45 to 70m) and operating in areas with smooth and predictable shear profiles (low exponent coefficients), the conventional definition of reference wind speed (hub height point measured) fits well with the rotor averaged definition for Ueq_{M1}, without turbulence. In all cases studied, the inclusion of turbulence term in the definition of the "rotor averaged wind speed", gives small but non-negligible difference to the IEC calculations and warranted. The above demonstrates the fact that, due to rotor size not all turbulent fluctuations sensed by a cup anemometer, can be converted to useful energy by a wind turbine rotor.

The cases studied in the present work are limited compared to the variety of operating conditions found in complex terrain sites. Additional cases should be analysed covering a wider range of operating conditions, focusing in sites with steep wind shear, i.e. where the I_T is rather low and wind speed stratification is noteworthy. However, provided the findings of the present analysis are verified at other cases as well, this could support the use of a test configuration with hub height mast and shear measuring anemometers for power performance measurements using alternative definition of the reference wind speed. This could serve as a less expensive alternative to "blade tip tall towers" or remote sensing systems (such as Lidars) for short to medium wind turbines.
A combination of short term operation of remote sensing systems with hub-height masts equipped with shear measuring anemometers could also be used for taller wind turbines, in combination with better monitoring of boundary layer stability conditions (temperature stratification etc).

14.5 Actions taken – improvements –response of wind energy community:

Anemometer recalibration interval

The Greek Accreditation organization, responsible for the accreditation of testing and measurements Laboratories (ESYD S.A), confirmed the acceptance of 18 months as recalibration interval for anemometers used in wind energy applications (http://www.esyd.gr/pweb/s/20/files/kanonismoi/kritiriaOdigies/KO_AIOLIKO.pdf, in Greek) .

Power performance measurements

MEASNET Network issued a new recommendation for Power performance Measurements (MEASNET Procedure "Power performance measurements ", Ver 5,2009, http://www.measnet.com/power5.pdf). In this procedure, it is recommended to include wind shear data in the documentation of each power curve measurement campaign.

14.6 References

[1]. Stefanatos N., Papadopoulos P., Binopoulos E., Kostakos A., Spyridakis G., "Effects of long term operation on the performance characteristics of cup anemometers" Proc. Of EWEC 2007, Milan

[2]. Stefanatos N., Papadopoulos P., "Verification of anemometer calibrations", Proc. of EWEC 2010, Warsaw

[3]. Stefanatos N., Mouzakis F., Binopoulos E., Kokkalidis F., Papadopoulos P. "Verification of power performance of active power control wind turbines in complex terrain" Proc. Of EWEC 2006, Athens

[4]. Stefanatos N., Zigras D., Foussekis D., Kokkalidis F., Papadopoulos P., Binopoulos E., "Revising reference wind speed definition for power performance measurements of multi-mw wind turbines" Proc. of EWEC 2008, Brussels.

[5]. Ioannis Antoniou et al. "Influence of Wind Characteristics on Turbine Performance" EWEC2007, Milan, Italy

Appendix A Aerodynamics & Aero-elastics, Rotor structures Materials, and Turbine Foundations

Table A.1 *List of parameters for WP2 Aerodynamics & Aero-elastics, WP3 Rotor structures and materials and WP4 Turbine Foundations*

Param No	Parameter / Signal	Unit	Desired Accuracy (Uncertainty)	Traceable (Y/N)	Sampling frequency range [Hz] (1)	Required / Optional	Measurement position	WP2 and WP3 Turbine Monitoring	Farm Monitoring	WP4 Design code verification	WP4 Advanced Control strategies
1	Displacements (2)	m	To be determined	Y	It should be 8 times larger than the highest frequency to be studied	O	Blade, hub, tower, nacelle, substructure, foundation and individual components	X	X	X	X
1	Velocities (3)	m/s	To be determined	Y	It should be 8 times larger than the highest frequency to be studied	O	Blade, hub, tower, nacelle, substructure, foundation and individual components	X	X	X	X
1	Accelerations (4)	m/s2	To be determined	Y	It should be 8 times larger than the highest frequency to be studied	O	Blade, hub, tower, nacelle, substructure, foundation and individual components	X	X	X	X
1	Nacelle acceleration in three directions (5)	m/s2	0.05 m/s2	Y	It should be 8 times larger than the highest frequency to be studied	R	Nacelle, measurement in more locations to capture all degrees of freedom	X		X	X
1	Tower bending moment on different height levels (fore-aft, side-side and torsional)	kNm	3%	Y	It should be 8 times larger than the highest frequency to be studied	R	Tower	X		X	X
1	Tower acceleration in three directions on different height levels	m/s2	0.05 m/s2	Y	It should be 8 times larger than the highest frequency to be studied	R	Tower	X		X	X
1	Substructure (monopile, tripod, floating) bending moment on different height levels above and below mudline (fore-aft, side-side and torsional if relevant)	kNm	3%	Y	It should be 8 times larger than the highest frequency to be studied	R	Substructure	X		X	X
1	Yaw moment	kNm	Target 3%	Y	It should be 8 times larger than the highest frequency to be studied	R	Nacelle, it could be measured from the rotating structure, or from the fixed structure.	X		X	X
1	Tilt moment	kNm	3%	Y	It should be 8 times larger than the highest frequency to be studied	R	Nacelle, it could be measured from the rotating structure, or from the fixed structure.	X		X	X
1	Main shaft bending (0° 90°)	kNm	3%	Y	It should be 8 times larger than the highest frequency to be studied	R	Main shaft	X		X	X
1	Main shaft torsion	kNm	3%	Y	It should be 8 times larger than the highest frequency to be studied	R	Main shaft	X		X	X
1	Strain distribution to determine local stress distributions and for instance shear (anywhere)	kN	3%	Y	It should be 8 times larger than the highest frequency to be studied	R	Blade, hub, tower, nacelle, substructure, foundation and individual components			X	
1	Blade bending moment along the blade length (flapwise and edgewise)	kNm	3%	Y	It should be 8 times larger than the highest frequency to be studied	R	Blade			X	X
1	Blade root bending moment (in-plane and out-of-plane)	kNm	Derived from blade bending moments and pitch angles	-	-	-		X	X	X	X
1	Blade torsional moment along the blade	kNm	3%	Y	It should be 8 times larger than the highest frequency to be studied	R	Blade			X	X

param No	Parameter / Signal	Unit	Desired Accuracy (Uncertainty)	Traceable (Y/N)	Sampling frequency range [Hz] (1)	Required / Optional	Measurement position	WP2 and WP3 Turbine Monitoring	Farm Monitoring	WP4 Design code verification	WP4 Advanced Control strategies
1	Blade deflection along the blade length (flapwise and edgewise)	m	1% of maximum deflection	Y	It should be 8 times larger than the highest frequency to be studied	O	Blade			X	
1	Blade twist along the blade length (flapwise and edgewise)	degree	0.01 degree from the mean value (wind still)	Y	It should be 8 times larger than the highest frequency to be studied	O	blade			X	X
1	Tower deflections on different height levels (fore-aft, side-side)	m	1% of maximum deflection	Y	It should be 8 times larger than the highest frequency to be studied	R	Tower			X	X
1	Tower torsional deflection on different height levels	degree	1% of maximum deflection	Y	It should be 8 times larger than the highest frequency to be studied	R	Tower			X	X
1	Tower torsional moment on different height levels	kNm	3%	Y	It should be 8 times larger than the highest frequency to be studied	R	Tower	X		X	X
1	Substructure (monopile, tripod, floating) deflections on different height levels above and below mudline (fore-aft and side-side)	m	1% of maximum deflection	Y	It should be 8 times larger than the highest frequency to be studied	R	Substructure			X	X
1	Substructure (monopile, tripod, floating) torsional deflection on different height levels	degree	1% of maximum deflection	Y	It should be 8 times larger than the highest frequency to be studied	O	Substructure			X	X
1	Subtructure and tower forces, such as anchor, tripod etc.	N	1% of maximum force	Y	It should be 8 times larger than the highest frequency to be studied	O	Substructure, Tower			X	X
1	Support structure natural frequencies (fore-aft, side-side and torsional)	Hz	Derived parameter	-	-	-	-			X	X
1	Rotor blade natural frequency (edgewise, flapwise)	Hz	Derived parameter	-	-	-	-			X	
1	Drive train natural frequencies	Hz	Derived parameter	-	-	-	-			X	
1	Applied pitch torque	kNm	3%	Y	It should be 8 times larger than the highest frequency to be studied	O	Hub			X	
2	Nacelle position (yaw)	degree	0.1 - 0.5 degrees	Y	>=1Hz	R	Nacelle	X	X	X	X
2	Rotor speed (low speed shaft)	rpm	0.1-1%	Y	It should be 8 times larger than the highest frequency to be studied	R	Nacelle	X	X	X	X
2	Rotor position (rotor azimuth)	degree	0.1 %	Y	It should be 8 times larger than the highest frequency to be studied	R	Nacelle	X	X	X	X
2	Generator speed (high speed shaft)	rpm	0.1-1%	Y	It should be 8 times larger than the highest frequency to be studied	R	Nacelle	X	X	X	X
2	Actual torque on high speed shaft	kNm	3%	Y	It should be 8 times larger than the highest frequency to be studied	R	Nacelle			X	X
2	Demanded torque on high speed shaft	kNm	0.1%	-	It should be 8 times larger than the highest frequency to be studied	R	Control system			X	X
2	Pitch angle	degree	0.01 degree	Y	It should be 8 times larger than the highest frequency to be studied	R	Nacelle	X	X	X	X
2	Demanded pitch angle	degree	0.1%	-	It should be 8 times larger than the highest frequency to be studied	R	Control system	X		X	X

Param No	Parameter / Signal	Unit	Desired Accuracy (Uncertainty)	Traceable (Y/N)	Sampling frequency range [Hz] (1)	Required / Optional	Measurement position	WP2 and WP3 Turbine Monitoring	Farm Monitoring	WP4 Design code verification	WP4 Advanced Control strategies
2	Pitch rate	degree/s	Derived signal					X		X	X
2	Active electrical power	kW	0.5%	Y	It should be 8 times larger than the highest frequency to be studied	R	Between wind turbine and electrical connection; It could be at different locations, such as stator, rotor etc.	X	X	X	X
2	Reactive electrical power	kW	0.5%	Y	It should be 8 times larger than the highest frequency to be studied	O	Between wind turbine and electrical connection; It could be at different locations, such as stator, rotor etc.	X	X	X	X
2	Controller mode	-	Derived from controller	Y	It should be 8 times larger than the highest frequency to be studied	R	Control system	X	X	X	X
2	Availability	-	Derived from controller	Y	It should be 8 times larger than the highest frequency to be studied	O		X	X	X	X
2	Failure	-	Derived from controller	Y	It should be 8 times larger than the highest frequency to be studied	O		X		X	X
2	Status	-	Derived from controller	Y	It should be 8 times larger than the highest frequency to be studied	R	Control system	X		X	X
2	Wind speed measured at nacelle	m/s	0.1 m/s	Y	>=1Hz	R	Nacelle	X	X	X	X
2	Wind direction measured at nacelle	degree	1 degree	Y	>=1Hz	R	Nacelle	X	X	X	X
3	Wind speed at different positions in the rotor plane (longitudinal, lateral and vertical)	m/s	0.1 - 0.25 m/s at 10 m/s	Y	>=1Hz	R	Rotor plane, free sector	X	X	X	X
3	Wind direction at different positions in the rotor plane	degree	2-5 deg	Y	>=1Hz	R	Rotor plane, free sector			X	X
3	Air Temperature	^{o}C	0.5-3 ^{o}C	Y	>=1Hz	R	Hub height			X	
3	Atmospheric pressure	hPa	5 hPa	Y	>=1Hz	R	Hub height			X	
4	Sea surface elevation	m	0.1 m	Y	>=1Hz	R	Sea level			X	
4	Wave direction	degree	5 degree	Y	>=1Hz	R	Sea level			X	
4	Current speed profile	m/s	0.1 m/s	Y	>= 0.1Hz	R	From mudline til sea level			X	
4	Current direction	degree	5 degree	Y	>= 0.1Hz	R	From mudline til sea level			X	
4	Ice parameters (thickness)	m	0.01m	Y	daily, hourly values	O	Sea level	X		X	
4	Water temperature (6)	^{o}C	0.3 degree C	Y	>=1Hz	R	Surface temperature			X	
5	Soil strata - Soil description as function of depth	-	-	Y	once, or larger than 1/year	R	Soil			X	X
5	Internal friction angle of soil	degree	5 degree	Y	once, or larger than 1/year	R	Soil			X	X
5	Cohesive strength	kN/m^2	?	Y	once, or larger than 1/year	?	Soil			X	X
5	Unit weight	kN/m3	?	Y	once, or larger than 1/year	?	Soil			X	X
5	Scour	?	?	Y	once, or larger than 1/year	?	Soil			X	X
5	Sea bed movement	?	?	Y	> 8 times the highest frequency to be studied	?	Soil			X	X

(1) For many parameters, it is noted that the sample frequency should be 8 times larger than the highest frequency to be studied.
This is most practical, since the parameters could be used for more purposes with own requirements.
(2) Displacements. Examples are gearbox displacements, angular displacements of flexible coupling, etc
(3) Velocities. Examples are pitch piston velocities, main shaft velocities etc.
(4) Acceleration. Examples are accelerations in subcomponents etc.
(5) The accelerometer should be applicable also for the lower frequencies encountered in larger wind turbines
(6) Water temperature is included for stability of the atmospheric boundary layer
In the future, the calibration by means of adding force on the turbine can be impossible, so new calibration methods should be defined

Appendix B Control systems and Condition Monitoring

Table B.1 *List of parameters for WP5 Control systems and WP7 Condition Monitoring*

Param No	Parameter / Signal	Unit	Desired Accuracy (Uncertainty)	Traceable (Y/N)	Sampling frequency range [Hz] (1)	Required / Optional	Measurement position	WP5 Operational Control Systems	WP5 Development of Control strategies	WP7 Condition Monitoring
1	Displacements (2)	m	To be determined	Y	It should be 8 times larger than the highest frequency to be studied	O	Blade, hub, tower, nacelle, substructure, foundation and individual components. (8)	X	X	X
1	Velocities (3)	m/s	To be determined	Y	It should be 8 times larger than the highest frequency to be studied	O	Blade, hub, tower, nacelle, substructure, foundation and individual components	X	X	X
1	Accelerations (4)	m/s2	To be determined	Y	It should be 8 times larger than the highest frequency to be studied	O	Blade, hub, tower, nacelle, substructure, foundation and individual components (9)	X	X	X (7)
1	Temperatures	C	To be determined	Y	It should be 8 times larger than the highest frequency to be studied	O	Individual components	X	X	X
1	Pressure	Pa	To be determined	Y	It should be 8 times larger than the highest frequency to be studied	O	Individual components	X	X	X
1	Liquid levels	m	To be determined	Y	It should be 8 times larger than the highest frequency to be studied	O	Individual components	X	X	X
1	Strain	microstrain	To be determined	Y	It should be 8 times larger than the highest frequency to be studied	O	Individual components		X	X
1	Nacelle acceleration in three directions	m/s2	0.05 m/s2	Y	It should be 8 times larger than the highest frequency to be studied	R	Nacelle, measurement in more locations to capture all degrees of freedom	X	X	X
1	Tower acceleration in three directions on different height levels	m/s2	0.05 m/s2	Y	It should be 8 times larger than the highest frequency to be studied	R	Tower	X	X	X
1	Yaw moment	kNm	Target 3%	Y	It should be 8 times larger than the highest frequency to be studied	O	Nacelle, it could be measured from the rotating structure, or from the fixed structure.	X	X	X
1	Tilt moment	kNm	3%	Y	It should be 8 times larger than the highest frequency to be studied	O	Nacelle, it could be measured from the rotating structure, or from the fixed structure.	X	X	X
1	Main shaft bending (0° 90°)	kNm	3%	Y	It should be 8 times larger than the highest frequency to be studied	O	Main shaft	X	X	X
1	Main shaft torsion	kNm	3%	Y	It should be 8 times larger than the highest frequency to be studied	O	Main shaft	X	X	X
1	Blade bending moment along the blade length (flapwise and edgewise)	kNm	3%	Y	It should be 8 times larger than the highest frequency to be studied	O	Blade	X	X	X
1	Blade root bending moment (in-plane and out-of-plane)	kNm	Derived from blade bending moments and pitch angles	-	-	-	-	X	X	X
1	Blade torsional moment along the blade	kNm	3%	Y	It should be 8 times larger than the highest frequency to be studied	O	Blade	X	X	
1	Blade deflection along the blade length (flapwise and edgewise)	m	1% of maximum deflection	Y	It should be 8 times larger than the highest frequency to be studied	O	Blade	X		X

param No	Parameter / Signal	Unit	Desired Accuracy (Uncertainty)	Traceable (Y/N)	Sampling frequency range [Hz] (1)	Required / Optional	Measurement position	WP5 Operational Control Systems	WP5 Development of Control strategies	WP7 Condition Monitoring
1	Blade twist along the blade length (flapwise and edgewise)	degree	0.01 degree from the mean value (wind still)	Y	It should be 8 times larger than the highest frequency to be studied	O	Blade	X	X	
1	Tower deflections on different height levels (fore-aft, side-side)	m	1% of maximum deflection	Y	It should be 8 times larger than the highest frequency to be studied	O	Tower	X	X	
1	Tower torsional deflection on different height levels	degree	1% of maximum deflection	Y	It should be 8 times larger than the highest frequency to be studied	O	Tower	X	X	
1	Tower-top accelerations (horizontal)	m/s2	to be determined	Y	It should be 8 times larger than the highest frequency to be studied	O	Tower	X	X	
1	Substructure and tower forces, such as anchor, tripod etc.	N	1% of maximum force	Y	It should be 8 times larger than the highest frequency to be studied	O	Substructure, Tower	X	X	
1	Support structure natural frequencies (fore-aft, side-side and torsional)	Hz	Derived parameter	-	-	O	-	X	X	X
1	Rotor blade natural frequency (edgewise, flapwise)	Hz	Derived parameter	-	-	O	-	X	X	X
1	Drive train natural frequencies	Hz	Derived parameter	-	-	O	-	X	X	X
2	Oil particle number	No.	10%	Y	<1Hz	R	Nacelle			X
2	Oil conductivity and pH value	S and PH	10%	Y	<1Hz	R	Nacelle			X
2	Nacelle position (yaw)	degree	0.1 - 0.5 degrees	Y	>=1Hz	R	Nacelle	X	X	X
2	Rotor speed (low speed shaft)	rpm	0.1-1%	Y	It should be 8 times larger than the highest frequency to be studied	R	Nacelle	X	X	
2	Rotor position (rotor azimuth)	degree	0.1 %	Y	It should be 8 times larger than the highest frequency to be studied	R	Nacelle	X	X	X
2	Generator speed (high speed shaft)	rpm	0.1-1%	Y	It should be 8 times larger than the highest frequency to be studied	R	Nacelle	X	X	X
2	Actual torque on high speed shaft	kNm	3%	Y	It should be 8 times larger than the highest frequency to be studied	O	Nacelle	X	X	X
2	Demanded torque on high speed shaft	kNm	derived from controller	Y	It should be 8 times larger than the highest frequency to be studied	O	Control system	X	X	
2	Pitch angle	degree	0.01 degree	Y	It should be 8 times larger than the highest frequency to be studied	R	nacelle	X	X	X
2	Demanded pitch angle	degree	derived from controller	Y	It should be 8 times larger than the highest frequency to be studied	R	Control system	X	X	
2	Pitch rate	degree/s	Derived signal	-	-	O	-	X	X	X
2	Voltage	V	0.5%	Y	It should be 8 times larger than the highest frequency to be studied	R	At several locations; before and after the converter, at stator, etc. Also in case of DC-lines, several locations might be required	X	X	X
2	Current	A	0.5%	Y	It should be 8 times larger than the highest frequency to be studied	R	At several locations; before and after the converter, at stator, etc. Also in case of DC-lines, several locations might be required	X	X	X
2	Active electrical power	kW	Derived parameter	-	-	-	-	X	X	X (10)

Param No	Parameter / Signal	Unit	Desired Accuracy (Uncertainty)	Traceable (Y/N)	Sampling frequency range [Hz] (1)	Required / Optional	Measurement position	WP5 Operational Control Systems	WP5 Development of Control strategies	WP7 Condition Monitoring
2	Reactive electrical power	kW	Derived parameter	-	-	-	-	X	X	X
2	Grid frequency	Hz	Derived parameter	-	-	-	-	X	X	
2	Controller mode (5)	-	derived from controller	Y	It should be 8 times larger than the highest frequency to be studied	R	Control system	X	X	X
2	Availability (5)	-	derived from controller	Y	It should be 8 times larger than the highest frequency to be studied	O	-	X	X	X
2	Failure (5)	-	derived from controller	Y	It should be 8 times larger than the highest frequency to be studied	O	-	X	X	X
2	Other parameters used in the controller	-	derived from controller	Y	It should be 8 times larger than the highest frequency to be studied	O	-	X	X	X
2	Wind speed measured at nacelle	m/s	0.1 m/s	Y	>=1Hz	R	Nacelle	X	X	X
2	Wind direction measured at nacelle	degree	1 degree	Y	>=1Hz	R	Nacelle	X	X	X
3	Wind speed at different positions in the rotor plane (longitudinal, lateral and vertical) (6)	m/s	0.1 - 0.25 m/s at 10 m/s	Y	>=1Hz	O (6)	Rotor plane	X	X	
3	Wind direction at different positions in the rotor plane	degree	2-5 deg	Y	>=1Hz	O	Rotor plane	X	X	
3	Air Temperature	C	0.5-3 ^{o}C	Y	>=1Hz	R	Hub height	X		X
4	Ice detection	-	-	-	-	O	Structure	X		X
6	Acoustic pressure measurements (11)	Pa	<0.1dB	Y	>22.4kHz	O	Individual components			X

Comments:
(1) For many parameters, it is noted that the sample frequency should be 8 times larger than the highest frequency to be studied.
This is most practical, since the parameters could be used for more purposes with own requirements.
(2) Displacements. Examples are gearbox displacements, angular displacements of flexible coupling, etc.
(3) Velocities. Examples are pitch piston velocities, main shaft velocities etc.
(4) Acceleration. Examples are accelerations in subcomponents etc.
(5) The controller should provide an output to monitor the state of the controller. It is not an input for the controller.
(6) If methods are developed to determine the wind characteristics in the rotor area in front of the turbine, this would be used.
(7) Cross sectional accelerations are required at each cross section in order to resolve flapwise as well as torsional vibrations.
(8) Main purpose for CM is monitoring of the main bearing.
(9) CM focuses on vibration analyses on all bearings, the gearbox as well as the blades.
(10) Is a requirement for CM. May be derived form turbine controller (IEC61400-25).
(11) Acoustic pressure measurements with the intention to early detect structural faults.

Analysis
1. We assume that vibrations or accelerations in the tower are used for the control, the tower bending moments are not applied.
2. We assume that strain distributions are not included for control or condition monitoring.
3. Condition monitoring tends to have the same signals as the control system.
Note that this is a consequence of the fact that when condition monitoring is a useful contribution to the turbine,
it is advantageous to include it in the control itself.
4. Insurance regulations have to be considered; If the CM is integrated in the controller, it requires a certificate, at least for the German market.

Appendix C Transmission and conversion and Electrical Grid

Table C.1 *List of parameters for WP1B2 Transmission and conversion and WP9 Electrical Grid*

Param No	Parameter / Signal	Unit	Desired Accuracy (Uncertainty)	Traceable (Y/N)	Sampling frequency range [Hz]	Required / Optional	Measurement position	WP9 Electrical Grid	WP1B2 Transmission and conversion	Power Quality Measurements
1	Displacements (1)	m	To be determined	Y	It should be 8 times larger than the highest frequency to be studied	O	Individual components		X	
1	Velocities (2)	m/s	To be determined	Y	It should be 8 times larger than the highest frequency to be studied	O	Individual components		X	
1	Accelerations (3)	m/s2	To be determined	Y	It should be 8 times larger than the highest frequency to be studied	O	Individual components		X	
1	Temperatures	C	To be determined	Y	It should be 8 times larger than the highest frequency to be studied	O	Individual components	X	X	
1	Pressure	Pa	To be determined	Y	It should be 8 times larger than the highest frequency to be studied	O	Individual components		X	
1	Yaw moment	kNm	Target 3%	Y	It should be 8 times larger than the highest frequency to be studied	R	Nacelle, it could be measured from the rotating structure, or from the fixed structure.		X	
1	Tilt moment	kNm	3%	Y	It should be 8 times larger than the highest frequency to be studied	R	Nacelle, it could be measured from the rotating structure, or from the fixed structure.		X	
1	Main shaft bending (0° 90°)	kNm	3%	Y	It should be 8 times larger than the highest frequency to be studied	R	Main shaft		X	
1	Main shaft torsion	kNm	3%	Y	It should be 8 times larger than the highest frequency to be studied	R	Main shaft		X	
1	Strain distribution to determine local stress distributions and for instance shear (anywhere)	kN	3%	Y	It should be 8 times larger than the highest frequency to be studied	R	Blade, hub, tower, nacelle, substructure, foundation and individual components		X	
1	Blade bending moment at the root of the blade (flapwise and edgewise)	kNm	3%	Y	It should be 8 times larger than the highest frequency to be studied	R	Blade		X	
1	Blade root bending moment (in-plane and out-of-plane)	kNm	Derived from blade bending moments and pitch angles	-	-	-	-		X	
1	Rotor blade natural frequency (edgewise, flapwise)	Hz	Derived parameter	-	-	-	-		X	
1	Drive train natural frequencies	Hz	Derived parameter	-	-	-	-		X	
2	Nacelle position (yaw) (4)	degree	0.1 - 0.5 degrees	Y	>=1Hz	R	Nacelle		X	
2	Rotor speed (low speed shaft)	rpm	0.1-1%	Y	It should be 8 times larger than the highest frequency to be studied	R	Nacelle		X	
2	Rotor position (rotor azimuth)	degree	0.1 %	Y	It should be 8 times larger than the highest frequency to be studied	R	Nacelle		X	
2	Generator speed (high speed shaft)	rpm	0.1-1%	Y	It should be 8 times larger than the highest frequency to be studied	R	Nacelle		X	X
2	Actual torque on high speed shaft	kNm	3%	Y	It should be 8 times larger than the highest frequency to be studied	R	Nacelle		X	

param No	Parameter / Signal	Unit	Desired Accuracy (Uncertainty)	Traceable (Y/N)	Sampling frequency range [Hz]	Required / Optional	Measurement position	WP9 Electrical Grid	WP1B2 Transmission and conversion	Power Quality Measurements
2	Demanded torque on high speed shaft	kNm	Derived from controller	Y	It should be 8 times larger than the highest frequency to be studied	R	Control system		X	
2	Voltage AC	V	0.5%	Y	It should be 8 times larger than the highest frequency to be studied, typically >= 2048Hz. Power Quality: sampling frequency >= 5kHz and harmonics with >=20kHz.	R	At several locations;before and after the convertor, at stator, etc. Power Quality: Measurement on MV side (10 to 20kV) may be required for (very large) wind farms.	X (4)	X	X
2	Current AC	A	0.5%	Y	It should be 8 times larger than the highest frequency to be studied, typically >= 2048Hz. Power Quality: sampling frequency >= 5kHz and harmonics with >=20kHz.	R	At several locations;before and after the convertor, at stator, etc. Power Quality: Measurement on MV side (10 to 20kV) may be required for (very large) wind farms.	X (4)	X	X
2	RMS values for voltage	V	Derived parameter	-	-	-	-	X	X	X
2	RMS values for current	A	Derived parameter	-	-	-	-	X	X	X
2	Absolute time (e.g. for assessing response to voltage drops)	sec	1microsec	Y	It should be 8 times larger than the highest frequency to be studied, typically >=10Hz	R	-			X
2	Grid Frequency	Hz	0.2% (may also be a derived parameter)	Y	It should be 8 times larger than the highest frequency to be studied, typically >=10Hz	R	-			X
2	Voltage DC	V	0.5%	Y	It should be 8 times larger than the highest frequency to be studied, typically >=10Hz	R	At several locations;before and after the convertor, at stator, etc. In case of DC-lines, several locations might be required	X (4)	X	X
2	Current DC	A	0.5%	Y	It should be 8 times larger than the highest frequency to be studied, typically >=10Hz	R	At several locations;before and after the convertor, at stator, etc. In case of DC-lines, several locations might be required	X (4)	X	X
2	Active electrical power	kW	Derived parameter	-	-	-	-	X	X	X
2	Reactive electrical power	kVAr	Derived parameter	-	-	-	-	X	X	X
2	Phases	-	Derived parameter	-	-	-	-	X	X	X
2	Controller mode	-	Derived from controller	Y	It should be 8 times larger than the highest frequency to be studied	R	Control system	X	X	X
2	Status	-	Derived from controller	Y	It should be 8 times larger than the highest frequency to be studied	R	Control system	X	X	X
3	Wind speed measured at nacelle	m/s	0.1 m/s	Y	>=1Hz	R	Nacelle	X	X	X
3	Wind direction measured at nacelle	degree	1 degree	Y	>=1Hz	R	Nacelle	X	X	
6	Acoustic pressure measurements	Pa	<0.1dB	Y	>22.4kHz	O	Individual components		X	

Comments:
(1) Displacements. Examples are gearbox displacements, angular displacements of flexible coupling, etc
(2) Velocities. Examples are pitch piston velocities, main shaft velocities etc.
(3) Acceleration. Examples are accelerations in subcomponents etc.
(4) In addition to these measurements, also high-frequency measurement campaigns might be required with sample frequencies >10kHz

Appendix D Flow and Remote Sensing

Table D.1 *List of parameters for WP8 Flow and WP6 Remote Sensing*

Param No	Parameter / Signal	Unit	Desired Accuracy (Uncertainty)	Traceable (Y/N)	Sampling frequency range [Hz]	Required / Optional	Measurement position	WP6 Remote Sensing	WP8 Flow Characterisation within and around wind farm
3	Wind speed (longitudinal, lateral and vertical) covering the rotor plane, below and above	m/s	0.1m/s	Y	>=1Hz	R	From 10m to one and a half times tip height; at several distances before and behind the turbine	X	X
3	Wind direction (longitudinal, lateral and vertical) covering the rotor plane, below and above	degree	1 degree	Y	>=1Hz	R	From 10m to one and a half times tip height; at several distances before and behind the turbine	X	X
3	Turbulence in the wind	%	derived parameter from horizontal wind speed	-	-	O	Rotor plane, free sector	X	X
3	Air Temperature	^{o}C	0.5-3 ^{o}C	Y	>=1Hz	R	Hub height, ground level	X	X
3	Temperature difference	^{o}C	0.01-0.1 ^{o}C	Y	>=1Hz	O	Rotor plane; offshore the difference between air temperature and sea water temperature may be dominating	X	X
3	Air relative humidity	%	3%	Y	>=1Hz	O	Hub height, ground level	X	X
3	Atmospheric pressure	hPa	5 hPa	Y	>=1Hz	R	Hub height, ground level	X	X
2	WT status signal	-	derived from controller	Y	>=1Hz	R	Control system		X
2	WT Grid Connected signal	-	derived from controller	Y	>=1Hz	O	Control system		X
2	Blade condition - icing, dust, insects	-	-	-	-	O	Blades		X
2	Rotor speed (low speed shaft)	RPM	0.1-1%	Y	1-10Hz	O	-		X
2	Pitch angle	degree	0.1-0.5 degree	Y	1-10Hz	R	-		X
2	Control Settings	-	derived from controller	Y	>=1Hz	O	-		X
2	Nacelle position (yaw)	degree	0.1-0.5 degree	Y	>=1Hz	R	Nacelle		X
2	Nacelle anemometer	m/s	0.1m/s	Y	>=1Hz	R	Nacelle		X
2	Active electrical power	kW	0.5%	Y	>=1Hz	R	Between wind turbine and electrical connection		X

Comments:
Remote sensing is performed from the ground, or could be performed from the wind turbine or mast.
Remote sensing from the nacelle could be

1. pointed to the front (inflow wind field),
2. pointed to the back (wake), pointed up (flow above wind farm).

Remote sensing from a mast could for instance assist the (complex terrain) power performance analysis.

Appendix EPower Performance analysis (IEC 61400-12-1)

Table E.1 *List of parameters for Power Performance analysis according IEC 61400-12-1.*

Param No	Parameter / Signal	Unit	Desired Accuracy (Uncertainty)	Traceable (Y/N)	Sampling frequency range [Hz]	Required / Optional	Measurement position	Power Performance	Site Calibration
2	Active electrical power	kW	0.5%	Y	>=1Hz	R	Between wind turbine and electrical connection	X	
2	Reactive electrical Power	kVAr	0.5%	Y	>=1Hz	O	Between wind turbine and electrical connection	X	
2	WT Availability Status signal	-	derived from controller	Y	>=1Hz	R	Control system	X	
2	WT Grid Connected signal	-	derived from controller	Y	>=1Hz	O	Control system	X	
2	Blade condition - icing, dust, insects	(1)	-	-	-	O	Blades	X	
2	Rotor speed (low speed shaft)	rpm	0.1-1%	Y	>=1Hz	O	-	X	
2	Pitch angle	degree	0.1-0.5 degree	Y	>=1Hz	O	-	X	
2	Control Settings	-	derived from controller	Y	>=1Hz	O	Control system	X	
2	Nacelle position (yaw)	degree	0.1-0.5 degree	Y	>=1Hz	O	-	X	
2	Yaw misalignment	degree	Derived parameter from nacelle position and wind direction	-	-	O	-	X	
3	Wind speed, horizontal component	m/s	0.1 - 0.25 m/s at 10 m/s	Y	>=1Hz	R	Hub height, free sector	X	X
3	Wind speed, horizontal component	m/s	0.1 - 0.25 m/s at 10 m/s	Y	>=1Hz	R	Hub height on a mast at the turbine location		X
3	Wind speed measured at other heights	m/s	0.1-0.25 m/s at 10 m/s	Y	>=1Hz	O	Rotor plane, free sector	X	X
3	Wind speed, vertical component	m/s	0.1 - 0.25 m/s	Y	>=1Hz	O	Rotor plane, free sector	X	X
3	Turbulence in the wind	%	Derived parameter from horizontal wind speed	-	-	O	Rotor plane, free sector	X	X
3	Wind direction	degree	2-5 deg	Y	>=1Hz	R	Rotor plane, free sector	X	X
3	Air Temperature	^{o}C	0.5-3 ^{o}C	Y	>=1Hz	Power performance: R Site calibration: O	Hub height	X	X
3	Temperature difference	^{o}C	0.01-0.1 ^{o}C	Y	>=1Hz	O	Rotor plane	X	X
3	Air relative humidity	%	3%	Y	>=1Hz	O	Hub height	X	X
3	Atmospheric pressure	hPa	5 hPa	Y	>=1Hz	Power performance: R Site calibration: O	Hub height	X	X
3	Atmospheric Stability	[-]	Derived from wind speed measurements in the rotor plane and temperature difference	-	-	O	-	X	X

Appendix F Noise Measurements (IEC 61400-11)

Table F.1 *List of parameters for Noise measurements according IEC 61400-11.*

Param No	Parameter / Signal	Unit	Desired Accuracy (Uncertainty)	Traceable (Y/N)	Sampling frequency range [Hz]	Required / Optional	Measurement position	Noise Measurements
2	Active electrical power	kW	0.5%	Y	>=1Hz	R	Between wind turbine and electrical connection	X
2	Rotor speed (low speed shaft)	rpm	0.1-1%	Y	>=1Hz	R	-	X
2	Pitch angle	deg	0.1-0.5 degree	Y	>=1Hz	R	-	X
2	Control Settings	-	Derived from controller	Y	>=1Hz	R	Control system	X
3	Wind speed horizontal	m/s	0.1 - 0.25 m/s at 10 m/s	Y	>=1Hz	R	Rotor plane, free sector	X
3	Wind speed horizontal	m/s	0.1 - 0.25 m/s at 10 m/s	Y	>=1Hz	R	Nacelle wind speed	X
3	Turbulence in the wind	%	Derived parameter from horizontal wind speed			R	Rotor plane, free sector	X
3	Wind direction	deg	2-5 deg	Y	>=1Hz	O	Rotor plane, free sector	X
3	Air Temperature	^{o}C	0.5-3 ^{o}C	Y	>=1Hz	R	Hub height	X
3	Air relative humidity	%	3%	Y	>=1Hz	O	Hub height	X
3	Atmospheric pressure	hPa	5 hPa	Y	>=1Hz	R	Hub height	X
3	Atmospheric Stability	[-]	Derived from wind speed measurements in the rotor plane and temperature difference			O	-	X
6	Acoustic pressure	Pa	<0.1dB	Y	>22.4kHz	R	On a ground plate behind the turbine	X